Involvement of Pattern Recognition Receptors in Coxsackievirus B Infection of Human Islets

Dissertation

zur Erlangung des Grades eines Doktors der Naturwissenschaften

im Fachbereich Biologie/Chemie
der Universität Bremen

vorgelegt von
Erna Domsgen

Bremen, 21.01.2013

1. Gutachter: Prof. Dr. Kathrin Mädler
2. Gutachter: Prof. Dr. Noel Morgan

Erklärung gemäß §6 Abs. 5 der Promotionsordnung

Ich versichere, dass ich die vorliegende Dissertation mit dem Titel „Involvement of Pattern Recognition Receptors in Coxsackievirus B Infection of Human Islets“ selbständig verfasst und keine anderen als die angegebenen Quellen und Hilfsmittel benutzt habe.

Bremen, den 21.01.2013

Erna Domsgen

Table of contents

Abbreviations

AP-1	Activating protein-1
APC	Antigen presenting cell
ATF-2	Activating transcription factor 2
CAR	Coxsackievirus and adenovirus receptor
CD8+ T-cell	T-cell receptors
CMV	Cytomegalovirus
CPE	Cytopathic effect
CTLA-4	T lymphocyte-associated protein 4
CVB	Coxsackieviruses B
DAF	Decay accelerating factor
DMEM	Dulbecco's Modified Eagle Medium
ECIT	European Consortium for Islet Transplantation
eIF2α	Eukaryotic translational initiation factor 2-alpha
ELISA	Enzyme-linked immunosorbent assay
ERK	Extracellular signalregulated kinase
EV	Enterovirus
FasL	Fas ligand
GAD65	Glutamic acid decarboxylase 65
GAD67	Glutamic acid decarboxylase 67
GLP-1, GLP-2	Glucagon-like peptide-1 and -2
GLUT2	Glucose transporter 2
GWAS	Genome wide association studies
HAV	Hepatitis A virus
HLA II	Human leukocyte antigen II
HSV-1	Herpes simplex virus-1
IA- 2	Insulinoma-associated antigen 2
ICA	Islet cell antibodies
IFIH1	Interferon-induced helicase 1
IFNs	Interferon
IIDP	Integrated Islet Distribution Program
IKKε	IκB kinase ε
IL-1R	Interleukin receptor 1
IL-1β	Interleukin 1 β

IL-2	Interleukin 2
IL-2Ralpha	Interleukin 2 receptor alpha
IL-6	Interleukin 6
IP	Immunoprecipitation
IP-10	Interferon-γ-inducible protein
IRES	Internal ribosomal entry site
IRF3	Interferon regulatory factor 3
ISG´s	Interferon stimulated genes
IκB	Inhibitory of κB
JNK	c-Jun N-terminal kinase
KRB	Krebs-Ringer bicarbonate buffer
LCMV	lymphocytic choriomeningitis virus
LCMV-GP	lymphocytic choriomeningitis virus glycoprotein
LGP2	Laboratory of Genetics and Physiology 2
LYP	lymphoid protein tyrosine phosphatase
MAVS	Mitochondrial antiviral signaling
MDA5	Melanoma differentiation associated gene-5
MHC	Major histocompatibility
MyD88	Differentiation primary response gene (88)
NDRI	National Disease Research Interchange
NK-cells	Natural killer cells
OAS1	2´-5´-oligoadenylate synthetase 1
p.i.	Post infection
PAMP	Pathogen associated molecular pattern
PCR	Polymerase chain reaction
PKR	Protein kinase regulated by RNA
Poly I:C	Polyinosine deoxycytidylic acid
PP	Pancreatic polypeptide
PPI	Preproinsulin
PRR	Pattern recognition receptor
PVDF	Polyvinylidene flouride-membrane
RIG-I	Retinoid-inducible gene I
RIP	Rat insulin promoter
RLR	Retinoid-inducible gene I like receptors
RT	Room temperature
RT-PCR	Reverse transcription-polymerase chain reaction

SNP	Single-nucleotide polymorphism
ssRNA	Single strand RNA
ssRNA	Single-stranded RNA
T1DM	Type 1 Diabetes mellitus
T2DM	Type 2 Diabetes mellitus
TAK1	Transforming growth factor β-activated protein kinase 1
TBK1	TANK-binding kinase 1
$TCID_{50}$	Tissue culture infectious dose 50 %
TCR	CD8+ cytotoxic T-lymphocyte
TEDDY	The Environmental Determinants of Diabetes in the Young
TIR	Toll/IL-1R
TLR	Toll-like receptor
TLR7	Toll-like receptor 7
TNFα	Tumor necrosis factors α
Tregs	Regulatory T-cells
TRIF	TIR-domain-containing adapter-inducing interferon-β
VNTR´s	Variable number of tandem repeats
VP	Viral protein
VRC	vanadyl ribonucleoside complexes
WHO	World Health Organization
ZnT8	Zink transporter 8

1 Summary

T1DM is an autoimmune disease in which β-cells are selectively destroyed by the immune system. As consequence of β-cell destruction insulin levels decline resulting in elevated blood glucose levels. The decline ends finally in complete insulin deficiency and manifestation of T1DM. At this step patients with T1DM require lifelong insulin therapy. The disease is highly associated with genetic susceptibility. The major susceptibility locus for T1DM is the HLA II region on chromosome 6. Over the last decades the overall incidence is rising especially in children under the age of 5. This increase is too big to be explained by genetic factors only, suggesting that environmental factors contribute to the manifestation of the disease [1, 2]. T1DM is thought to result from the interaction between genetic predisposition, immune system and environmental factors [3]. Such environmental factors may be viral infections, which have been associated with T1DM for many years. So far, the best investigated viral environmental factors with the best documented connection to T1DM are human EVs [4]. Epidemiological studies and analysis of pancreatic tissue samples show the clear involvement of EVs and among those, coxsackievirus B (CVB) in T1DM. However, the molecular mechanisms of islet infection and how viruses can lead to the disease are still not discovered.

In the present study isolated human islets were infected with two serotypes CVB3 and CVB4 and molecular mechanisms of infections were investigated. Infections with both viruses showed that mainly β-cells were infected which resulted in specific β-cell apoptosis and impaired β-cell function. Gene expression analysis revealed that upon CVB3 and CVB4 infections genes encoding pro-inflammatory proteins were highly expressed, especially those of *CXCL10* and *IFNβ*. Induction of genes encoding cytokines and chemokines is mediated by the interaction of PAMPs (pathogen associated molecular patterns), as dsRNA, with pathogen recognition receptors (PRRs). The present study showed the binding or CVB3 and CVB4 RNA to PKR and in addition to TLR3 and TLR7 which are members of the PRR family. This observation was further supported by the RNA interference analysis. TLR3 depleted human islets infected with CVB3 and CVB4, showed lower expression levels of cytokine and chemokine genes, especially of *CXCL10* and *IFNβ* genes, indicating that induction of gene expression was TLR3 mediated. In addition, TLR3 depleted and CVB3 and CVB4 infected human islets showed less apoptosis, suggesting that the TLR3 pathway was involved in virus-induced β-cell death. Further studies on virus mediated apoptosis induction revealed that JNK also was involved in cell death.

High expression of cytokines and chemokines such as CXCL10 contribute to the activation and the attraction of immune cells to the side of the infection. Apoptotic β-cells can be

phagocytised by APCs leading to the presentation of viral but also of β-cell antigens. This results in activation of cytotoxic T-cells. Both effects can be crucial for the initialization of autoimmunity in genetically susceptible individuals.

1 Zusammenfassung

Typ 1 Diabetes Mellitus (T1DM) ist eine Autoimmunerkrankung, bei der das eigene immunsystem gezielt die β-Zellen der Langerhans Inseln zurstört. Als Folge der Zerstörung wird nicht ausreichend Insulin produziert, um den Glucosespiegel im Blut nach Mahlzeiten zu reduzieren und auf einem gesunden Niveau zu halten. Letzendlich führt die β-Zell Zerstörung dazu, dass Betroffene ein Lebenlang von zugefügtem Insulin, in Form von Injektionen, abhängig sind. Die Krankheitsurasache hat einen genetischen Ursprung. Es ist etabliert, dass bestimmte HLA Allele mit dem T1DM stark assoziiert sind. In den letzten Jahrzehnten wurde ein stetiger Anstieg der Krankheitshäufigkeit beobachtet, der nicht durch die Genetik alleine erklärt werden kann [1, 2]. Es wird angenommen, dass zusätzlich zu den genetischen Faktoren auch Umweltfaktoren eine Rolle spielen und zu dem Anstieg beitragen. Zu den Umweltfaktoren zählen Virusinfektionen, die seit vielen Jahren mit T1DM assoziiert sind. Verschiedene Studien haben einen Zusammenhang zwischen Enteroviren, die zur Familie der *Picornaviridae* gehören, und T1DM gezeigt [4]. Dabei wurden vorallem Coxsackieviren der Gruppe B (CVB) besonders oft assoziiert. Eine Erklärung, wie eine Virusinfektion zum Ausbruch des T1DM führen kann, wurde noch nicht beschriben.

In der vorliegenden Arbeit wurden humane Inseln mit zwei verschiedenen Serotypen, CVB3 und CVB4, *in vitro* infiziert und molekulare mechanismen der Infektionen wurden untersucht. In der Arbeit konnte gezeigt werden, dass beide Serotypen zu einer β-Zell spezifischen Infektion führen, die wiederum eine Induktion der β-Zell Apoptose und die beeinträchtigung der β-Zell Funktion zur Folge hatte. Des Weiteren konnte durch Genexpressionsanalysen gezeigt werden, dass die Infektionen zu gesteigerten Expressionen der Gene führte, die während der Aktivierung des angeborenen und adaptiven Immunsystems, eine Rolle spielen. So konnte die höchste Expression der *CXCL10* und *IFNβ* Gene beobachtet werden. Eine solche Induktion wird durch die Bindung von Molekülen, wie der dsRNA, an sogenannte Pattern Recognition Receptors (PRRs) ausgelöst. In der vorliegenden Arbeit konnte gezeigt werden, dass die CVB3 und CVB4 RNA Moleküle von der PKR, und den PRRs TLR3 und TLR7 gebunden wird. Die TLR3-RNA Interaktionen wurden zusätzlich durch RNA Interferenz Studien unterstützt. Inseln, die mittels siTLR3 transfiziert und mit CVB3 und CVB4 infiziert wurden, zeigten eine Reduktion der beobachteten Genexpressionen, vorallem der der *CXCL10* und *IFN β* Gene, was eindeutig für eine TLR3 vermittelte Aktivierung des angeborenen Immunsystems spricht.

Des Weiteren, konnte in siTLR3 transfizierten und mit CVB3 und CVB4 infizierten Inseln, eine Reduktion der CVB3 und CVB4 induzierten Apoptose beobachtet werden. Weitere

Apoptose Untersuchungen zeigten dass neben TLR3 auch die JNK Kinase eine Rolle in der Virus induzierten Zell Apoptose spielte.

Die Induktion der Expressionen von Inflammatorischen Genen und die Induktion der Apoptose können beide entscheidene Faktoren bei der Entstehung des T1DM sein. Cytokine und Chemokine aktivieren und locken zytotoxische T-Zellen zum Ort der Infektion, wo apoptotische Zelle von Antigen presentierenden Zellen phagozytiert werden und so virale und β-Zell Antigene presentiert werden können.

2 Introduction

2.1 Islets of Langerhans

The pancreas is a gland organ located partially behind the stomach and in close proximity to the spine in the abdomen. It consists of the tail region located close to the spleen, the body region and the head region that is connected to the duodenum. The gland has two functional parts; the exocrine and the endocrine part. The exocrine part contains acinar cells which produce digestive enzymes important for food digestion in the duodenum. They are positioned around central ducts that drain into the pancreatic duct allowing the digestive enzymes to enter the small duodenum via the major duodenal papilla where they contribute to break down carbohydrates, proteins and lipids. The endocrine pancreas is made by the islets of Langerhans, first described by the German anatomist Paul Langerhans in 1869. They consist of clusters of different hormone producing cells, endothelial cells, nerves and fibroblasts. The size of the islets ranges from few to many thousand cells. Islets are scattered throughout the whole organ in about 1 million clusters and constitute around 1-2% of the mean pancreatic weight. Islets are highly vascularised mini-organs so that produced hormones are absorbed rapidly into the blood stream and thus distributed throughout the whole body. A collagen capsule around the islets separates the endocrine and the exocrine part [5].

Five cell types are located in the islets; glucagon producing α-cells, insulin producing β-cells, somatostatin producing δ-cells, pancreatic polypeptide producing PP-cells and ghrelin producing ε-cells [6]. All hormones regulate glucose homeostasis.

Glucagon increases blood glucose levels during starvation. Low levels of blood glucose trigger its secretion and hepatic glucose output increases to supply organs with glucose. The source of glucose is maintained by glucogenogenesis and glycogenolysis, two mechanisms leading to synthesis of D-glucose from carbon substrates like pyruvate, lactate or glycerol and to the breakdown of glycogen in glucose respectively [7]. Glucagon is a 29-aminoacid peptide that is derived from the 180-aminoacid proglucagon by proteolytic cleavage. Other proglucagon cleavage products are glucagon-like peptide-1 and -2 (GLP-1, GLP-2). The number of α-cells per islet varies from 15 to 20% [6, 8].

β-cells build the majority of cells per islet ranging from 50 to 80% [6, 8]. Insulin is secreted by the β-cells in response to high blood glucose levels and acts on different tissues leading to glucose uptake from the blood, thus preventing hyperglycemia. It suppresses the glucose

output and increases the uptake by the liver and the skeletal muscles. In those organs it stimulates glucogenesis and inhibits gluconeogenesis and lipolysis in the fat tissue.

Glucose molecules are taken up by β-cells via the glucose transporter 2 (GLUT2) and are phosphorylated by glucokinase, the essential enzyme for gycolysis. During this metabolic process glucose is cleaved into 2 pyruvate molecules, which are decarboxylated and added to coenzyme A forming Acetyl-CoA, which enters the Krebs cycle. ATP is produced as result of the Krebs Cycle and during oxidative phosphorylation, in which electrons are transferred from electron donors to electron acceptors. The increase in the ATP/ADP ratio leads to the closure of potassium channels which in turn leads to membrane polarization. Consequently, calcium channels open and induce the release of insulin by exocytosis of insulin-containing granules [9].

Insulin is generated by cleavage of a preproinsulin molecule composed of an A-chain, B-chain and a C-chain. Proinsulin is formed by catalytic cleavage of the signal sequence in the Golgi apparatus and further cleaved in insulin in maturing granules. Its active form is a 51-aminoacid protein containing two peptide chains, A-chain and B-chain that are combined by two disulfide bonds (Fig. 1) [10]. The C-chain (C-peptide) is released together with insulin at a 1:1 ratio.

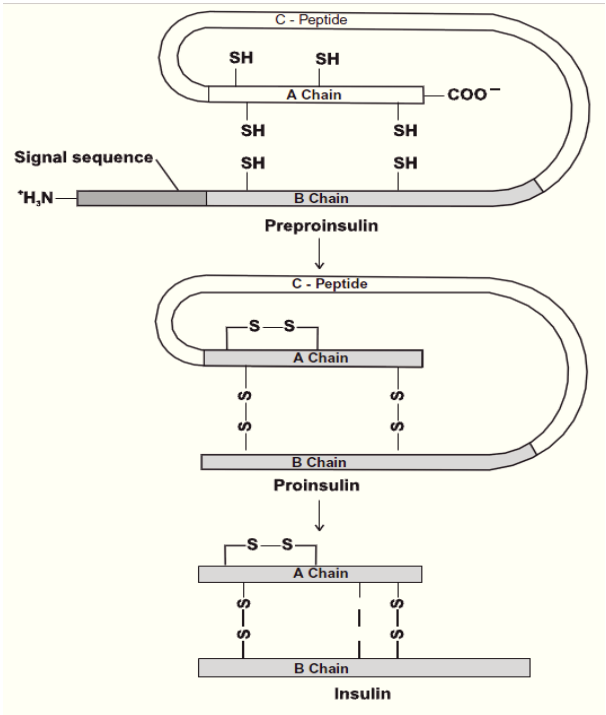

Figure 1: Posttranslational processing of preproinsulin to mature insulin [10].

δ-cells produce somatostatin, a hormone which inhibits insulin and glucagon release. The hormone exists in two forms, a 14 and a 28 aminoacid-peptide. Islets contain only 5-7% of δ-cells [6, 8].

PP-cells produce pancreatic polypeptide (PP), a hormone that is involved in appetite regulation after food intake. Its release is mainly stimulated by food intake. PP is under vagal control and exerts its regulatory functions in different tissues, including the inhibition of digestive enzyme secretion from acinar cells and gallbladder motility. It is a 36 aminoacid-peptide and belongs to and shares high homology to neuropeptides like neuropeptide Y [11]. There are few PP-cells in the islet; islets located in the head part of the pancreas contain larger numbers of PP-cells, while there are rarely any PP-cells in the tail part [12].

The last discovered islet cell type are ε-cells which secrete ghrelin hormone acting on growth hormone secretion and regulation of metabolism. Little is known about this cell type, and further investigations are necessary [6].

The architecture of human islets shows a distribution of cell types without any obvious organization. Mouse islets have a typical construction where β-cells form the core of islets that is encircled by remaining cell types (Fig. 2) [8]. The most common disease associated with islets is Diabetes mellitus.

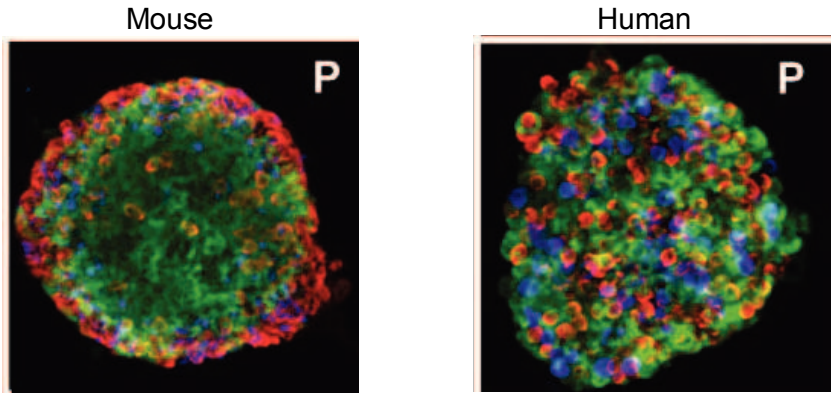

Figure 2: Comparison of architecture between human and rodent islets. β-cells are stained in green, α-cells in red and δ-cells in blue [8].

2.2 Diabetes mellitus

Diabetes mellitus is a disease with high prevalence worldwide. Based on WHO (World Health Organization) 347 million people worldwide have diabetes. Studies on estimation of diabetes prevalence suggest that this number is expected to double to more than 500 million diabetes cases by the year 2030.

This is mainly due to population growth, longer life expectation, urbanization and increasing incidence of obesity and physical inactivity. Especially in developing countries diabetes prevalence is expected to increase drastically by 2030 because of demographic change [13].

Diabetes mellitus is characterized by abnormal high blood glucose concentrations, hyperglycemia. Such elevated blood glucose levels over a long period of time lead to microvascular and macrovascular complications. This can result in impairment of neurons and blood circulation leading to neuropathy, retinopathy and blindness and nephropathy. The risk for stroke is highly increased in patients with diabetes, and poor wound healing and perfusion together with neuropathy can lead to the diabetic foot syndrome resulting in limb amputation.

The main causes of hyperglycemia are insufficient blood insulin levels or in case of insulin resistance, failure in biological insulin functions. Massive destruction of insulin producing β-cells leads to insufficient secretion of insulin to maintain glucose levels in a normal range resulting in elevated blood glucose levels.

The most common forms of Diabetes mellitus are Type 1 Diabetes mellitus (T1DM) and Type 2 Diabetes mellitus (T2DM). T1DM results from autoimmune destruction of β-cells and displays an autoimmune disorder, while T2DM is considered to result from insulin resistance together with the relative insulin insufficiency and decline in β-cell function and mass.

2.2.1 Type 1 Diabetes

T1DM is an autoimmune disease which is characterized by the destruction of β-cells by the own immune system, leading to reduced and finally no insulin production. It is estimated that approximately 5-10% of all diabetic patients suffer from T1DM [14]. The disease manifests itself usually in people younger than 30 years, and it is therefore also termed juvenile-onset diabetes. In the last decades the overall incidence is rising, especially in children under the age of 5 [1, 2]. During the last 100 years hygiene standards have drastically changed. The so-called “hygiene hypothesis” has been proposed as possible explanation for the T1DM increase and for allergy development. It suggests that lack of pathogen exposure in developed countries leads to malfunction of the immune system and increases allergies and autoimmune disorders [15]. This hypothesis correlates very well with the high T1DM incidence in children from 0 to 14 years in developed countries (Fig. 3) [16]. A similar hypothesis has been suggested for poliomyelitis [17].

From 1989-2003 the annual increase in T1DM incidence in Europe was 3.9%, and it is predicted that T1DM cases in European children younger than 5 years will double between 2005 and 2020 [18]. This increase is too big to be explained by genetic factors only. The concordance rate between monogenetic twins is only ~50% [19]. This implicates that environmental factors such as viral infections, early exposure to cow´s milk, wheat proteins

or vitamin D insufficiency also contribute to T1DM. The disease is thought to result from the interaction between genetic predisposition, immune system and environmental factors (Fig. 4) [3].

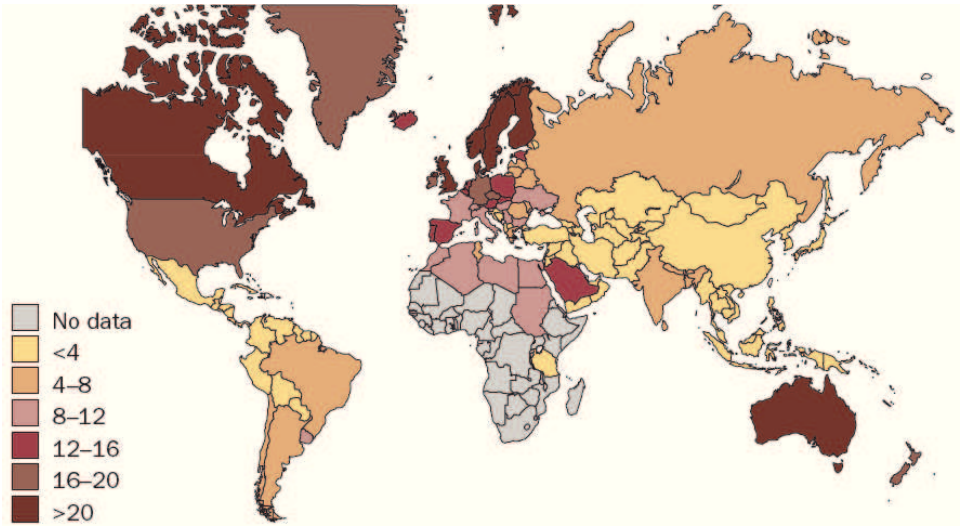

Figure 3: Worldwide incidence of Type 1 diabetes. The world map shows the T1DM incidence in children from 0-14 years. Numbers account for new cases per year/100,000 individuals. Adapted from [16].

T1DM is strongly associated with genetic susceptibility (poplygenic). The major susceptibility locus for T1DM is the MHC class II (major histocompatibility complex class II) or HLA II (human leukocyte antigen II) region on chromosome 6p21 or IDDM1 (insulin-dependent-diabetes mellitus locus) [20].

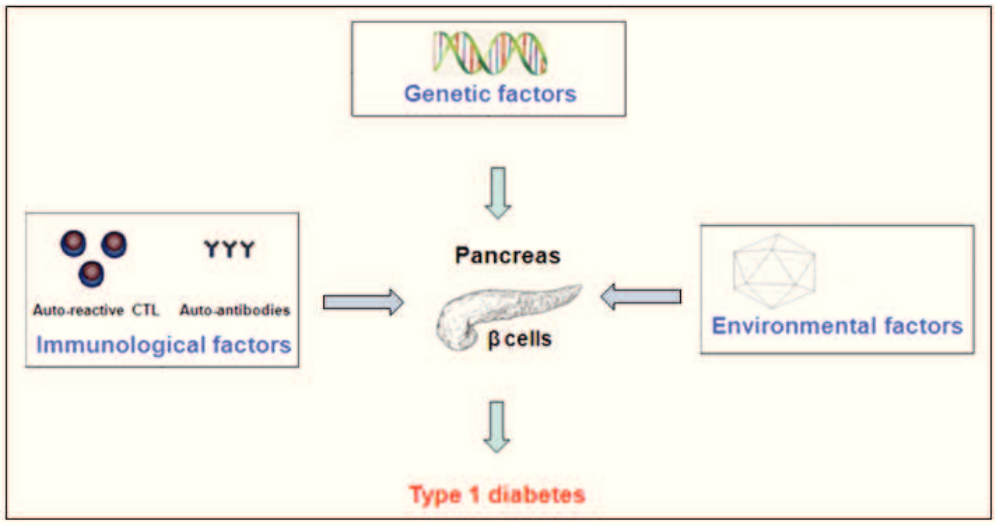

Figure 4: Contributors in T1DM. The interplay between genetic factors, the immune system and environmental factors leads to breakdown of self tolerance and outcome of T1DM. Adapted from [21].

2.2.1.1 HLA class I and II

The locus of *HLA* codes for MHC molecules, class I and class II. MHC class I is expressed by all nucleated cells. These complexes present intracellular antigens on their surface-like viral epitopes- and are bound by the T-cell receptors (TCR) of $CD8^+$ cytotoxic T-lymphocytes ($CD8^+$ T-cells). MHC class II molecules are expressed on antigen presenting cells (APC) like dendritic cells, macrophages and B-lymphocytes. They present extracellular antigens to $CD4^+$ TCR´s. Genes encoding MHC class I molecules are MHC-A, MHC-B and MHC-C, and MHC class II are HLA-DP, HLA-DQ and HLA-DR. Every locus has a high number of variant alleles, making the HLA system highly polymorph (Fig. 5).

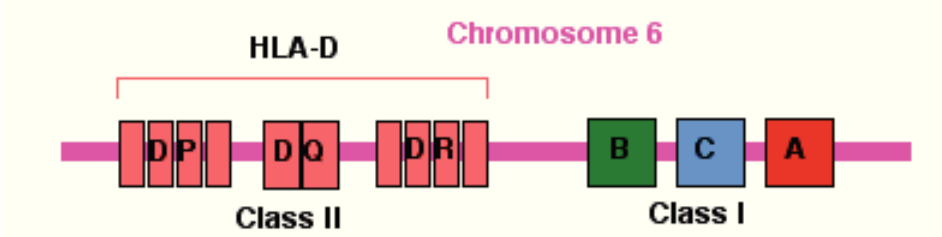

Figure 5: Schematic representation of the HLA class I and class II system. Genes coding for the MHC class I and II molecules are located on chromosome 6.

The *HLA II* genotype is a useful determinant to define inherited risk for T1DM. The genotype associated with the highest risk tor T1DM is *HLA DRB1*03,*04; DQB1*0302* [22-24]. In children with these haplotypes and a T1DM relative the risk to develop T1DM is around 25% and with two or more affected family members even around 50% [25]. This predisposing HLA class II haplotypes are found in around 90% of T1DM cases [24]. 20% of the population have the haplotype DRB1*1501-DQA1*0102-DQB1*0602, but only 1% of T1DM patients, demonstrating a protective haplotype for T1DM [26]. Susceptibility loci were also found in the HLA I region [27-29]. HLA-A*02 increases the risk for T1DM in individuals with the high-risk class II DR3/4-DQ8 haplotype [30]. Among those, HLA-A *0201 is one of the most prevalent class I alleles, with an incidence rate of around 60% in T1DM patients [22]. Other non-HLA genes were also found to contribute to susceptibility.

2.2.1.2 Non-HLA genetic factors

The insulin gene region itself contributes to T1DM susceptibility. The mutation in the variable number of tandem repeats (VNTR´s) of the insulin gene promoter determines the susceptibility [31-33]. The number of the VNTR´s correlates with either protection or predisposition [33, 34]. It is hypothesized that VNTR´s regulate the insulin expression in the

thymus. Less VNTR´s would lead to less insulin gene transcription, which might reduce self tolerance and T1DM outcome [35].

PTPN22 encoding the lymphoid protein tyrosine phosphatase (LYP) is another T1DM susceptibility gene [36]. LYP is expressed in lymphocytes where it acts as a strong suppressor of Src family kinases which mediate TCR signaling. It is a strong inhibitor of T-cell activation [36]. The mechanisms of how LYP leads to autoimmunity are still not fully understood [22].

Genetic risk for development of T1D has also been found in the gene encoding Interleukin 2 (IL-2) receptor alpha (IL-2Ralpha) [37]. The IL-2R appears in two forms as a moderate binding IL-2R not containing the IL-2Ralpha subunit expressed on T-cells, NK-cells (natural killer cells), and monocytes, and a high-affinity IL2-R containing the IL-2Ralpha subunit expressed on regulatory T-cells (T_{regs}). IL-2 binding to its receptor provides survival and growth of T_{regs} [38]. T_{regs} are specialized subsets of T-cells that suppress autoreactivity at the peripheral level. In T1DM, abnormalities in T_{reg} function have been reported and implicated in the development of the disease [39].

Other T1DM susceptibility genes are T lymphocyte-associated protein 4 (CTLA-4), which is involved in the regulation of immune response, and Interferon-induced helicase 1 (IFIH1) that has been identified in genome wide association studies (GWAS) [22, 40]. *IFIH1* encodes melanoma differentiation associated gene-5 (MDA5) that acts as an intracellular pattern recognition receptor (PRR) for viral double stranded RNA (dsRNA). Upon binding to dsRNA, MDA5 interacts with the adaptor protein mitochondrial antiviral signaling (MAVS) to induce type I interferons (IFNs) [41, 42]. GWAS demonstrated rare variants protecting from T1DM, whereas the majority of the population carries alleles predisposing to the disease [40]. IFIH1 variants identified to be protective are encoding MDA5 proteins with reduced function due to truncation or failure in splicing [40, 43]. Other candidate genes that can have a function in host response against viruses are toll-like receptor 7 (TLR7) and TLR8 that recognize single-stranded RNA (ssRNA) molecules from different viruses and initiate the upregulation of type I IFNs. A single-nucleotide polymorphism (SNP) in TLR7 and TLR8 has been associated with the risk for T1DM [44].

2.2.1.3 Pattern recognition receptors (PRRs)

Microorganism trying to invade hosts need to be detected and eliminated. During evolution, different detection receptors, so-called PRRs, developed to sense the invaders. In case of RNA viruses, dsRNA and ssRNA serve as pathogen associated molecular patterns (PAMPs) for specialized PRR´s to induce the first line of defence, the innate immune response. This includes upregulation and secretion of chemokines and cytokines like type 1 IFNs that in turn induce upregulation of many interferon stimulated genes (ISG´s) which have antiviral

properties to eliminate infection. The antiviral receptors or sensors are classified in two groups toll-like receptor (TLR) family members and retinoid-inducible gene I (RIG-I) like receptors (RLRs).

TLRs are type I transmembrane proteins consisting of extracellular leucine-rich-repeats responsible for binding of PAMPs, a transmembrane region and a cytosolic domain homologous to the interleukin receptor 1 (IL-1R) named Toll/IL-1R (TIR) domain [45, 46]. So far 10 TLRs are identified in humans which are responsible for the detection of distinct PAMPS derived from viruses, bacteria, fungi, parasites and mycobacteria. They are located in cellular membranes or in intracellular vesicles like endosomes, the endoplasmatic reticulum, lysosomes or endolysosomes [45, 47]. Binding of distinct PAMPs to TLRs results in the recruitment of adapter proteins such as myeloid differentiation primary response gene (88) (MyD88) or TIR-domain-containing adapter-inducing interferon-β (TRIF) to the TIR domain and induction of a signal cascade inducing secretion of inflammatory cytokines, chemokines and type I IFN through translocation of the transcription factors NF-κB and interferon regulatory factor 3 (IRF3) and IRF7 [45, 46].

Viral dsRNA or the synthetic analogue polyinosine deoxycytidylic acid (Poly I:C) are recognized by TLR3, whereas ssRNA is bound by TLR7 and TLR8 [45, 48] . Upon binding of dsRNA or Poly I:C to TLR3, TRIF and other adaptor proteins associate with the intracellular region TIR leading to phosphorylation of TRIF. This results in TRIF dependent phosphorylation of TANK-binding kinase 1 (TBK1) and IκB kinase ε (IKKε) leading to phosphorylation and translocation of IRF3 and IRF7, which are critical transcription factors in type 1 IFN induction [49]. NFκB is released from the inhibitor of κB (IκB) due to TRIF dependent activation of transforming growth factor β-activated protein kinase 1 (TAK1) and the IKK complex causing phosphorylation and ubiquitination of IκB. Released NFκB translocates to the nucleus where it induces type 1 IFN and inflammatory cytokine gene expression (Fig. 6) [50, 51]. Simultaneously, TAK1 activates the MAP kinase pathway resulting in activation of the transcription factor activating protein-1 (AP-1) composed of c-Jun and activating transcription factor 2 (ATF-2). MAP kinases involved in this pathway are c-Jun N-terminal kinase (JNK), p38 and extracellular signalregulated kinase (ERK) [52].

Another feature of TRIF in TLR3 signalling is its induction of apoptosis as important antiviral action restricting the spreading of viruses [53, 54]. Binding of ssRNA to TLR7 recruits the essential adapter protein MyD88, which together with other adaptor proteins leads to TLR3 signalling and eventually induction of inflammatory proteins and type I IFN through NFκB and IRF translocation [45, 47].

RLRs are intracellular dsRNA sensors which include MDA5, RIG-I and Laboratory of Genetics and Physiology 2 (LGP2) and contain a DExD/H-box RNA helicase domain. After binding to dsRNA, RIG-I and MDA5 interact with the mitochondrial adaptor protein MAVS

[55-57]. MAVS triggers the activation of TBK1 and IKKε, resulting in phosphorylation and translocation of IRF3 and IRF7 to the nucleus. Secondary NFκB is released from IκB in a MAVS dependent fashion (Fig. 6) [57, 58].

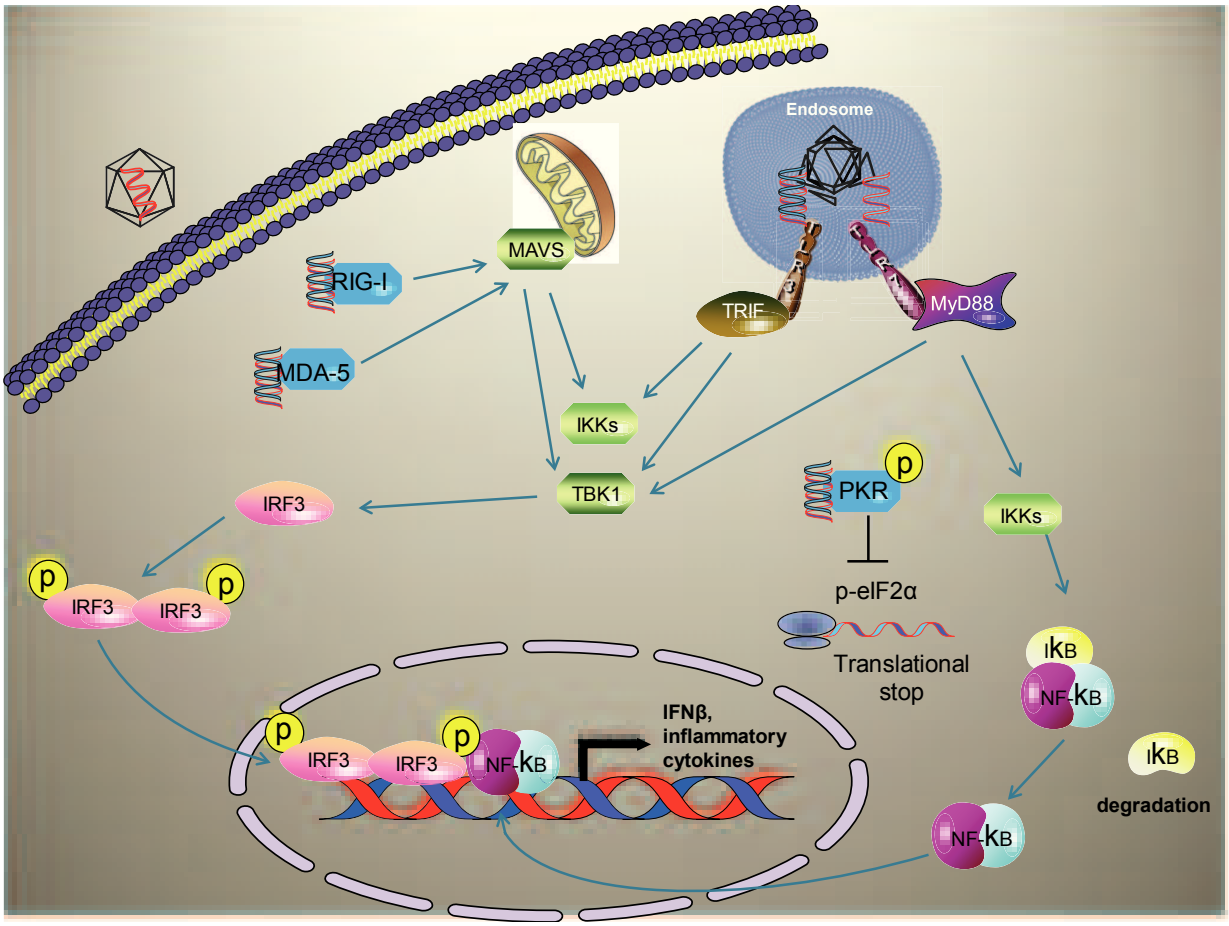

Figure 6: Induction of type I interferons upon binding of PRR to dsRNA and ssRNA. dsRNA or ssRNA, which can be present in the endosomes after uncoating of the viral capsid, bind to TLR3 or TLR7 leading to recruitment of adaptor proteins TRIF and MyD88. This activates IKKs and TBK1, resulting in phosphorylation and dimerization of IRF3 and degradation of IkB, leading to translocation of the transcription factors into the nucleus where they induce IFNβ gene expression. On the other hand intracellular PRR RIG-I and MDA5 can bind to intracellular dsRNA and activate IKKs and TBK1 in a MAVS dependent fashion leading also to translocation of IRF3 and NFkB.

Protein kinase regulated by RNA (PKR) is an IFN-inducible, dsRNA binding antiviral protein. Its antiviral property is mediated trough translational stop after infection. dsRNA binding leads to dimerisation and phosphorylation of PKR. Activated PKR is phosphorylating eukaryotic translational initiation factor 2-alpha (eIF2α) leading to general inhibition of translation [59]. PKR has been shown to be involved in insulin resistance through phosphorylation of the insulin receptor and activation JNK [60].

2.2.1.4 Autoantibodies and immune mediated destruction of β-cells

The etiology of T1DM is very complex. It is still under investigation how genetic susceptibility can lead to autoreactivity resulting in loss of β-cells and finally to the onset of the disease. T1DM is characterized as an autoimmune mediated disease with selective destruction of β-cells by islet infiltrating immune cells, a process also called insulitis. Environmental factors as pathogens can be triggering events responsible for autoimmunity. The first indication of self reactivity and autoimmunity in T1DM is the appearance of autoantibodies. Insulitis can persist for years before clinical symptoms occur (Fig. 7).

Autoantibodies can be present in the sera of individuals many years before diabetes onset. Until now four groups of autoantibodies binding to islet antigens are identified recognizing preproinsulin (PPI) and insulin, glutamic acid decarboxylase 65 or 67 (GAD65 or GAD67), insulinoma-associated antigen 2 (IA-2) and zink transporter 8 (ZnT8). Other islet-specific antibodies exist which are called islet cell antibodies (ICA) [23]. Those four different groups of autoantibodies are used as biomarkers to predict the risk for T1DM progression in children and young adults with and without family history [61, 62]. Thereby mostly the number of different autoantibody groups determines the risk. The presence of one autoantibody raises, but two or more autoantibodies markedly increase the risk for T1DM [23].

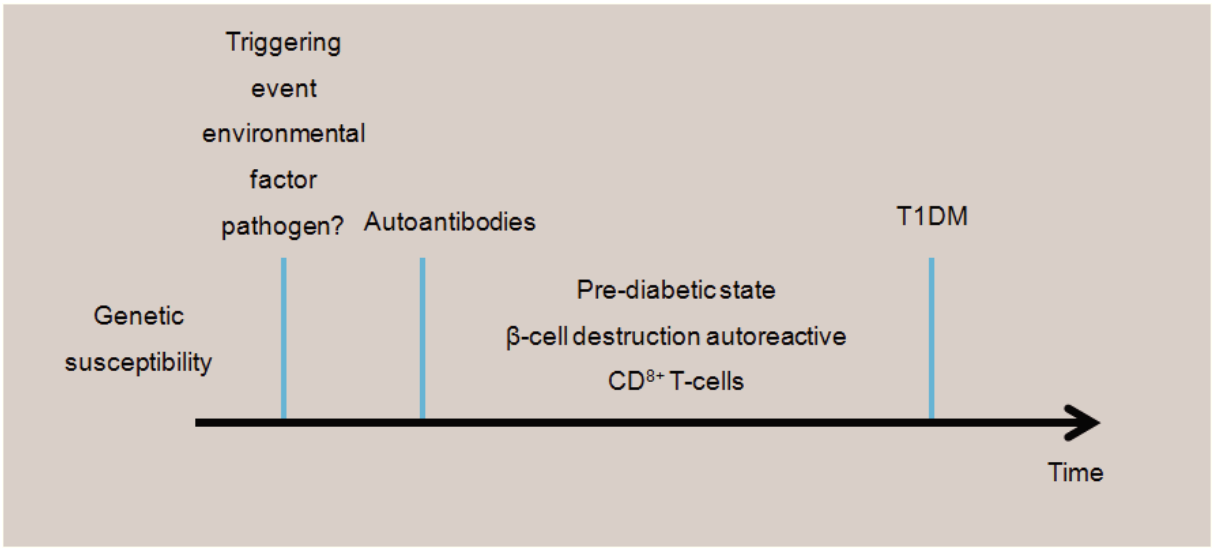

Figure 7: Pathogenesis of T1DM. In genetic susceptible individuals, triggering events like environmental factors such as pathogen infections can lead to the appearance of autoantibodies. In the pre-diabetic state autoreactive $CD8^+$ destroy the β-cells T1DM manifests after destruction of ~70-80% the β-cells.

Autoantibodies can appear in the early stage long before the onset of the disease, indicating involvement of plasma B-cells in the initial phase of the disease. T1DM susceptibility or resistance HLA II genotypes are mapped to peptide binding pockets of the MHC class II receptors present on APC [63]. B-cells are APC that become plasma B-cells producing and

secreting antibodies upon activation. Indeed, a study by Pescovitz et al. showed that B-lymphocytes contribute to the pathogenesis of T1DM, since application of an anti-CD20 monoclonal antibody rituximab preserved β-cell function. CD20 is present on B-cells until plasma B-cell differentiation and the application of anti-CD20 monoclonal antibody rituximab can selectively deplete B-lymphocytes [64].

Another hallmark of prediabetic stage and early onset of T1DM are autoreactive T-cells. $CD8^+$ T-cells are thought to be the most important β-cell killers [65]. APCs such as B-cells can actively contribute to autoimmunity by presenting autoantigens to diabetogenic $CD4^+$ and $CD8^+$ T-cells [22]. The main autoreactive T-cell epitopes are also the major antibody targets, namely proinsulin and PPI, GAD65, IA-2 and ZnT8 [66]. Autoreactive $CD8^+$ T-cells can destroy β-cells upon binding to MHC class I molecules which are shown to be upregulated on β-cells in $CD8^+$ T-cell infiltrated islets from T1DM patients [67].

Recent immunohistochemical investigations of a collection of samples confirmed pre-existing observations and gave more insight into chronological events. Modern immunohistochemical techniques were applied on old samples from 29 patients with recent onset T1DM collected from 1960 to 1985 [68]. Here the investigators separated islets according to their β-cell mass in different categories from islets with normal β-cell mass to islets where only very few or no β-cells were present. $CD8^+$ T-cells were the most prominent immune cells in insulitis and the cell number correlated with the degree of β-cell demise. Macrophages followed the same pattern suggesting a role in β-cell death. $CD20^+$ B-cells were present in low number but were increased during β-cell demise. $CD4^+$ T-cells were present with no increase in number at any stage and T_{regs} were not present in inflamed islets. β-cell deficient islets showed no infiltration of immune cells or any signs of insulitis [69].

Programmed cell death or apoptosis is probably the main form of β-cell death in T1DM [70]. β-cell loss during insulitis is most likely caused by direct contact with $CD8^+$ T-cells or macrophages. Upon ligation of the TCR with MHC class I molecules, $CD8^+$ cytotoxic T-cells induce apoptosis through release of granules containing perforin and granzymes. Perforin is introducing holes in the target cell membrane allowing granzymes to enter the cytosol where they can activate caspases and nucleases, the main apoptotic effector proteins. Another possibility is the ligation of Fas expressed on target cells with Fas ligand (FasL) present on T-cells. Fas/FasL interaction leads to activation of intracellular proapoptotic proteins and consequently to cell death [70, 71]. Macrophages and other immune cells can induce secretion of proinflammatory cytokines like IL-1β, TNFα, IFNγ and NO (nitric oxide) leading to cytokine induced cell death [72, 73] (Fig. 8).

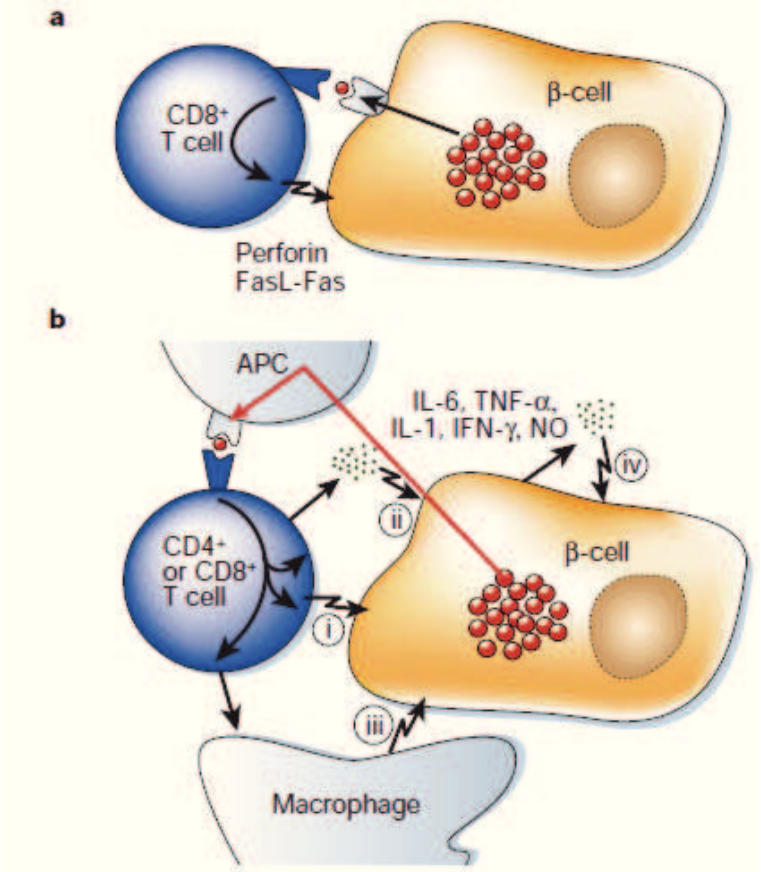

Figure 8: Possible mechanisms of β-cell death. A: $CD8^+$ T-cell directly recognizes β-cell antigens presented by MHC I on β-cells. Apoptosis can be induced via perforin or the Fas/FasL system. **B:** $CD4^+$ or $CD8^+$ T-cells recognize β-cell antigens presented by APC´s. This results inβ -cell killing possibly through (i) the Fas/FasL system, (ii) secretion of soluble death mediators like IL-6, TNFα, IL-1, IFNγ or nitric oxide (iii) activation and stimulation of macrophages and (iv) stimulation of secretion of soluble cell death mediators by β-cells [74].

The triggers which induce the initial autoimmune process leading to appearance of autoantibodies are still largely unknown. The precipitating event must include release of β-cell antigens due to β-cell death resulting in β-cell antigen presentation by APC.

2.3 Viruses in the etiology of T1DM

Accumulating evidence suggests viral infections as inducers for T1DM. Infections can lead to activation of the innate and adaptive immune system and local inflammation. *IFIH1* encoding a sensor protein for dsRNA molecules which are generated during certain RNA virus replication, has been identified as a susceptible gene for T1DM [40]. Epidemiological data imply that T1DM onset follows a seasonal pattern which strongly correlates with viral infections [75]. During the last decades many different viruses have been associated with the induction of T1DM.

2.3.1 Viruses associated with T1DM

Scientific observations connect different virus infections with T1DM. Among those, mumps virus was one of the first viruses associated with T1DM due to a case of diabetes onset after mumps infection in 1898. Infections were also connected with the appearance of autoantibodies [75] and recently mumps infection was implicated in a fulminant T1DM case [76]. However, vaccination programs against mumps had no impact on the rise of T1DM [77].
Rotaviruses were investigated due to sequence homologies between rotavirus proteins and autoreactive T-cell epitopes IA-2 and GAD, suggesting possible cross-reactivity between rotavirus and islet antigens [78]. Studies in Australian children at risk to develop T1DM showed increased frequency of islet autoantibodies soon after rotavirus infection [79]. However, this was challenged by a study in children at risk from Finland where no association between autoantibodies and rotavirus infection was observed [80]. Finland is the country with the highest T1DM incidence rate.
Approximately 20% of patients suffering from the congenital rubella syndrome develop T1DM in their life. However, it is thought that rubella infection does not contribute to autoimmunity but leads to an abnormal development in β-cell mass. Vaccination programs against rubella almost eliminated the virus, suggesting that it is not involved in recent T1DM increase [77].
Cytomegalovirus (CMV), a member of the herpes virus family, has also been associated with T1DM. The first connection was observed in a child that developed T1DM after suffering from congenital CMV infection. Studies of patients with T1DM and their healthy siblings showed a strong correlation between autoantibodies and anti-CMV antibodies [81]. However, further studies failed to correlate CMV with autoantibodies or T1DM [75].
So far, the best investigated viral environmental factors with the most strongly documented connection to T1DM are human enteroviruses (EV) [4].

2.3.1.1 Human enteroviruses

Epidemiological and serological studies have linked human enteroviruses, and among those especially CVB (group B coxsackieviruses), to the etiology of T1DM [15].

The EV genus belongs to the large family of *Picornaviridae*. Among this genus human EV are classified in different species namely human EV-A, human EV-B, human EV-C and human EV-D. The six different serotypes of CVB1-6 belong to the human EV-B species [82].

Human EV consists of non-enveloped virus particles having an icosahedral shape and a size of 25-30 nm. The viral capsid is built up by four different viral structural proteins, viral protein 1 to 4 (VP1 to VP4). VP1, VP2 and VP3 form the surface of the capsid while VP4 is located in the inner surface (Fig. 9A). Particles contain a positive-sense single strand (ss) RNA (+ssRNA) genome of about 7500 bp which is linear, not segmented and can be directly translated after infection. The genome codes for structural as well as non-structural proteins and is flanked by 5´- and 3´- noncoding regions (Fig. 9B).

Human EVs enter cells through distinct receptors resulting in endocytosis of the particle, uncoating of viral proteins and release of +ssRNA into the cytoplasm. The translation of the +ssRNA occurs in a 5´-cap independent fashion. Instead, EVs possess an internal ribosomal entry site (IRES) at the 5´end, which serves to initiate translation of the RNA to a large polyprotein. This is processed by autocatalytic cleavage resulting in different structural and non-structural proteins. The virally encoded RNA-dependent-RNA polymerase performs RNA replication, which takes place in the replication complex at the outer surface of virus-induced membrane vesicles. During this step dsRNA is formed as a replication intermediate. Generated minus sense single strand RNA (-ssRNA) serves as template for the synthesis of new +ssRNA molecules. Newly synthesized particles are probably released due to cell lysis (Fig. 9C) [83].

A

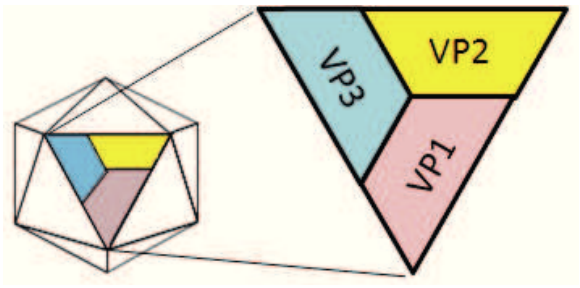

B

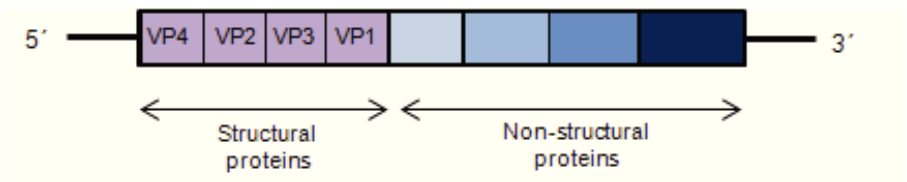

C

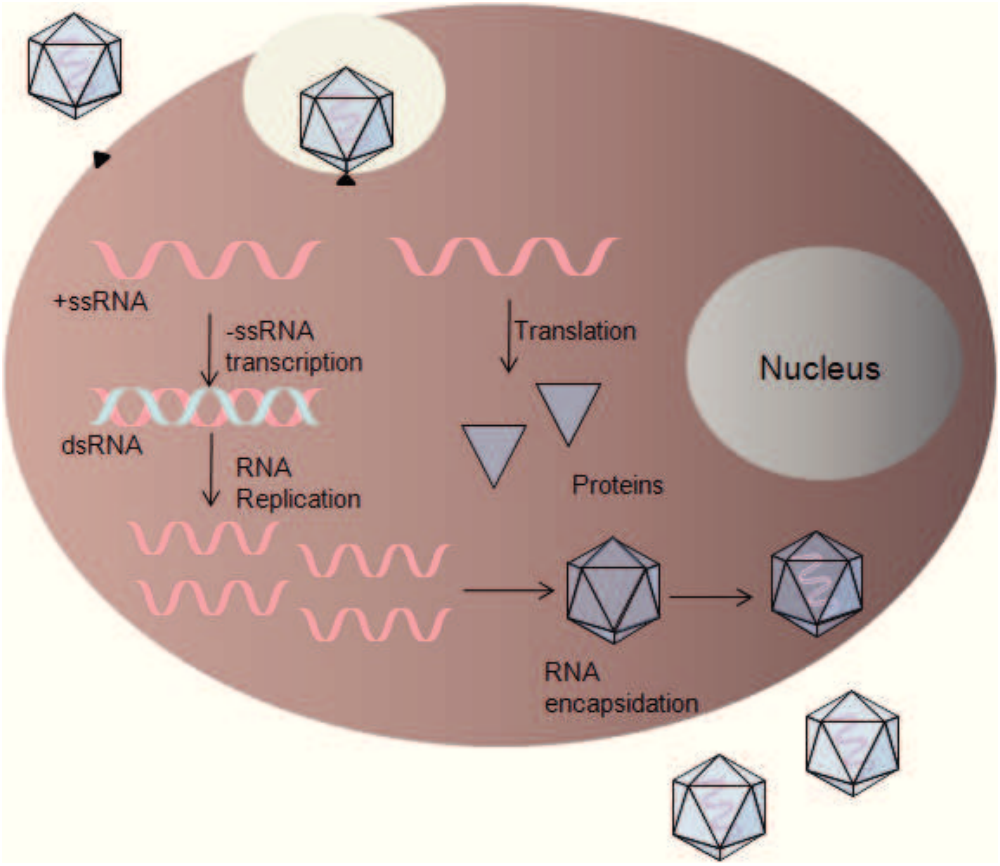

Figure 9: Enterovirus structure and replication. A: The viral capsid has an icosahedral shape and consists of four different viral structure proteins VP1 to VP4. **B** The viral genome is ssRNA which is flanked by 5´- and 3´- noncoding regions. It codes for structural and nonstructural proteins. **C** The virus enters the cell by receptor mediated endocytosis. Viral RNA is released into the cytoplasm where it can be directly translated into the polyprotein which is autocatalytically cleaved into different proteins. For viral RNA replication -ssRNA needs to be generated that serves as template for further +ssRNA replication. RNA encapsidation and assembly of viral proteins leads to formation of new viral particles that are released.

The transmission between individuals occurs through the fecal-oral route. Most infections are asymptomatic or lead to mild respiratory syndromes. In some cases virus can spread to other organs and lead to severe disease. CVB infection is the most common infectious cause for myocarditis and delayed cardiomyopathie. In addition, CVB infection can cause meningitis, encephalitis pancreatitis and T1DM [84].

2.3.2 Evidence for human enteroviruses as inducers of T1DM

2.3.2.1 Cross-sectional and prospective studies

The first evidence for a connection between EV and the etiology of T1DM arose from studies by Gamble et al. in 1969, showing higher concentrations of neutralization antibodies against CVB in the serum of recent onset patients compared to controls [85]. Ten years later CVB was strongly linked to diabetes based on the finding by Yoon et al. who isolated the CVB4 from the pancreas of a 10 year old boy who died due to ketoacedosis in 1979 [86]. Another study tested the serum of recent onset patients for the presence of antibodies against different viruses and found the most significant association with CVB [87]. Human EV RNA was detected in 64% of children at onset of diabetes compared to 4% control children using the reverse transcription-polymerase chain reaction (RT-PCR) technique. The sequences of human EVs detected in positive patients showed strong homology to CVB3 and CVB4 [88]. Other cross-sectional studies found human EV RNA in the blood of T1DM patients, again linking EVs to T1DM [89].

These studies suggest that human EV and especially CVB are associated with autoimmunity and T1DM. But it is still not clear whether infections cause autoimmunity or T1DM or whether EV infections are more frequent in T1DM patients, possibly due to weaker immune response. To answer this question, prospective studies were carried out. The advantage of such studies is that patients can be followed up for a long period of time until disease occurs. The timing between the appearance of viral infections and the development of autoantibodies can be analysed. Prospective studies in the Finnish population showed that human EVs were more frequent in children who developed diabetes later in life [90-94]. However, other prospective studies from Germany or the USA showed no association of EV infection in autoantibody positive children [95, 96]. These findings can be due to differences in methodology or population. Scientists hope to gain more knowledge from large international studies such as The Environmental Determinants of Diabetes in the Young (TEDDY) which is currently in progress [89]. Cross-sectional and prospective studies can be additionally complicated by the fact that infections can be “hit and run” effects and therefore difficult to determine. For more details about prospective studies see reference [97].

2.3.2.2 Pancreas and *in vitro* studies

In addition to cross-sectional and prospective studies, direct evidence for the association of human EV infection and diabetes comes from observations of pancreatic tissues from T1DM patients.

Positive EV VP1 immunostaining was observed in the gut mucosa, which is closely located to the pancreas, in patients with T1DM [98], showing a virus reservoir in close proximity to the pancreas. However, this could not be confirmed in a recent study [99]. Richardson et al. showed the presence of VP1 immunostaining in β-cells in more than 60% of patients with recent-onset T1DM and in only 6% of control patients. In addition, VP1 positive cells were also positive for PKR, a kinase involved in antiviral defence, indicating that virus induces signal transduction in infected β-cells [100]. This was also confirmed by Dotta et al. showing specific VP-1 colocalization in β-cells in pancreatic tissues from T1DM patients, suggesting a β-cell specific infection *in vivo*. The isolated and sequenced virus was CVB4 [101]. EVs were also detected in β-cells in cases of fulminant T1DM [102].

All CVBs use one major receptor coxsackievirus and adenovirus receptor (CAR) to enter the cell, but decay accelerating factor (DAF), also called CD55, was also reported [103, 104]. Immunostaining of post mortem pancreatic tissues from a donor positive for islet autoantibodies showed CAR expression solely colocalizing with Islet cells, while the exocrine tissue showed no CAR expression. Islets in this study were VP1 positive [105]. The restricted expression of the coxsackievirus receptor CAR can contribute to virus tropism [102, 106]. A recent meta-analysis of 33 prevalence studies in which virus infection was detected by various molecular methods like RT-PCR, in situ hybridization, or immunostaining showed a significant association between EV infection and islet autoimmunity or T1DM [107].

In summary these findings show the presence of human enteroviruses including CVB in islets from post-mortem pancreatic tissue of T1DM, patients implicating a direct role of islet CVB infection in T1DM. This indicates that virus particles can reach the pancreas and that infection occurs specifically in islets and β-cells which express the CVB receptor CAR. Although human EVs are linked to T1DM, and serotypes belonging to human EV-B species were found to be associated with T1DM and can be responsible for T1DM outcome in at least some cases, no specific causative virus serotype or strain has been identified yet.

To investigate mechanisms underlying human EV infection of human islets, *in vitro* studies were performed on isolated human islets infected with different serotypes and strains of human EVs. Most of the analyzed human EVs, especially CVB, efficiently infect and replicate in isolated human islets, reaching high titres in a period of about 24h [108]. Different serotypes of CVB induce destruction of islet cells indicated by loss of islet integrity and rounded cells detaching from the whole islets, a condition also called cytopathic effect (CPE) [109]. In addition to β-cell destruction, adequate β-cell response to glucose challenge was

impaired after infection with different human EVs [110]. The property of virus replication and subsequent islet cell destruction is not only serotype specific, it also varies in different virus stains [108].

To investigate changes in gene expression patterns after CVB infection, microarray studies were carried out. Human islets infected with CVB3, CVB4 and CVB5 showed increased expression levels of genes specifically linked to inflammation and antiviral defence. Inflammatory cytokines and chemokines like IL-1b, IL-6, IL-8, CXCL10 (IP-10), CX3CL1 (fractalkine), CXCL1 (MIP-2α), CXCL2 (MIP-2β), CXCL3 (GRO-γ), CXCL5 (ENA78), CXCL11 (I-TAC), CCL8 (MCP-2), CCL5 (RANTES), CCL3 (MIP-1α) and CCL4 (MIP-1β) were significantly increased upon infection as well as IFN-β, a strong antiviral protein; an increased secretion of some of those cytokines and chemokines was also confirmed [111-113].

Genes involved in dsRNA recognition like TLR3, RIG-I and MDA5 as well as ISGs, which act as antiviral proteins like PKR and 2´-5´-oligoadenylate synthetase 1 (OAS1) were shown to be upregulated upon infection [113]. An additional study performed by Ylipaasto et al. showed upregulation of MHC class I molecules and several other genes involved in the antigen presentation and processing. Genes involved in β-cell function like glycolysis and insulin secretion were downregulated suggesting a role in impaired insulin secretion [114].

In summary, those studies show that infection of human islets initiates an antiviral response including MHC class I, IFN and inflammatory cytokine and chemokine expression and secretion which *in vivo* can contribute to attraction of immune cells and autoimmune destruction of β-cells initiating T1DM.

2.3.3 Possible mechanisms of virus triggered T1DM

Although human EVs and especially CVB are associated with autoimmunity or T1DM, the mechanism how infections contribute to accelerate or trigger T1DM is not yet well established.

Direct infection of β-cells can result in cell lysis and a rapid decrease in β-cell mass resulting in diabetes in a non autoimmune fashion. This form of diabetes induction can probably be responsible for rare cases of fulminant T1D [75].

Another possible mechanism that has been proposed is induction of autoimmunity due to molecular mimicry which has been implicated in autoimmune stromal keratitis following HSV-1 (herpes simplex virus-1) [115]. This term describes a condition where TCR of T- and BCR of B-cells recognize an epitope from pathogens which shares similarity to self epitopes

resulting in cross-reactivity. In this case immune cells directed against a pathogen can cross-react with self antigens leading to autoimmunity. It was shown that the CVB4 non-structural protein 2C shares similarities with GAD65 [116]. It was suggested that those similarities result in cross-reactivity leading to autoimmunity and T1DM [117, 118]. However, studies performed in mice failed to establish a relationship between molecular mimicry and autoimmunity [119]. In addition, studies on autoreactive T-cell clones specific for GAD65 failed to proliferate upon viral epitope stimulation [120].

Autoimmune disease can result from “bystander activation”. This concept has also been applied as mechanism in virus induced T1DM. Damage of β-cells and release of sequestered islet antigens can induce autoantigen presentation by activated APC. Here the APC presents β-cell antigens to pre-existing autoreactive T-cells resulting in bystander activation and proliferation. This can lead further to autoimmune destruction of β-cells by autoreactive T-cells [115]. Accordingly, it has been shown in mice that phagocytosis of CVB4 infected β-cells by macrophages lead to an increase in islet antigen presentation which was associated with T1DM [121]. Release of soluble inflammatory factors can induce bystander damage of non infected cells in a T-cell independent fashion [122].

The initial damage of β-cells resulting in uptake and presentation of autoantigens by APC seems to be crucial in initiation of autoimmunity. Damage to β-cells can occur through limited β-cell infection or through inflammatory factors secreted by immune cells or β-cells themselves.

During an infection of cells the first line of defence is the induction of the innate immune system. This defence system consists of different receptors called PRR´s which bind to molecules that are normally not present in the extracellular space or in the cell called PAMPs. The engagement of PAMPs with PPRs results in the induction of an innate immune response [123]. In the case of human EV infection, specialized PRRs recognize dsRNA. This results in upregulation of chemokines and cytokines, and among those type I IFNs.

Upon EV infection *in vitro*, interferon-γ-inducible protein (IP-10) or CXCL10 is secreted from human islets [113, 124]. CXCL10 attracts CXCR3 expressing cells like activated T-cells, monocytes and natural killer cells and thus initiates immune attraction during insulitis [125]. In T1DM CXCL10 serum levels are elevated in newly diagnosed and in patients with high risk to develop the disease [126-128]. Immunohistochemical staining of pancreatic sections from 3 patients with fulminant T1DM showed presence of VP1 and β-cell specific CXCL10 expression. In addition, islets were infiltrated by $CXCR3^+$ T-cells and CXCL10 serum levels, were elevated suggesting a key role for CXCL10 in insulitis [102]. A study performed in mice showed that LCMV (lymphocytic choriomeningitis virus) infection of RIP-GP mice leads to early expression of CXCL10 in the pancreas and induction of T1DM, which was prevented by application of CXCL10 neutralizing antibodies, demonstrating a role of CXCL10 in virus

induced T1DM [129]. RIP-GP mice are transgenic mice expressing the lymphocytic choriomeningitis virus glycoprotein (LCMV-GP) under the control of the rat insulin promoter (RIP) resulting in expression of LCMV-GP in β-cells).

Immunohistochemistry analysis showed IFNα in islets of recent onset T1DM patients [101]. Type 1 IFNs are potent inducers of MHC class I molecules. In 1987, Foulis et al. showed hyperexpression of MHC class I molecules and IFNα on islets of a recently diagnosed diabetic child [130]. This has been confirmed by other studies showing hyperexpression of MHC class I in inflamed islet cells of T1DM patients. No such observations were made in healthy individuals [131]. With the expression of MHC class I molecules on β-cells the destruction by $CD8^+$ T-cells would be very efficient. A model of virus induced T1DM is still not established and needs further investigation.

The aim of this study was to investigate possible consequences of in vitro infection of islets with CVB3 and CVB4.

3 Materials and methods

3.1 Isolated human islets and cell lines

Isolated human islets were obtained through the European Consortium for Islet Transplantation (ECIT) – Islet for Basic Research program and through the Integrated Islet Distribution Program (IIDP), administered by the ABCC, and supported by NCRR, NIDDK, JDRF and the Chicago Diabetes Project. Human pancreatic sections were provided by the National Disease Research Interchange (NDRI).
Mouse pancreatic sections were kindly provided by Brigitte Glück, Universitätsklinikum Jena. Germany.
Human insulinoma CM cell line was kindly provided by Dr Paolo Pozzilli, Barts and the London School of Medicine, Queen Mary, University of London, UK.
The fetal rhesus monkey kidney cell line FRhK-4 was kindly provided by Prof. Dr. Andreas Dotzauer, Institut für Virologie, University of Bremen, Germany.

3.2 Viruses

Hepatitis A virus PI (HAV PI), Cytomegalovirus, (CMV), coxsackievirus B2 (CVB2), CVB3 (Nancy) and CVB4 (JVB) were kindly provided by Prof. Dr. Andreas Dotzauer, Institut für Virologie, University of Bremen, Germany.

3.3 Plasmids

pcDNA3-Flag Jnk1a1 (apf) (dnJNK) plasmid was purchased from addgene. The plasmid codes for the dominant negative JNK1 isotype with a FLAG-tagg. The phosphorylation motif Thr(183)-Pro-Tyr(185) was replaced with Ala-Pro-Phe, which resulted in an inactive form of JNK1.
pEGFP-N2 plasmid encodes a red-shifted variant of wild-type green fluorescent protein (GFP) which has been optimized for brighter fluorescence and higher expression in mammalian cells.

3.4 Inhibitors

The JNK inhibitor SP600125 (Sigma Aldrich, Steinheim, DE) is a reversible ATP-competitive inhibitor.

2-Aminopurin (2-AP) (Sigma Aldrich, Missouri, USA) is a highly mutagenic base analog. It inhibits the PKR kinase activity due to interaction with the ATP-binding site.

PKRi (Calbiochem, San Diego, CA) is an imidazolo-oxindole compound that acts as a potent ATP-binding site directed inhibitor of PKR.

Protease and phosphatase inhibitor (100x Halt™ Protease and Phosphatase Inhibitor Cocktail, Thermo Scientific, Bonn, Germany) was diluted to 1x in protein-lysis buffer.

3.5 Human islet and cell line culture

Obtained islets were normally approximately 95 % viable and 85 % pure, as assessed after islet isolation. After arriving isolated human islets were centrifuged and washed in CMRL-1066 (Gibco, life technologies, UK) medium. Isolated human islets were cultured on extracellular matrix coated dishes (ECM) from bovine corneal endothelial cells (Novamed, Jerusalem, Israel) in CMRL-1066 containing 5.5 mM glucose supplemented with 10% FBS (PAA Laboratories GmbH Pasching, Austria), 2 mM L-glutamine (PAA Laboratories GmbH Pasching, Austria), 100 U/ml penicillin (PAA Laboratories GmbH Pasching, Austria) and 0,1 mg/ml streptomycin (PAA Laboratories GmbH Pasching, Austria) (complete media) at 37°C and 5 % CO_2. To allow islets to attach to the surface, islets were cultured for two to three days before experiments were started.

Cell lines

CM cells were cultured on 10 cm tissue culture dishes and maintained in RPMI-1640 (PAA Laboratories GmbH, Pasching, Austria) supplemented with 10 % FBS, 2 mM L-glutamine, 25 mM Hepes (Sigma Aldrich, Steinheim, DE), 1 mM sodium pyruvate (Sigma Aldrich, Steinheim, DE), 100 U/ml penicillin and 0,1 mg/ml streptomycin (complete media) at 37°C and 5 % CO_2. Every three to five days cells were split at a ratio of 1:3. Firstly, cells were washed with PBS (140 mM NaCl, 2.7 mM KCl, 6.5 mM Na2HPO4 and 1.5 mM KH2PO4, pH of 7.4 was adjusted with HCl) followed by incubation with trypsin/EDTA (PAA Laboratories GmbH Pasching, Austria) for 3 to 5 min at RT (room temperature). Detached cells were resuspended in complete RPMI media and seeded on new tissue culture dishes. Media was changed every two days. For western blot experiments detached cells were counted using the Neubauer chamber and around 2.5 x 10^5 cells were seeded per 35mm dishes.

FRhK-4 cells were cultured on 80 cm^2 tissue culture flasks in DMEM (Dulbecco's Modified Eagle Medium) (Sigma Aldrich, Steinheim, DE) supplemented with 1% FBS, 100 U/ml penicillin and 0,1 mg/ml streptomycin at 37°C 5 % CO_2 (maintenance media). Media was changed twice weekly. Every seven to ten days cells were split at a ratio of 1:8. Therefore cells were firstly washed with trypsin/EDTA following incubation with trypsin/EDTA for 5 to 10 min at 37°C and 5 % CO_2. Detached cells were resuspended in DMEM containing 10 % FBS (growth media) and placed in new tissue culture flasks. Next day, media was changed to maintenance media which contained 1 % FBS. For titration assays FRhK-4 cells were seeded in 96-well plates and for virus stock preparations on 180 cm^2 cell culture flasks at a ratio of 1:6.

3.5.1 Islet treatment and neutralization study

Isolated human islets were treated with 1, 5, 10, 50, 100, or 500 U of recombinant IFNβ (Antigenix America, NY, USA). 24 h after treatment cells were lysed and RNA was extracted.
For the CXCL10 neutralization study isolated human islets were pre-treated for 1 h with 10 µg/ml CXCL10 antibody MDX1100 (Medarex) or with the same concentration of human IgG (Medarex) before infection. After infection islets were treated the same way with same concentrations.
Treatment of islets with 25 µg Poly I:C (Sigma Aldrich, Sigma Aldrich, Steinheim, DE) for 24 h was used to induce expression of pro-inflammatory genes.

3.6 Virus preparations

3.6.1 Production of virus stocks

To produce sufficient amount of virus to perform infection experiments, CVB3 and CVB4 virus stocks needed to be expanded. Virus stocks were generated using FRhK-cells because this cell line showed to be permissive for different picornaviruses [132]. Therefore, FRhK-4 cells were seeded on 180 cm^2 tissue culture flasks and cultured at 37°C and 5 % CO_2 until cells reached around 90 % confluency. For each condition three flasks were prepared. Cells were overlaid with 15 ml of DMEM maintenance media containing or not containing diluted virus for 2h at 37°C and 5 % CO_2. Then tissue culture flasks were filled up to 30 ml with maintenance medium and cultured for three days at 37°C and 5% CO_2. Three days post

infection (p.i.) a clear CPE (cytopathic effect) was visible in cells from infected flasks in contrast to non-infected, showing detachment of cells and lesions in the cell monolayer. When almost all cells showed a CPE, flasks were freeze and thawed three times and media containing cell debris was centrifuged for 10 min at 2000 rpm. The cleared supernatant was aliquoted and stored at -80°C. Supernatants from non-infected lysed cells represent the mock stocks which were used as control.

3.6.2 Virus purification

To omit the mock condition and contamination of virus stocks with cell proteins, virus stocks were purified using a sucrose gradient. FRhK-4 cells were grown in six 180 cm^2 flasks, three were infected with CVB3 and three with CVB4 as described. Following three freeze and thaw cycles, media containing cell lysate was centrifuged two times at 5000 rpm for 10 min and after that transferred in ultracentrifugation tubes (Beckman Polyallomer Centrifugation Tubes, CA, USA). Then tubes were ultracentrifuged (Beckman Ultracentrifuge LE-70) at 15000 rpm for 10 min and 8°C in a SW 28 rotor. 10 ml of the sucrose containing solution (40% sucrose (Sigma Aldrich, Steinheim, DE), 10 mM Tris pH 7.5 100 mM NaCl and 1 mM EDTA) was added in ultracentrifugation tubes and cleared supernatant was carefully overlaid, which resulted in a gradient. Tubes were ultracentrifuged overnight at 25000 rpm and 8°C in a SW 28 rotor. Next day both phases were discarded and purified non visible virus pellet was resuspended in 250µl PBS. To get high yield of virus the 250 µl PBS were transferred from one tube to another to concentrate virus particles.10 µl virus stock aliquots were stored at -80°C.

3.6.3 Virus titration

The $TCID_{50}$ (tissue culture infectious dose 50 %) was determined using serial dilutions of virus stocks or media supernatants containing lysates from infected islets. Firstly, Frhk-4 cells were grown in 96-well plates in 10 % FBS containing DMEM (growth media). When cells reached confluence titration study was performed. Virus stocks were serially diluted from 10^{-1} to 10^{-11} in duplicate. Per virus serotype two 96-well plates were infected. For that, 900 µl 1 % FBS containing DMEM was added in eleven tubes. In the first tube virus stock or supernatant from infected islets were diluted 1:10 and 100 µl of this dilution was transferred to the next tube and so on. The first 11 columns were infected with 100 µl of 10^{-1} to 10^{-11} virus dilutions. The 12^{th} column was left uninfected or treated with mock and was used as

control. Cells were incubated for 2h at 37°C and 5 % CO_2 to allow absorption of virus particles to cells. Then, cells were washed three times with PBS and fresh 1 % FBS containing DMEM was added to each well; subsequently cells were incubated for 7 days at 37°C and 5 % CO_2. To determine the $TCID_{50}$ each well was investigated using a light microscope; wells with a clear CPE showed lesions in the cell monolayer and were declared as positive. The $TCID_{50}$/ml was calculated using the Spearman-Kärber formula [133]. Average of $TCID_{50}$ from two plates was calculated.

3.6.4 CM cell and human islet infections

CM cells were infected with indicated viruses at MOI (multiplicity of infection) of 5. To infect CM cells with CVB3 or CVB4, virus serotypes were diluted in FBS free RPMI complete media and cells were inoculated with 750 µl for 2h at 37°C and 5% CO_2. As controls CM cells were incubated with 750 µl of diluted mock or media alone. Cells were then washed twice with PBS and overlaid with 2 ml of fresh complete RPMI media containing 10 % FBS. After certain time infections were stopped. Therefore supernatants were discarded and cells were washed thrice with PBS.

Infection of isolated human islets with CMV, HAV, CVB2, CVB3 or CVB4 were performed either on 35 mm ECM dishes or 35 mm suspension dishes dependent on which experiment was performed with a MOI of 5, 10 or 20. To infect isolated human islets with indicated viruses, those were diluted in FBS free CMRL complete media and islets were inoculated with 750 µl for 2h at 37°C and 5% CO_2. Human islets incubated with 750 µl of diluted mock or media alone were used as controls. Cells were then washed twice with PBS and overlaid with 2 ml of fresh complete CMRL media containing 10 % FBS. This time point represents the 0 h of infection.

3.6.5 Inhibition of JNK and PKR in CM cells and human islets

To investigate JNK and PKR dependent effects in CVB infected CM cells and isolated human islets JNK was inhibited using the inhibitor SP600125 and PKR using 2-AP or PKRi. Prior to infection cells and human islets were pre-incubated with 25 mM of SP600125 for 1h at 37°C and 5 % CO_2. Then media containing SP600125 was removed and cells and islets were inoculated with virus containing media supplemented with 25 mM SP600125. Infection was performed as described. After infection fresh media was added to the cells and islets, again supplemented with 25 mM SP600125.

Inhibition of PKR was performed using either 2-AP or PKRi. After infection islets were treated with 10 mM 2-AP. Inhibitor was kept on the islets throughout the whole experiment. Control islets were treated with the same volume like 2-AP only with the diluent (PBS:glacial acetic acid 200:1).
CM cells or human islets were pre-treated with different concentrations of PKRi ranging from 1 µM to 2.5 µM for 12 h at 37°C and 5 % CO_2. Transfections, infections and further culturing were carried out in the presence of the inhibitor.
This procedure made sure that the inhibitor was present in the cell supernatants throughout the whole experiment.

3.7 Protein analysis

3.7.1 Protein extraction

Proteins from CM cells and human islets were isolated and analysed by western blot. Experiments were performed with 200 islets per ECM dish or 2.5 x 10^5 CM cells per 35 mm tissue culture dish, respectively. After indicated time p.i. (post infection) supernatants were either kept for further analysis or discarded, cells were washed twice with PBS and 55 µl of RIPA buffer (50 mM Tris HCl pH 8, 150 mM NaCl, 1% NP-40, 0.5% sodium deoxycholate, 0.1% SDS) containing 1x protease and phosphatase inhibitor (100x) (Thermo Scientific, Bonn, Germany) was applied per dish to lyse the cells. Then dishes were wrapped with parafilm and frozen at -80°C. CM cells were thawed on ice and cells were scraped off.
Dishes with isolated human islets were freeze and thawed thrice. During the last freeze and thaw cycle dishes were thawed on ice and islets were scraped off. Lysis buffer containing proteins and islet debris was transferred to tubes. To obtain higher protein yields tubes were vortexed for 2 to 3 min following centrifugation at 12000 rpm for 15 min at 4°C. Protein containing supernatants were collected and transferred to new tubes. Cell debris pellets were discarded. To prevent degradation protein samples were always kept on ice.

3.7.2 BCA Assay for quantification of proteins

Concentration of proteins was quantified using the BCA (bicinchoninic acid assay) assay (Pierce, Thermo Scientific, Rockford, IL USA) according to manufacturers' instructions. 25 µl of 1:5 diluted protein samples (dilution was performed in RIPA buffer supplemented with protease and phosphatase inhibitor) and 25 µl of standards were added in wells of a 96-well plate. Sufficient amount of BCA reagent was prepared by dilution of 1 part of reagent A in 50 parts of reagent B. 200 µl of reagent was added to protein or standard samples per well. Plate was covered with aluminium foil and incubated at 37°C for 30 min in the dark. In proportion to protein concentration the colour is changing from green to purple. After incubation measurement of the absorption spectra at 570 nm was assessed using a photometer (Multiskan Ascent, Thermo Scientific). Protein amounts were calculated by comparing absorption spectra from sample and standards with known protein concentrations. RIPA buffer with proteinase and phosphatase inhibitor alone was representing the blank.

3.7.3 Co-Immunoprecipitation (Co-IP)

For each condition three ECM dishes with around 250 islets were cultured. Islets were infected as described for 24 h. Then Islets were washed twice with PBS followed by addition of 1 ml 1 % formaldehyde (37 %, Merck, Darmstadt, Germany) (diluted in PBS) to fix the protein-RNA interactions. Islets were incubated for 30 min on a shaker. The formaldehyde solution was discarded and 2 mM glycine (Riedel de Haen, Germany) was added to the dishes which were incubated for 15 min on a shaker. Islets were washed twice and around 150 µl RIPA buffer was added to each dish. Dishes were freeze and thawed three times and proteins were extracted and concentration was determined as described above. To pre-clear proteins, around 250 µg of proteins in 500 µl of RIPA buffer were incubated with 2 µg of an antibody of the same species and isotype as the IP antibody for 30 min with gentle agitation at 4°C. In the mean time protein A agarose beads (protein A Agarose, Fast Flow, Millipore, California, USA) were washed with RIPA buffer. 70 µl of slurry beads were added to the proteins, followed by incubation with gentle rotation for 30 min at 4°C. The beads were pelleted and discarded. Aliquots of around 30 µl were kept at -80°C (input fraction) and pre-cleared lysates were mixed with 2 µg K1 antibody (English and Scientific Consulting Bt) and incubated overnight at 4°C. The K1 antibody binds dsRNA, and it has been used successfully in a previous study [134].

70 µl protein A agarose beads were added to the lysates followed by incubation for 4 - 6 h with gentle rotation. Then the beads were spun down and supernatants (output fraction) were

kept for further analysis. Beads were three times washed with RIPA buffer. After the last washing beads (IP-fraction) were mixed with 50 µl 2x loading buffer (1:2 diluted with RIPA buffer) (NuPAGE® LDS Sample Buffer (4x), Invitrogen, Darmstadt, Germany) and 4 µl reducing agent (1:7 dilution of β-mercaptoethanol (Merck, Darmstadt, Germany) in H_2O). Before western blot analysis IP-fractions were incubated 45 min at 95°C, beads were spun down and around 30 µl of supernatants were applied in the western blot. 15 µl of input and output fractions were mixed with 7,5 µl loading buffer (4x), 2 µl reducing agent and 5,5 µl RIPA buffer. Tubes were incubated 10 min at 95°C before western blot analysis.

3.7.4 Western blot

For western blot studies 200 islets were cultured per ECM dish. After protein extraction and determination of concentrations 15-30 µg proteins were analyzed. Equal amount of proteins were mixed with 1X protein loading buffer (NuPAGE® LDS Sample Buffer (4x), Invitrogen, Darmstadt, Germany) 2 µl of reducing reagent (2 µl / 50 µl reaction volume) and ddH_2O. Samples were heated up for 10 min at 95°C and then chilled on ice. Proteins were applied on precast gels (NuPAGE® 4 %-12 % Bis-Tris, Invitrogen Darmstadt, Germany) and separated according to their kDa size. Protein separation was performed in running buffer (NuPAGE® MES SDS Running Buffer, Invitrogen, Darmstadt, Germany) supplemented with 0.1 % antioxidant (NuPAGE® Antioxidant, Invitrogen, Darmstadt, Germany). Following separation proteins were blotted on polyvinylidene flouride-membrane (PVDF) (Roti, Karlsruhe, Germany). Therefore, membranes were incubated for 1 min in methanol and for 30 sec in H_2O. Proteins were blotted in transfer buffer (500 mM Bis-Tris, 20.5 mM EDTA, 500 mM Bicine, 20 % v/v methanol 0,1 % antioxidant). Membranes were blocked with 2.5 % dry milk (Cell Signaling, Frankfurt Main, Germany) and 2.5 % bovine serum albumine (BSA) (Sigma-Aldrich, Steinheim, DE) in TBS-T (50mM Tris, 150 mM NaCl pH 7.6 with HCl, 0.1 % Tween-20 (Sigma- Aldrich). Following the blocking step membranes were incubated over night at 4°C with primary antibodies diluted in TBS-T containing 5 % BSA.

Following are the different primary antibodies used and the respective dilutions along with the product information.

Cl. caspase 3	1:1000	Cell Signalling # 9664
PARP	1:1000	Cell signalling # 9542
VP1	1.1000	Dako clone 5-D8/1
β-actin	1:1000	Cell signalling # 4967
pPKR	1:1000	Abcam E120
PKR	1:1000	Cell signalling # 3072

RIG-I	1:1000	Cell signalling # 4200
MDA5	1:1000	Cell signalling #5321
peIF2α	1:1000	Cell signalling # 9721
pJNK	1:1000	Cell signalling # 9251
JNK	1:1000	Cell signalling # 9252
p c-Jun	1:1000	Cell signalling # 9261
Tubulin	1:1000	Cell signalling # 2146
CXCL10	1:5000	RnD systems BAF266

Membranes were washed three times for five minutes in TBS-T. Secondary antibodies HRP (horse radish peroxidase) conjugated goat anti mouse IgG (Jackson Immuno Research, USA) was diluted 1:3000 and HRP-conjugated goat ant rabbit IgG (Jackson Immuno Research, USA) 1:10000 in TBS-T containing 2.5 % dry milk and membranes were incubated for 1h at RT. Then membranes were washed four times in TBS-T on a shaker, each time for 10 min. Peroxidase was activated by applying HRP substrate solution (Immobilon Western, Millipore, Schwalbach, Germany). Protein bands were visualized using UVP BioSpectrum AC Imaging System (UVP, Upland, Canada).

3.7.5 Glucose Stimulated Insulin Secretion (GSIS)

Infected human islets were tested for their ability to secrete insulin upon acute glucose challenge. 24, 48 and 72h p.i., islets were washed and pre-incubated for 30 min in KRB (Krebs-Ringer bicarbonate buffer) (115 mM NaCl, 5 mM KCl, 2.5 mM $CaCl_2$, 1.2 mM KH_2PO_4, 1,2 mM $MgSo_4$, 1M Hepes, 5mM $NaHCO_3$, 0,5 % BSA) containing 2.8 mM glucose at 37°C. KRB was replaced with 1 ml of fresh KRB containing 2.8 mM glucose and islets were incubated for 1h at 37°C. Then supernatant was collected (basal insulin secretion) and replaced with 1 ml of KRB containing 16.7 mM glucose and incubated again for 1h at 37°C. Supernatant was collected (stimulated insulin secretion). To avoid contamination with cells, tubes containing basal and stimulated insulin were centrifuged at 2000 rpm for 5 min and supernatants were transferred to new tubes and kept at -20°C. The insulin secretion stimulation index was calculated by dividing the amount of stimulated insulin by the amount of insulin produced at basal conditions.

3.7.6 Human insulin and CXCL10 ELISA

Human Insulin ELISA

Insulin secreted under basal and stimulated conditions was analysed using the human insulin enzyme-linked immunosorbent assay (ELISA) (ALPCO Diagnostics, Salem, NH) according to manufacturers' instructions. Concentration was determined photometrically at 450 nm (Molecular Devices, Emax precision microplate reader).

Human CXCL10 ELISA

Islet culture supernatants were collected and frozen at -20°C until measurement. Human CXCL10 (ELISA) (DB OptEIA^{TM} Set human IP-10) was obtained from BD Biosciences (BD Biosciences, San Diego, CA, USA) and performed according to manufacturers' instructions. 96-well ELISA-plates (BD Biosciences, Heidelbach, Germany) were pre-coated with 100 µl per well of capture anti-human IP-10 antibody diluted 1:250 in coating buffer (0.1 M sodium carbonate, pH 9.5; 7.13 g NaHCO3, 1.59 g Na2CO3; pH to 9.5 with 10 N NaOH) (BD Biosciences). Concentration was determined photometrically at 450 nm (Molecular Devices, Emax precision microplate reader).

3.8 RNA analysis

3.8.1 RNA isolation

For RNA analysis 100 islets were cultured on 35 mm ECM dishes. RNA extraction was performed using peqGOLD TriFast (peqlab, Erlangen, Germany). Islets were lysed with 1 ml of peqGOLD reagent and either kept at -80°C or further processed. Reagent containing lysate was transferred to tubes and mixed with 200 µl chloroform. Then Tubes were shaken for 15 sec and incubated for 2 – 3 min at RT. Then Tubes were centrifuged at 12000 rpm for 15 min at 4°C. The upper aqueous phase was collected and mixed with 10 µg glycogen (Fermentas). 500 µl of isopropanol were added in each tube, followed by centrifugation at 12000 rpm for 30 min at 4°C. Isopropanol was discarded and RNA pellets were washed with 1 ml of Ethanol. For washing, pellet was centrifuged again at 12000 rpm for 30 min at 4°C. RNA pellet was dried and resuspendet in 10 µl DEPC-H_2O.

RNA concentration was determined using the spectrophotometer at 260 nm (NanoDrop ND1000).

3.8.2 RT-reaction

Around 500 ng RNA was reverse transcribed using the RevertAid^{TM} Reverse Transcriptase and reaction buffer (Fermentas). Before this, RNA was treated with 1 U DNase I (Fermentas) for 1,5 h at 37°C in a reaction volume of 10 µl. Reaction was stopped by adding 1 µl EDTA (Fermentas) followed by the incubation for 15 min at 65°C. RNA was mixed with random hexamer primers (Fermentas Life Sciences) and incubated for 5 min at 65°C. The tubes were chilled on ice and 5x reaction buffer (Fermentas Life Sciences), 10 mM dNTPs (each) (Thermo Scientific) and 100 U of Moloney Murine Leukemia virus (*M-MuLV*) reverse transcriptase (Fermentas) were added. Reactions were incubated for 10 min at 25°C followed by 60 min at 42°C and 10 min at 70°C in the PCR cycler (eppendorf Mastercycler gradient).
For each sample a negative control was included, where the reverse transcriptase was exchanged with DEPC-H_2O (-RT samples).

3.8.3 Polymerase chain reaction (PCR)

Before qPCR analysis, cDNA and –RT samples were checked in a regular PCR. A 10 µl reaction contained 1x buffer (DreamTaq™ 10x Buffer, Thermo Scientific) 1 U polymerase (DreamTaq™ Polymerase, Thermo Scientific) 200 µM dNTPs (each), 500 pM tubulin primers (each), 25ng cDNA and ddH_2O. PCR was performed in a PCR cycler with a primer annealing temperature at 60°C.
PCR products were run in a 1 % agarose gel (LE Agarose, Biozym, Oldendorf, Germany) and visualized with DNA stain G (Serva, Heidelberg, Germany).

3.8.4 Real-Time PCR (qPCR)

qPCR was performed using Sybr Green (Power Sybr Green, Applied Biosystems) and TaqMan primer probes. For sybr Green, each reaction was performed in a volume of 10 µl and contained 10 ng cDNA, 5 µl Sybr Green, 0.25 µM primers (each) and ddH_2O. All primers annealed at 60°C and qPCR was run for 40 cycles.
Following are the sequences of the primers used in this study:
TLR3 fw 5´ AGCCTTCAACGACTGATGCT 3´ rev 5´ TTTCCAGAGCCGTGCTAAGT 3´
MDA5 fw 5´ ACCAAATACAGGAGCCATGC 3´ rev 5´ RGCGATTTCCTTCTTTTGCAG 3´
RIG-I fw 5´ FAGAGCACTTGTGGACGCTTT 3´ rev 5´ RTGCAATGTCAATGCCTTCAT 3´

PKR fw 5´ FACGCTTTGGGGCTAATTCTT 3´ rev 5´ RTTCTCTGGGCTTTTCTTCCA 3´
18s fw 5´ FAAACGGCTACCACATCCAAG 3´ rev 5´ RCCTCCAATGGATCCTCGTTA 3´
Cyclophillin fw 5´ F TTCATCTGCACTGCCAAGAC 3´
rev 5´ TCGAGTTGTCCACAGTCAGC 3´

For TaqMan probes, reactions were also carried out in 10 µl using 1x PCR master mix (TaqMan Fast Universal PCR Master mix (2x), Applied Biosystems), 1x TaqMan primer probes (TaqMan Assay (20x), Applied Biosystems) 10 ng cDNA and ddH_2O.
Following TaqMan Assays were used in this study:
CXCL10 Hs00171042_m1
IFNβ Hs02621180_s1
IL-6 Hs99999032_m1
IL-1β Hs00174103_m1
TNFα Hs99999043_m1
Cyclophillin Hs99999904_m1
qPCR was performed using the StepOnePlus (Applied Biosystems) qPCR machine. Results were analysed with the StepOnePlus software.

3.8.5 RNA-Immunoprecipitation (RIP)

For each condition three ECM dishes with around 250 islets were cultured. Islets were infected as described for 24 h and 48 h. Human islets were washed once with PBS at room temperature and fixed with 1% formaldehyde in PBS at RT for 10 min. Cells were quickly rinsed twice in ice-cold PBS and 100µl of lysis buffer A was added (100mM KCl, 5mM MgCl2, 10mM Hepes pH 7, 0.5% NP40, 1mM DTT, 100U/ml RnaseOUT (Invitrogen), 400 µM vanadyl ribonucleoside complexes VRC (New England Biolab), Protease/phosphatase inhibitor cocktail). The samples were freeze and thawed followed by pipetting and vortexing to completely lyse the cells. 2 mg of total protein was used for RNA-IP. Protein-A Sepharose beads were pre-swelled in buffer B (50mM Tris-HCl pH7.4, 150mM NaCl, 1mM MgCl2, 0.05% NP-40) supplemented with 5 % BSA to a final ration of 1:5 for 2h at 4°C before use. 2 µg TLR3 antibodies (IMG-315A, Imgenex, USA) or 2 µg TLR7 antibodies (IMG-581A, Imgenex, USA) were added to the slurry beads and incubated overnight tumbling end over end at 4°C. The following day the antibody-coated beads were washed with 1ml of ice-cold buffer B for 5 times. After the final wash the beads were resuspended in 850 µl of ice-cold buffer B supplemented with 200 U RNase inhibitor, 400 µM VRC, 1,2 mM DTT and 20 mM EDTA. 100µl were removed as imput fraction. RNA-protein complexes were incubated with

beads-antibody for 5h at 4°C tumbling end over end. After incubation the supernatant was saved as output fraction and the beads washed 5 times with 1ml of ice-cold buffer B supplemented with 1% SDS to reduce background. The beads were resuspended in 100µl of buffer B supplemented with 30ug of Proteinase K and the mixture incubated for 60 min at 55°C with occasional vortexing. RNA was isolated using PeqGold reagent following manufacturer instructions. RNA was reverse transcribed and analysed by qPCR using CVB primes. Values were expressed as arbitrary units.

3.9 Immunocyto- and histochemistry

TUNEL Assay and immunocytochemistry

For TUNEL assay usually 30 islets were plated per ECM dish. Cells were fixed for 30 min at room temperature (RT) with 4 % paraformaldehyde following cell permeabilisation with 0,5 % Triton X-100 for 4 min at RT and blocking with 3 % BSA for 1 h. Cell death was detected using the terminal deoxynucleotidyl transferase-mediated dUTP nick-end labeling (TUNEL) technique according to the manufacturer's instructions (In situ cell death detection kit, Roche, Mannheim, Germany). Islets were incubated overnight with primary antibodies guinea pig anti-insulin (Dako) diluted 1:100 and mouse anti-VP1 (Dako clone 5-D8/1) diluted 1:500. Islets were washed thrice with PBS and incubated with secondary antibodies Cy3-conjugated donkey anti guinea pig IgG (Jackson ImmunoResearch Laboratories, West Grove, PA) and VP1 was visualized using the biotin HRP-conjugated streptavidin system (Histostain®, Invitrogen, USA) according to manufacturer's instructions, following AEC chromogen incubation. Islets were mounted using mounting media containing DAPI (Vector Laboratories, Burlingame, CA).

Immunohistochemistry

Islets were washed with PBS and fixed with Bouin´s fixate (Sigma Aldrich) for 15 min at RT and added to melted 2 % agarose. Islets were spun down and dehydrated in ethanol (70 %, 80 %, 95 %, 100 %, each for 2h and toluene for 4 h). Agarose pellets were embedded in paraffin and microtome sections were cut (4µm). Tissue sections were deparaffinized, rehydrated (toluene, 100 %, 95%, 70 % ethanol and H_2O) and antigen retrieval was performed in low pH antigen unmasking solution (Vector Laboratories, Burlingame, CA) using a microwave. Slides were microwaved three times for 5 min. After permeabilisation in 0,4% Triton X-100 in PBS and blocking in 3% BSA sections were incubated with primary

antibodies over night, biotinylated anti-human CXCL10 (RnD, Minneapolis, USA) diluted 1:200, mouse anti-VP1 diluted 1:500, donkey anti-glucagon (Dako) 1:100, guinea pig anti-insulin 1:100. After incubation with primary antibodies, islets were washed thrice with PBS and incubated for 1 h at RT with 1:100 diluted secondary antibodies, Cy3-conjugated donkey anti guinea pig IgG, AMCA-conjugated donkey anti guinea pig IgG, Cy3-conjugated donkey anti mouse IgG, FITC-conjugated donkey anti rabbit IgG and FITC-conjugated donkey anti guinea pig IgG (all Vector Laboratories, Burlingame, CA). CXCL10 was visualized using the biotin HRP-conjugated streptavidin system (Histostain®, Invitrogen, USA) according to manufacturer's instructions, following AEC chromogen incubation.

For TUNEL staining, slides were not treated with antigen retrieval solution and tissue was not permeabilized. Instead sections were treated with protease K (Roche, Mannheim, Germany) diluted 1:1000 in 10 mM Tris-HCl pH was adjusted to 7.4.

Cryosections were covered with PBS and blocked for 30 min with 3% BSA at RT. Due to optimizations, tissue sections were not fixed. Sections were incubated over night with mouse anti-TLR3 (Imgenex, IMG315-A, San Diego, USA), rabbit anti-TLR7 (Imgenex, IMG-581A, San Diego, USA), guinea pig anti-insulin and donkey anti-glucagon antibodies. All antibodies were diluted 1:100. After incubation with primary antibodies, islets were washed thrice with PBS and incubated for 1 h at RT with secondary antibodies, Cy3-conjugated donkey anti-mouse IgG, FITC-conjugated donkey anti-guinea pig IgG, Cy3-conjugated donkey anti rabbit IgG and followed by secondary antibody incubation and TLR7 was visualised using biotin HRP-conjugated streptavidin system (Histostain®, Invitrogen, USA) according to manufacturer's instructions, following AEC chromogen incubation.

Sections were mounted in mounting media containing DAPI or glycerol gelatin (Sigma, Steinheim, Germany).

3.10 Human islet transfection

Around 200 islets per dish were dispersed with accutase (PAA Laboratories GmbHPasching, Austria) for 5 min at 37°C to improve the access of the transfection mixes to islet cells. Dispersion was aborted by addition of fresh complete media. Islets were cultured for two days and experiments were carried out. TLR3 knockdown in human islets was performed using the siTLR3 (ON-TARGETplus SMARTpool, Dharmacon). The siRNA is a mix of ON-TARGETplus siRNAs directed against the following sequences: GAACUAAAGAUCAUCGAUU, CAGCAUCUGUCUUUAAUAA, AGACCAAUCUCUCUCCAAUUU, UCACGCAAUUGGAAGAUUA. Before transfection, islets

were incubated for 1 h in an optimized Ca^{2+}-KRH transfection medium (KCl 4.74 mM, KH_2PO_4 1.19 mM, $MgCl_26H_2O$ 1.19 mM, NaCl 119 mM, $CaCl_2$ 2.54 mM, $NaHCO_3$ 25 mM, HEPES 10 mM) at 37°C. Transfection was carried out with 100 nM siTLR3 or siScr or with DNA plasmids dnJNK and GFP. For gene silencing, 100 pM siRNA was mixed with 5 µl of transfection reagent, for overexpression studies DNA was mixed at a ratio 2,5:1 and 800 ng Poly I:C were mixed with 5µl lipofectamine (Lipofectamine2000, Invitrogen). Mixes were incubated at RT for 45 min and added to the islets. Transfection was carried out in half of the volume. After 6 h 2x media containing 20 % FBS was added to the dishes.

4 Results

4.1 Establishment of CVB infection in isolated human islets

In the beginning of this study, infection of isolated human islets was established and confirmed with the published data. For this purpose, isolated human islets were infected as indicated and different experiments were carried out to investigate the properties of the infection. I focused on virus effects on human islets including proof of infection, destruction of islet cells, replication of viral particles and effects on function and cell specific actions. The infection was studied in a time frame of 72 h.

4.1.1 CVB3 and CVB4 infect human islet cells and induce cell death

Isolated human islets were infected *in vitro* with the 3 different CVB serotypes- 2, 3 or 4, HAV (Hepatitis A virus) another representative of the *Picornaviridae* or CMV (Cytomegalovirus) belonging to the *Herpesviridae.* 72 h after infection the destruction of islet cells was investigated using the TUNEL technique. TUNEL and insulin double positive cells were quantified and results represented as percentage of TUNEL positive β-cells.

Infection of human islets with CVB2, 3 or 4 resulted in 8-fold, 6-fold and 7-fold increase in apoptosis, respectively, as compared to mock treatment, whereas CMV and HAV had no effect on apoptosis (Fig. 10A).

CMV and HAV were excluded from further experiments. Due to the frequent association of CVB3 and CVB4 serotypes in virus induced diabetes, further experiments were performed with those serotypes; CVB2 was excluded.

TUNEL staining detects DNA fragmentation which occurs during apoptosis. Due to the fact that TUNEL was shown to label inappropriate DNA strand breaks during necrosis, western blot analysis was performed to confirm apoptosis [135]. Protein analysis showed cleavage of pro-apoptotic proteins PARP and caspase 3 during CVB3 and CVB4 infections of human islets 48 h p.i., in contrast to non-infected control islets. VP1 bands confirmed CVB3 and CVB4 infections, and β-actin bands were used as protein loading controls (Fig. 10B).

To determine whether infected cells were mainly apoptotic, triple immunostaining of VP1, insulin and TUNEL was performed. CVB3 and CVB4 infected islets showed TUNEL specific black staining of nuclei accompanied with red stained VP1 positive cells indicating apoptosis in infected islet. In contrast, media and mock treated islets showed no signs of infection or cell death (Fig. 10C).

All further studies were performed using purified virus stocks; hence mock treatment was discontinued. As control, media treated islets were included in all further experiments. Infection of islets with purified CVB3 or CVB4 had the same effect on apoptosis as non-purified virus stocks and led to 4- and 3-fold induction of apoptosis, respectively as compared to control (*p< 0.05) (Fig. 10D).

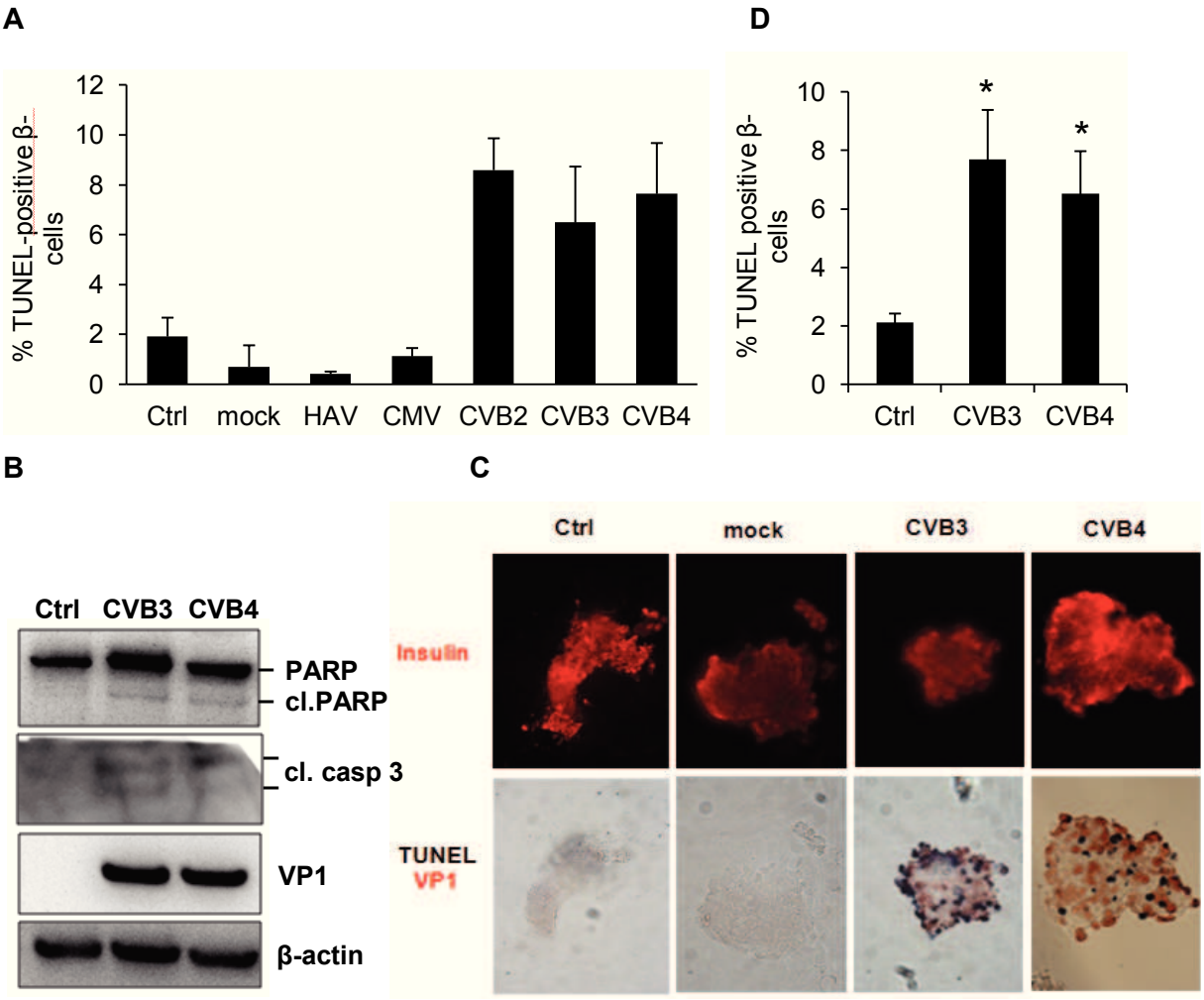

Figure 10: CVB3 and CVB4 induce cell death in isolated human islets. A: Isolated human islets were cultured for two days followed by infection with HAV, CMV, CVB2, CVB3 or CVB4 (MOI of 10). Media and mock treatment were included as controls. 72 h p.i. islets were fixed and double stained with

TUNEL and insulin. TUNEL positive black stained nuclei in insulin positive cells were quantified and expressed as percentage of total insulin positive cells (error bars represent ± SD from triplicate). **B:** Western blot analysis of proteins from control and CVB3 or CVB4 infected islets (MOI of 5) isolated 48 h after infection showed cleavage of PARP and caspase 3. VP1 bands confirmed infection and β-actin was used as control for equal protein input. **C:** Isolated human islets infected with CVB3 or CVB4 (MOI of 5), or treated with media or mock were fixed 48 h p.i. and triple immunostaining was performed. Upper panel shows fluorescent insulin staining in red and lower panel black stained TUNEL positive nuclei surrounded by red stained VP1 positive cells in bright field (magnification: x 400). **D:** In order to ensure that purified virus stocks had the same effects on apoptosis as not purified stocks, human islets were infected (MOI of 5) and TUNEL assay performed. TUNEL positive black stained nuclei in insulin positive cells were quantified and expressed as percentage of total insulin positive cells (error bars represent ± SEM from five independent experiments from 5 different donors; *p< 0,05).

4.1.2 CVB3 and CVB4 reach high titers in isolated human islets

To investigate if infection of isolated human islets leads to progeny of viruses, titration assays of infected islets were carried out. Supernatants and lysates from CVB3 or CVB4 infected islets obtained at 0 h, 24 h, 48 h and 72 h were titrated using FRhK-4-cells. CVB3 and CVB4 replicated regularly in human islets and the maximum of titre was reached 24 h p.i. (Fig. 11).
The time point 0 h indicated bound viral particles which were not washed off. Titres stayed constant over the observed time. To investigate if virus particles were released during infection, supernatants were titrated, showing the same pattern of virus replication (data not shown).

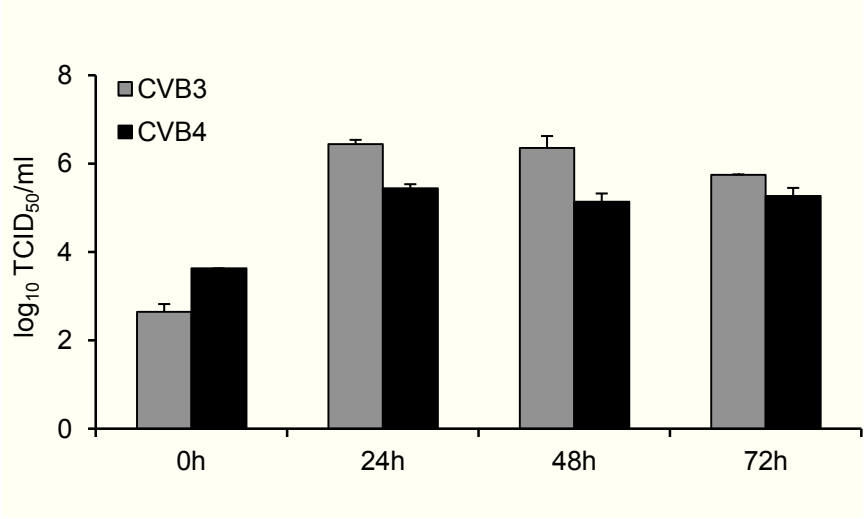

Figure 11: CVB3 and CVB4 replicate in isolated human islets. Human islets infected with CVB3 or CVB4 (MOI of 5) were lysed at 0 h, 24 h, 48 h and 72 h p.i. and cell debris were pelleted. Serial dilutions of cleared supernatants were titrated on FRhK-4-cells. Results show the $TCID_{50}$/ml in logarithmic

manner of one representative result out of three from three different donors (error bars indicate ± SD from technical replicate).

4.1.3 CVB3 and CVB4 impair β-cell function

The results achieved showed that infection of human islets *in vitro* led to apoptosis of β-cells and progeny of virus. The next question was whether CVB3 and CVB4 infections have an impact on β-cell function. To investigate the CVB3 and CVB4 effects on β-cell function, glucose stimulated insulin secretion (GSIS) was performed. Isolated human islets were infected with CVB3 or CVB4 *in vitro* for 24 h and 48 h, respectively, and at indicated time points, islets were challenged for 1 h with a low glucose concentration of 2.8 mM, which corresponds to the basal insulin secretion. Then the islets were challenged for an additional hour with a high glucose concentration of 16.7 mM, corresponding to the stimulated insulin secretion. Secreted insulin amounts were measured and stimulatory indices calculated based on the ratio of stimulated to basal insulin levels.
24 h p.i. GSIS was unaffected by infections. CVB3 as well as CVB4 significantly reduced stimulatory indices from 5.7 ± 1.17 in the control to 3.2 ± 0.76 and 2.7 ± 0.21 respectively 48 h p.i. (*p< 0.05) (Fig. 12).

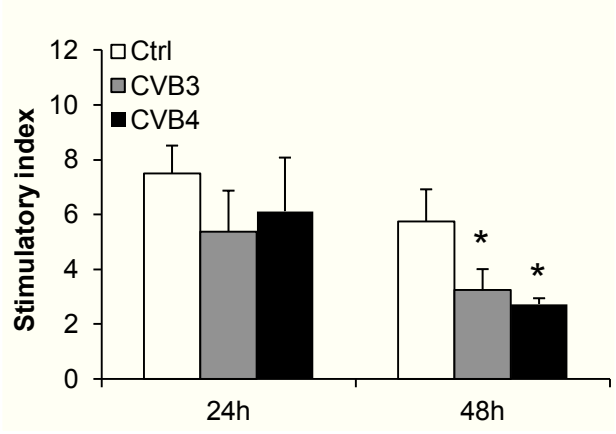

Figure 12: CVB3 and CVB4 infections impair glucose stimulated insulin secretion in human islets. Isolated human islets were infected with CVB3 or CVB4 (MOI of 5) and GSIS was performed 24 h and 48 h p.i. Islets were incubated with 2.8 mM followed by 16.7 mM glucose concentrations for 1 h, respectively. Secreted insulin was measured using insulin ELISA. Stimulatory indices were calculated by dividing stimulated insulin amount by basal insulin amount (error bars indicate ± SED from three independent experiments from three different donors, *p< 0.05 compared to control at 48 h).

4.1.4 CVB3 infect mainly β-cells while CVB4 infect β- and a certain portion of α-cells

To investigate if CVB3 or CVB4 infect all islet cells or show any tropism towards a specific islet cell type, immunostaining was performed. Microtome sections from paraffin embedded islets infected with CVB3 or CVB4 for 24 h, 48 h and 72 h were prepared. Triple immunostaining was performed for insulin glucagon and VP1. Sections were microscopically analyzed and colocalization of VP1 with either insulin or glucagon was quantified. Results are expressed as percentage of VP1 positive α- or β-cells, respectively.

CVB3 VP1 staining was observed in 60.6% ± 9.6% and CVB4 in 53.5% ± 4.9% of β-cells 24 h p.i. The later time points displayed similar high values, which decreased gradually. CVB3 infected only 3.3% ± 0.8% and 2.5% ± 0.3% of α-cells at 48 h and 72 h p.i., in contrast to CVB4, which showed significantly higher VP1 positive α-cell values of 12.1% ± 4.0% and 8.1% ± 2.8% at 48 h and 72 h p.i. (*p< 0,05) (Fig. 13A).

Results showed that both virus serotypes infected α-, but mainly β-cells. Immunofluorescence staining showed no VP1 positive cells in control islets but strong colocalization of CVB3 VP1 with insulin positive cells and of CVB4 VP1 with insulin and glucagon positive cells (Fig. 13B).

A

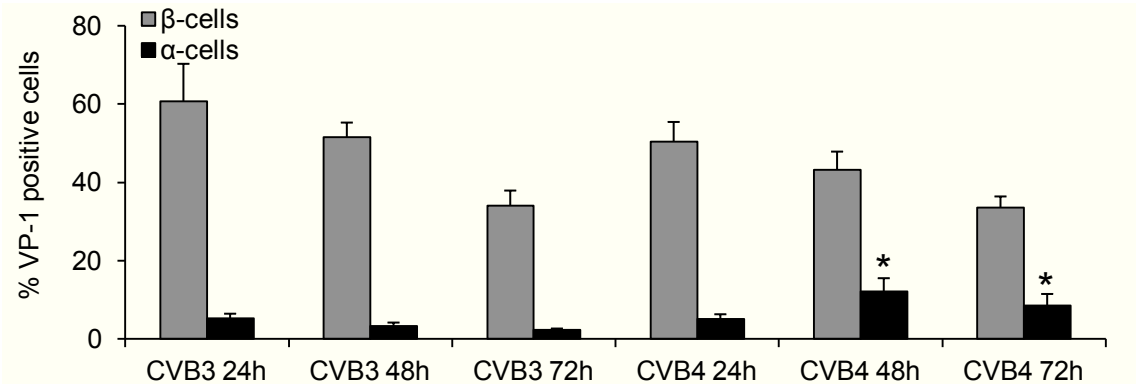

B

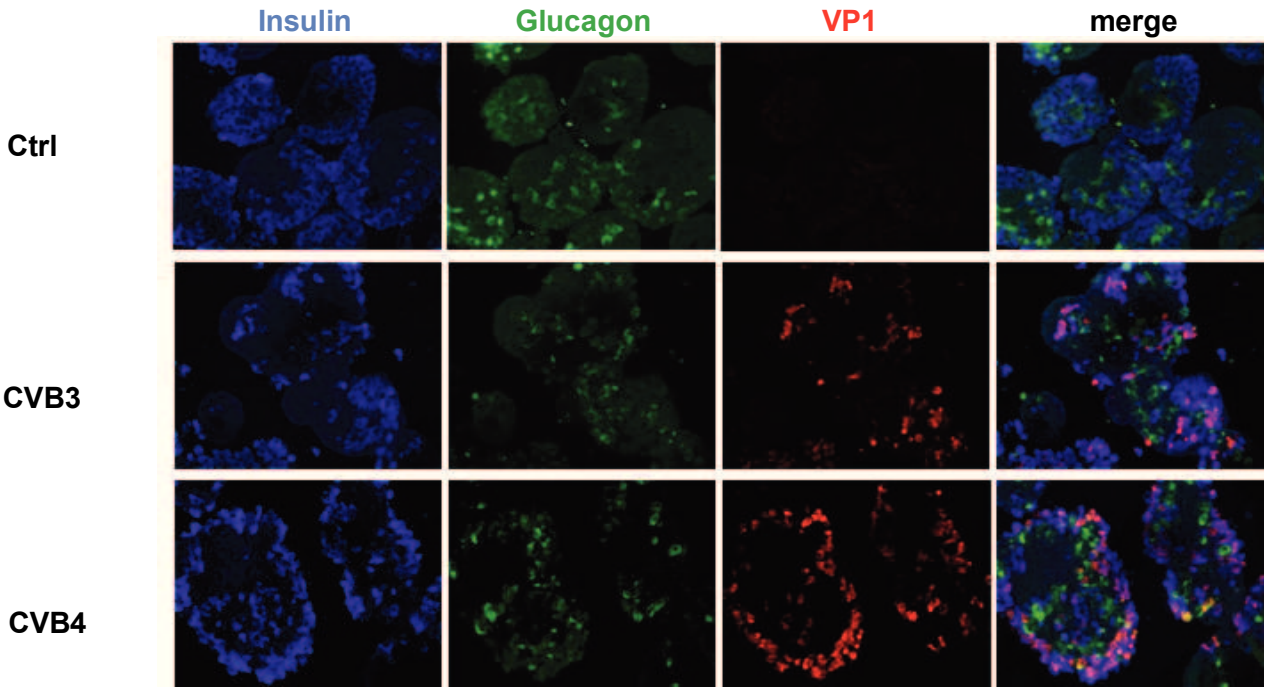

Figure 13: CVB3 and CVB4 infect mainly β-cells and CVB4 additionally a certain portion of α-cells. A: Isolated human islets were infected with CVB3 or CVB4 (MOI of 5) for 24 h, 48 h and 72 h. Islets were fixed, pelleted and paraffin embedded. Pellets were microtome sectioned and stained for insulin, glucagon and VP1. Colocalization of VP1 with either insulin or glucagon was quantified; results are expressed as percentage of VP1 positive α- or β-cells (error bars indicate ± SEM from three independent experiments from three different donors, $^{*}p< 0.05$). **B:** Immunofluorescence analysis of paraffin embedded sections from islets infected with CVB3 or CVB4 (MOI or 5) demonstrate individual staining for insulin in blue, glucagon in green and VP1 in red 48 h p.i. Merge images show the colocalization of insulin and VP1 indicated by purple colour in islets infected with CVB3; and insulin, glucagon and VP1 indicated by purple and yellow staining in islets infected with CVB4 (magnification x 400).

4.1.5 CVB3 and CVB4 induce β-cell death

As CVB3 and CVB4 mainly infected β-cells, it was investigated whether cell death was restricted to β-cells or if it occurred in all islet cell types. Paraffin embedded sections from islets infected with CVB3 or CVB4 were analyzed for cell specific apoptosis by TUNEL assay. Sections were stained for insulin or glucagon and colocalization with TUNEL positive nuclei was quantified and expressed as percentage of total amount of α- or β-cells. Both virus serotypes increased apoptosis significantly in β-cells at 48 h and 72 h from 1.1% ± 0.1% and 1.6% ± 0.6% in control

islets to 8.4% ± 1.6% (#p< 0.01) and 6.7% ± 0.4% (#p< 0.01) in CVB3 and to 4.4% ± 0.8 (#p< 0.01) and 6.4% ± 1.3% (*p< 0.05) in CVB4 infected islets, at indicated time points (Fig. 14A).

Contrary to β-cells, there was no significant change in α-cell apoptosis at any time point after CVB4 infection, which was in contrast to the elevated α-cell infection by CVB4. Results imply that CVB mainly infected β-cells, resulting in increased β-cell specific apoptosis.

Immunofluorescent staining showed CVB3 and CVB4 induced β-cell apoptosis indicated by red stained TUNEL positive nuclei in green stained β-cells merging with DAPI 48 h p.i. In contrast to that, glucagon positive cells showed no increase in TUNEL positive staining. Control islets showed basal moderate apoptosis rates 48 h p.i. (Fig. 14B).

A

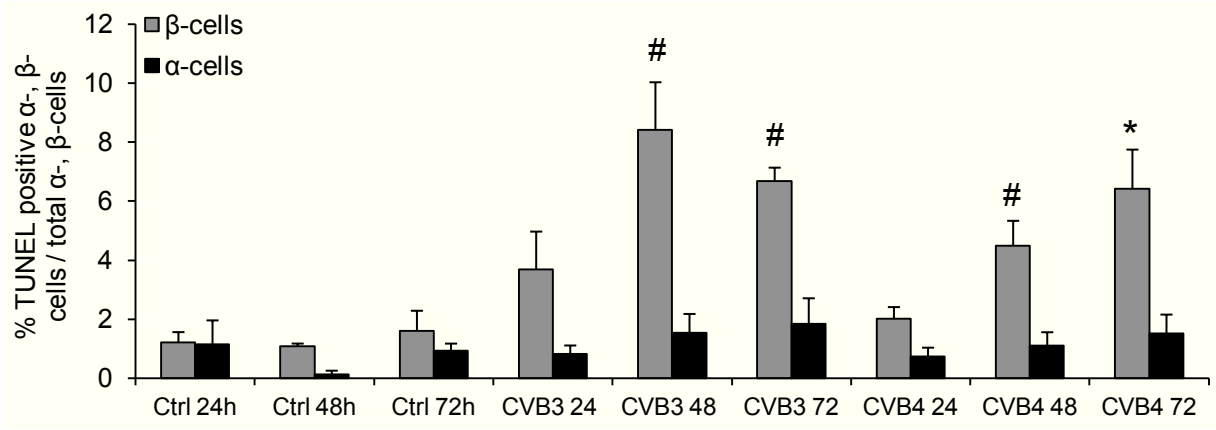

B

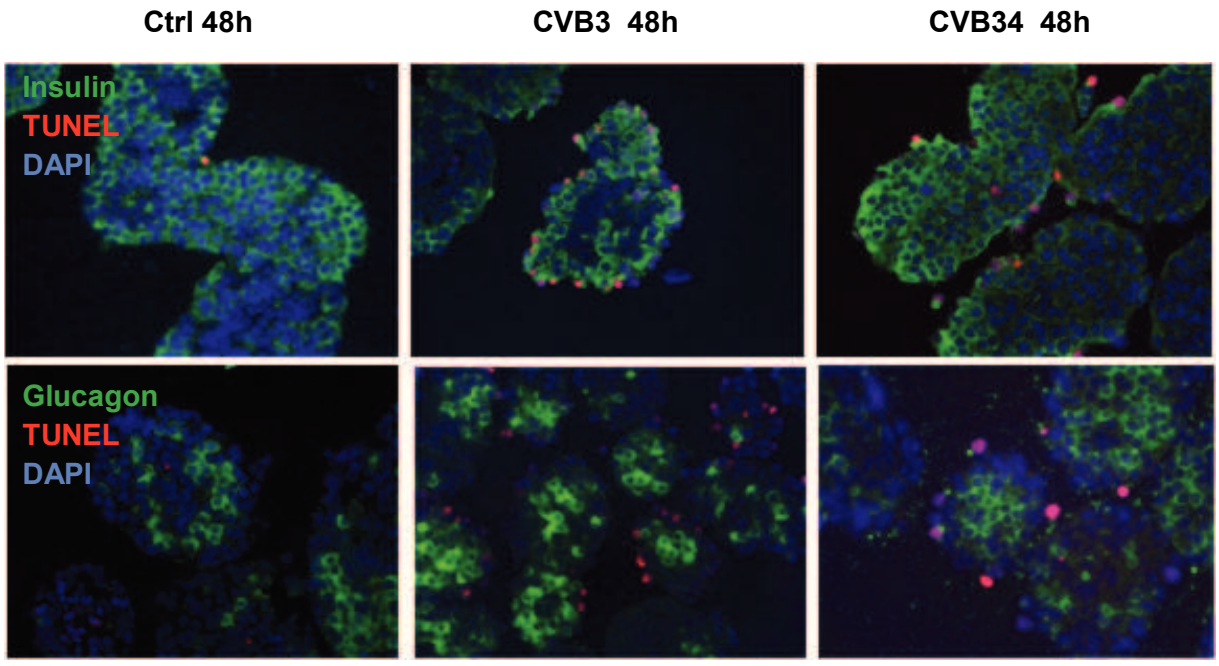

Figure 14: CVB3 and CVB4 infections of islets induce cell death specifically in β-cells. A: Isolated human islets infected with CVB3 or CVB4 (MOI of 5) for 24 h, 48 h and 72 h were subsequently fixed, pelleted and paraffin embedded. Islet sections were double stained for TUNEL and insulin or TUNEL and glucagon. Insulin or glucagon positive cells containing a TUNEL positive nuclei were quantified; results are expressed as percentage of TUNEL positive α- or β-cells (error bars indicate ± SEM from three independent experiments from three different donors; *$p< 0.05$, $^{\#}p< 0.01$ compared to controls at the same time points). **B:** Paraffin embedded islet sections from control, CVB3 or CVB4 (MOI of 5) infected islets were triple stained for insulin in the upper panel or glucagon in the lower panel in green, TUNEL in red and DAPI in blue 48 h p.i. TUNEL positive nuclei were indicated by purple staining due to colocalization with DAPI (magnification x 400).

In this part of the study, CVB3 and CVB4 *in vitro* infections of isolated human islets were established and revealed that both virus serotypes replicated efficiently in isolated human islets, and led to infection and induction of apoptosis mainly in β-cells resulting in impaired β-cell function to respond to elevated glucose concentrations. CVB4 infected a certain portion of α-cells in contrast to CVB3; however, an increase in α-cell apoptosis was not observed. The MOI of 5 did not result in rapid cell death, and therefor infection could be analyzed in a time frame of 72 h. This MOI was used in all experiments, unless stated otherwise. In all further studies a media treated control was included.

4.2 Induction of inflammation-related genes as result of CVB3 and CVB4 islet infections

CVB infected human islets upregulate several genes involved in inflammation like cytokines and chemokines [111-113]. Pro-inflammatory proteins can contribute *in vivo* to activation and attraction of immune cells resulting in the destruction of pancreatic tissue. In this study the transcription of different inflammatory genes was investigated using Real-time PCR (qPCR) technique.

4.2.1 *In vitro* CVB3 and CVB4 infections of human islets induce transcription of inflammatory cytokine and chemokine genes

In order to confirm that infection of human islets *in vitro* induces expression of different genes involved in virus defence and inflammation, isolated human islets were infected with CVB3 or CVB4 and gene expression analyses were performed.

In accordance with previous reports, mRNA transcription of the pro-inflammatory cytokines and chemokines *CXCL10*, *IL-6*, *TNFα* and *IFNβ* was increased after CVB3 or CVB4 infections, in which the highest gene expressions were observed 72h p.i. Values represent the relative gene expression as compared to control islets at the same time points. *CXCL10* mRNA showed 2194.3- and 1117.7-, *IL-6* 28.0- and 5.8-, *IFNβ* 157.7- and 140.3- and *TNFα* 4.7- and 2.1-fold increase in expression in CVB3 or CVB4 infected islets respectively, compared to control islets. In addition Poly I:C, the viral dsRNA analog, which is known to induce *CXCL10* gene transcription was added as positive control. Treatment or transfection of human islets with Poly I:C resulted also in the increase of expression of tested genes, however, highest gene expressions were observed 24 h p.i. possibly due to Poly I:C degradation at later time points (Fig. 15A).

Among the probes tested, *CXCL10* showed the highest gene expression levels after both CVB3 and CVB4 infections. *IFNγ,* the classical inducer of CXCL10, was not detected at any time point, suggesting an IFNγ independent *CXCL10* induction. Cell culture supernatants from CVB3 and CVB4 infected islets showed significantly elevated CXCL10 levels of 1.6 ng/ml ± 0.7 ng/ml and 2.8 ng/ml ± 0.8 ng/ml 48h and 72h after CVB3 and 2.0 ng/ml ± 0.8 ng/ml and 2.5 ng/ml ±

1.4 ng/ml 48 h and 72 h after CVB4 infections, compared to control at same time points (*p< 0.05; #p< 0.01). Treatment with Poly I:C resulted in high secretion of CXCL10 up to 4.9 ng/ml ± 0.05 ng/ml and 6.3 ng/ml ± 1.2 ng/ml at 48 h and 72 h (#p< 0.01) (Fig. 15B).

The *IFNβ* gene expression was highly increased upon infection, but the secreted IFNβ could not be detected in cell culture supernatants using ELISA (data not shown).

Based on the finding that CVB3 and CVB4 infect mainly β-cells, the cell type secreting CXCL10 was investigated. Immunostaining revealed that CXCL10 was highly colocalized with β-cells 48 h after CVB3 and CVB4 infections, suggesting β-cells as source of CXCL10. In contrast, control islets showed no positive staining for CXCL10 (Fig. 15C).

It has been shown, that IFNα treatment of isolated human islets leads to gene upregulation of *CXCL10* [136] In order to confirm that human islets can be stimulated *in vitro* with IFNβ, islets were treated with two different concentrations and gene expression of *CXCL10* was investigated by qPCR 24 h after treatment. Results showed a 5-fold and a 43-fold increase in *CXCL10* mRNA after treatment with 50 U and 500 U of IFNβ, compared to untreated control islets, confirming that isolated human islets are responsive to IFNβ (Fig. 15D).

A

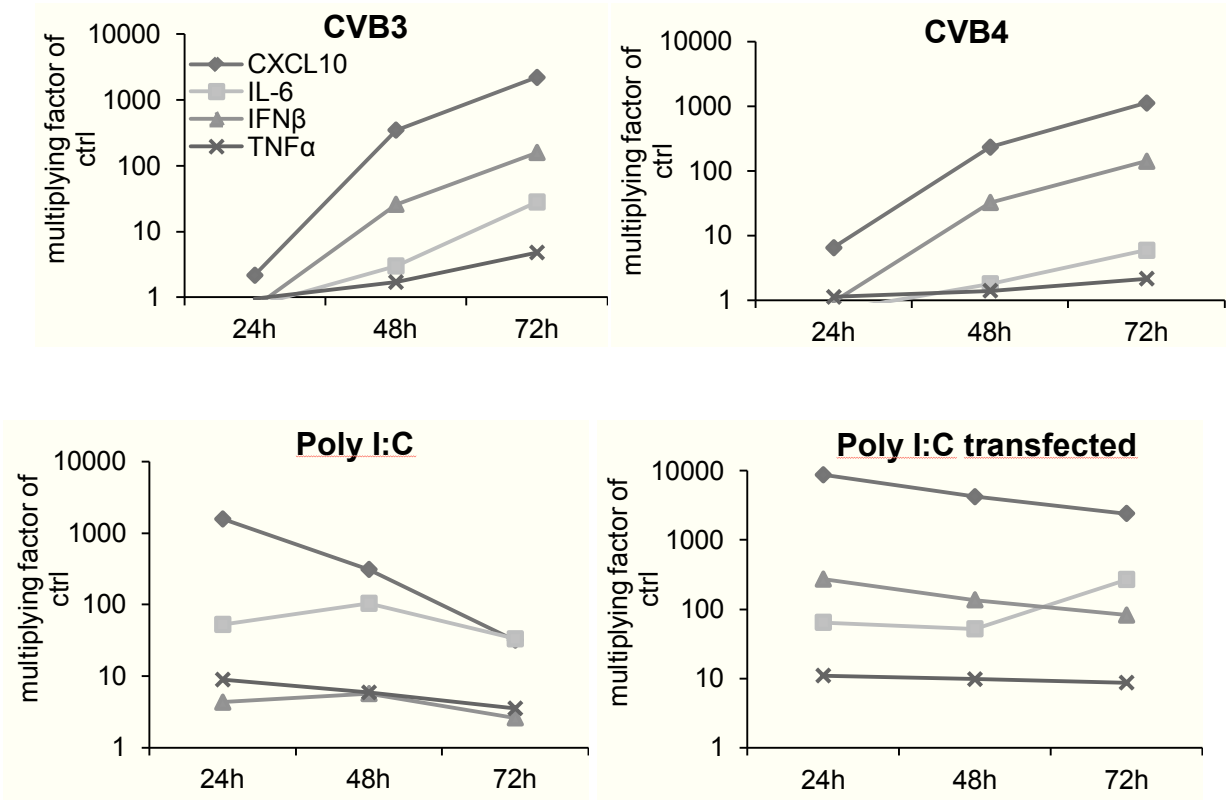

B

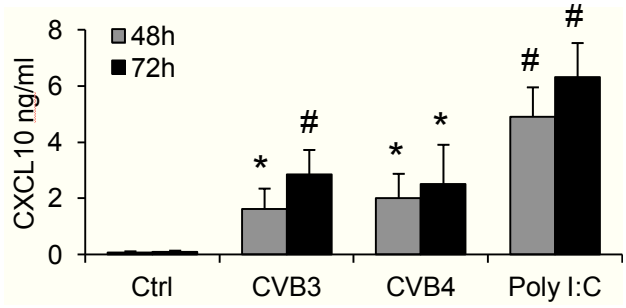

C

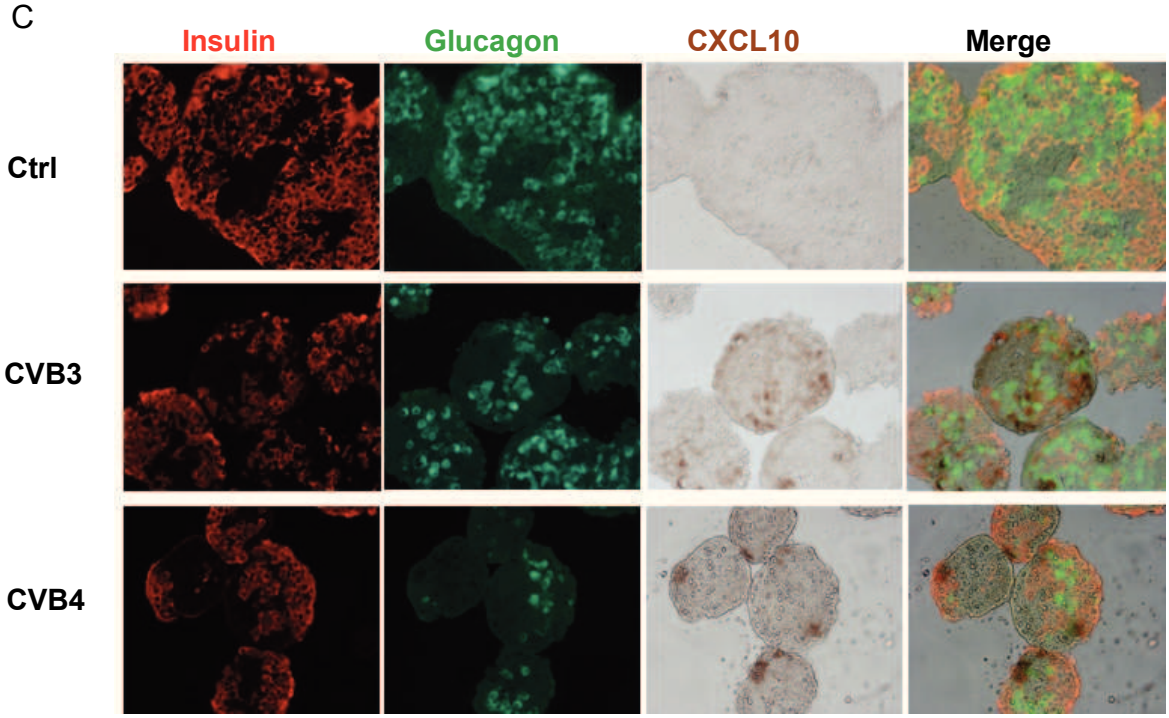

D

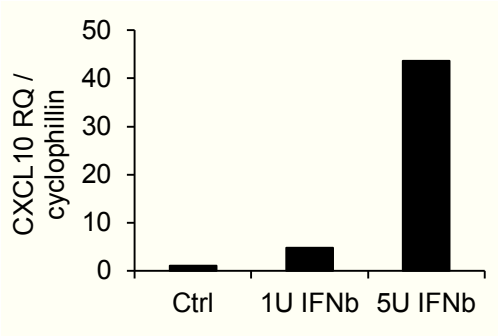

Figure 15: CVB3 and CVB4 induce cytokine and chemokine gene transcription and secretion of CXCL10 in isolated human islets. A: Human pancreatic islets were infected with CVB3 or CVB4, or treated (25 µg/ml) or transfected (5 µg) with Poly I:C. RNA was extracted 24 h, 48 h and 72 h p.i cDNA was generated and mRNA expression levels were analysed using qPCR technique. Reference gene was cyclophilin; shown are the mRNA amounts as multiplying factors of the mRNA amount obtained without virus or Poly I:C (controls) in a logarithmic scale (values show one representative

result out of three from three different donors). **B:** CXCL10 secretion was analysed in the supernatants from infected and Poly I:C (25 ng/ml) treated human islets by ELISA, 48 h and 72 h after infections and treatment (error bars indicate ± SEM from three independent experiments from three different donors, *p<0.05; # p<0.01). **C:** Paraffin embedded sections from CVB3 and CVB4 infected islets were immunostained for insulin in red, glucagon in green and CXCL10 in brown 48 h after infection. Merge shows colocalization of CXCL10 with insulin or glucagon positive cells (magnification x 400). **D** Isolated human islets were treated with 50 U and 500 U of IFNβ, and 24 h after treatment RNA was isolated and reversely transcribed. *CXCL10* mRNA transcription was analysed; cyclophilin was used as reference gene (result shows one experiment).

4.2.2 Neutralization of CXCL10 does not protect from virus induced β-cell apoptosis

Infection of isolated human islets resulted in a strong *CXCL10* gene expression and protein secretion. Treatment of isolated human islets *in vitro* with the recombinant CXCL10 protein resulted in increased β-cell apoptosis [137]. To investigate a possible involvement of CXCL10 on β-cell survival and function, isolated human islets were infected with CVB3 or CVB4 and were additionally treated with a CXCL10 neutralizing antibody. IgG was included as control. CVB3 and CVB4 infections of isolated human islets resulted in a 2.3-fold and 1.7-fold induction of apoptosis. Application of the CXCL10 neutralizing antibody had no effect on virus induced apoptosis (Fig. 16).

CXCL10 neutralization also showed no effects on GSIS, which was performed with the same samples (data not shown).

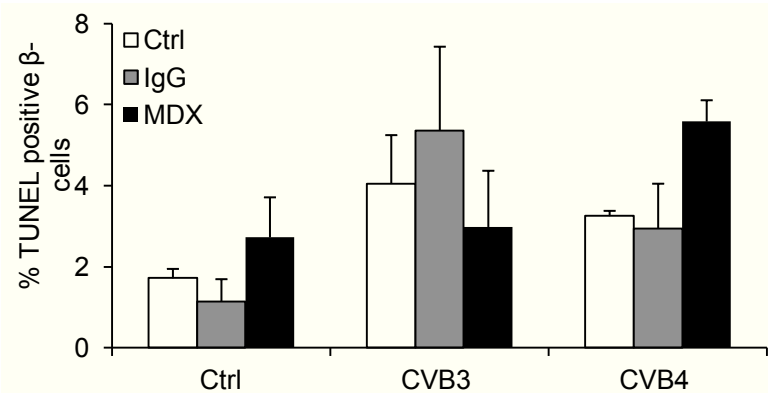

Figure 16: CXCL10 neutralization shows no effect on β-cell survival and function. Isolated human islets were infected with CVB3 or CVB4. CXCL10 neutralizing antibody (MDX1100) (10 µg/ml) or human IgG (10 µg/ml) were added to the islets at the beginning of the infection. 48 h p.i. GSIS analysis was performed. Then the islets were fixed and double stained for TUNEL and insulin. TUNEL positive β-

cells were quantified and results expressed as percentage of TUNEL positive cells (error bars indicate ± SD from triplicate, result shows one representative experiment of three from three different donors).

4.2.3 PRRs are upregulated upon infection of isolated human islets

PRRs recognizing viral ss/dsRNA are involved in the induction of several cytokines and chemokines and especially type 1 IFN genes. To investigate if the gene expression of certain PRRs was increased in CVB3 or CVB4 infected islets, qPCR analysis was performed. *TLR3*, *RIG-I*, *MDA5* and *PKR* mRNA showed a time-dependent increase with highest expression levels detected at 72 h after CVB3 or CVB4 infections. Values represent the relative gene expression compared to control islets at the same time points. *TLR3* mRNA transcription was 6.2- and 4.7-, *RIG-I* 23.5- and 15.4-, *MDA5* 17.5- and 13.0- and *PKR* 7.3- and 6.1-fold increased upon CVB3 or CVB4 infections, respectively, compared to control at 72 h. In this experiment, too, poly I:C treatment and transfection was included and resulted in increased expressions of PRR genes analyzed (Fig. 17A).

To investigate whether IFNβ treatment of isolated islets results in induction of PRR gene expression, isolated human islets were treated with increasing concentrations of IFNβ. Treatment for 24 h resulted in a concentration-dependent increase of mRNA levels of investigated PRRs, showing the IFNβ stimulation of human islets (Fig. 17B).

The reference genes used in this study were cyclophillin and 18s. To exclude the effect of CVB3 or CVB4 infections on the stability of the reference genes, a qPCR of cDNAs from CVB3 or CVB4 infected and non-infected control islets was performed 48 h p.i. Results revealed that both housekeeping genes were equally expressed (Fig. 17C).

A

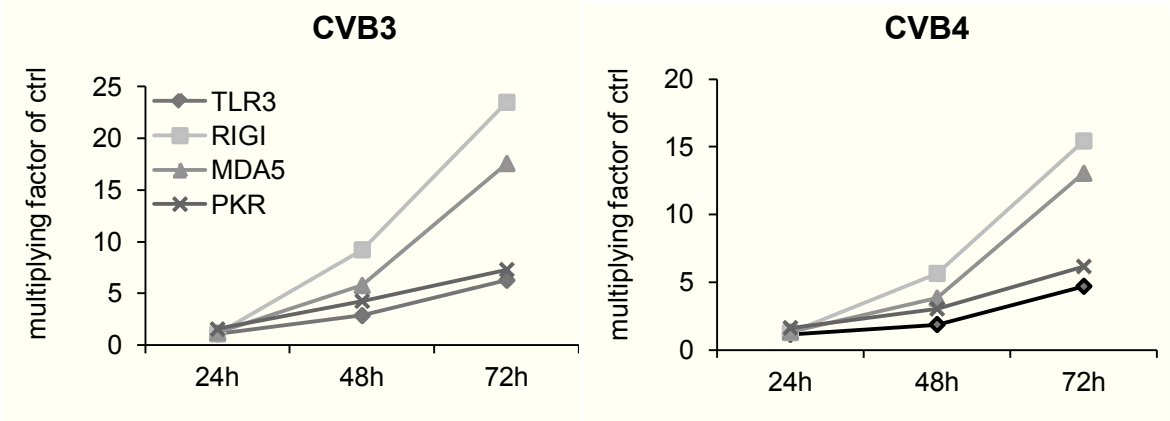

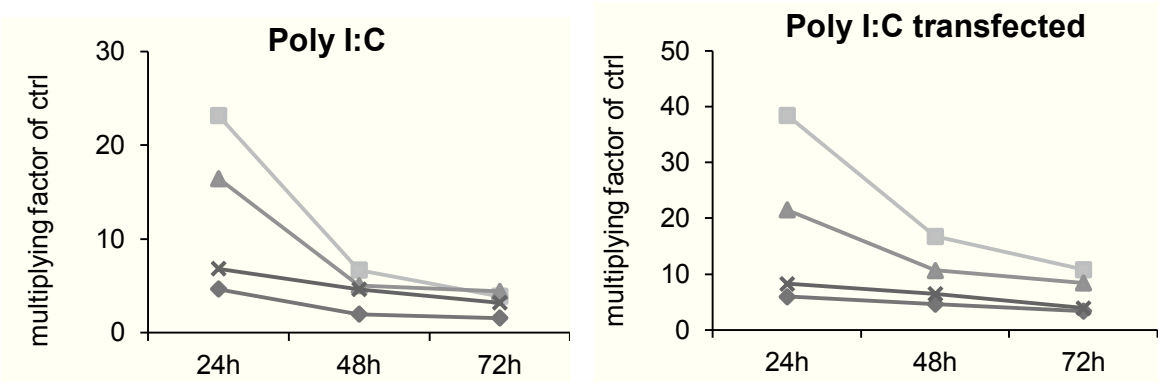

B

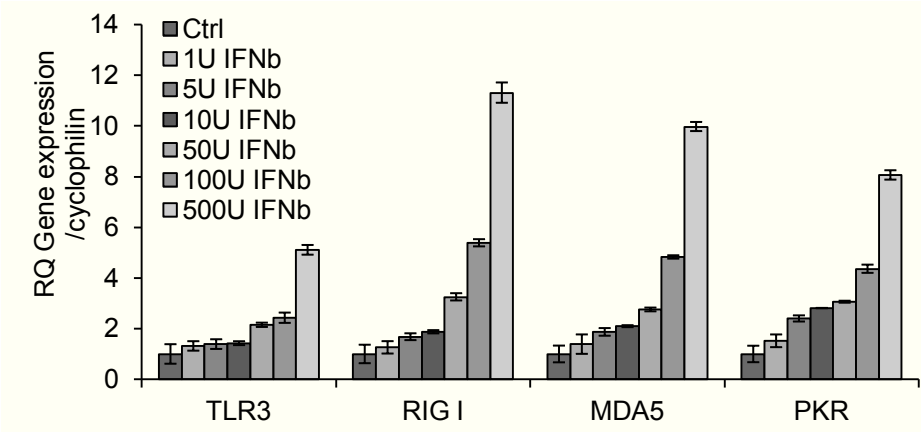

C

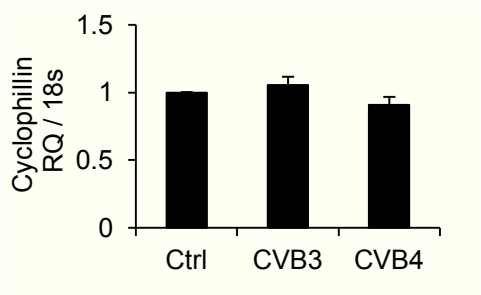

Figure 17: Distinct PRR genes are upregulated in isolated human islets after CVB3 and CVB4 infections, and Poly I:C treatment and transfection. Human pancreatic islets were infected with CVB3 or CVB4, or treated (25 µg/ml) or transfected (5 µg) with Poly I:C, and RNA was extracted 24 h, 48 h and 72 h after infection and treatment. RNA was reversely transcribed and PRR mRNAs were analysed using qPCR technique. The reference gene was 18s; shown are the mRNA amounts as multiplying factors of the mRNA amount obtained without virus or Poly I:C (controls) in a logarithmic scale (values show one representative result out of three, from three different donors). **B:** Isolated human islets were treated with indicated Units of IFNβ for 24 h, following RNA extraction and reverse transcription. PRR mRNAs were analysed by qPCR (result shows one experiment). **C:** Human pancreatic islets were infected with CVB3 or CVB4 and RNA was extracted 48 h after infection. RNA was reversely transcribed and the expression of cyclophilin mRNA was analysed using qPCR technique. 18s was used as reference gene (error bars indicate ± SD from technical replicate, result shows one experiment).

4.3 Involvement of PRRs in CVB sensing

The increase of cytokine, chemokine and especially type I IFN gene expressions are the first defence mechanisms of the innate immune system in virus infected cells, which belong. The first step leading to the initiation of the signal cascade leading to the induction of gene transcription is the binding of viral nucleic acids to PRRs. So far, a specific PRR sensing CVB RNA in isolated human islets has not been found. In order to investigate which receptor binds to CVB3 or CVB4 nucleic acids, protein- and RNA- immunoprecipitation studies were performed.

4.3.1 CVB3 RNA is sensed by TLR3 and PKR and CVB4 RNA by TLR3, PKR, as well as by TLR7

Protein- and RNA-immunoprecipitation studies were performed in collaboration by Dr. Federico Paroni.

To immunoprecipitate proteins bound to CVB dsRNA, protein lysates from CVB3 or CVB4 infected islets and control islets were incubated with the K1 antibody, which is directed against dsRNA. Input protein lysates (in), supernatants after immunoprecipitation (out) and immunoprecipitated (IP) fractions were analysed by western blotting. RIG-I and MDA5 showed no bands in the immunoprecipitated fractions of CVB3, CVB4 infected and control islet lysates in contrast to out- and input fractions, suggesting no binding of dsRNA to RIG-I and MDA5 24 h p.i. the analysis of the same fractions for presence of PKR showed a strong band in the immunoprecipitated fractions of CVB3 and CVB4 infected islets, while no bands were observed in the control, indicating that CVB3 and CVB4 RNA was bound by PKR during infection of islets (Fig. 18A).

PKR is phosphorylated and activated following dsRNA binding, which leads to the phosphorylation of its downstream target eIF2a and consequently to the inhibition of translation, as an antiviral effect. Western blot analyses of lysates obtained from CVB3 or CVB4 infected islets showed phosphorylation of PKR as well as its downstream target eIF2a in contrast to lysates from control islets, confirming the immunoprecipitation results (Fig. 18B).

Using the same strategy, positive bands for TLR3 and TLR7 could not be obtained. To investigate if TLR3 or TLR7 were involved in CVB3 or CVB4 RNA binding an opposite strategy, RNA-immunoprecipitation (RNA-IP), was performed. Lysates from CVB3- or CVB4-infected and

control islets were incubated with antibodies directed against TLR3 and TLR7, respectively. RNA was precipitated from the immunoprecipitated fractions. Only, RNA which was bound to TLR3 or TLR7 was reversely transcribed to cDNA and analysed by qPCR. CVB3 RNA was bound by TLR3 while CVB4 RNA was bound by both receptors, TLR3 and TLR7, 24 h and 48 h p.i. suggesting an involvement of TLR3 and TLR7 in the CVB3 and CVB4 RNA sensing in the early phase of infection. Binding of CVB RNA by TLR3 and TLR7 increased over time. RNA precipitated from control islets showed no binding to TLR3 or TLR7 (Fig. 18C). Values represent arbitrary units.

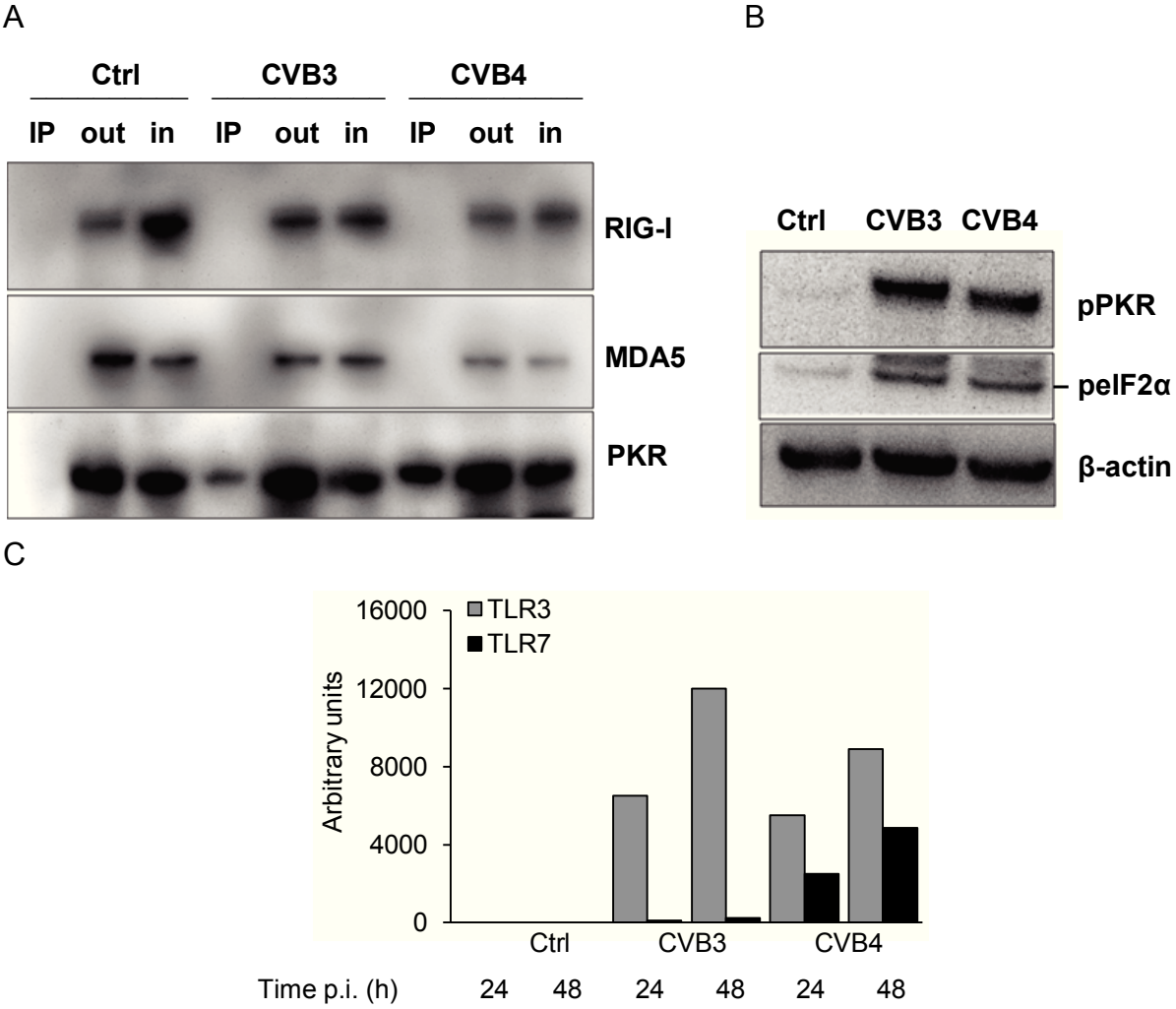

Figure 18: PKR, TLR3 and TLR7 are involved in CVB3 and CVB4 RNA binding. A: 24 h after CVB3 or CVB4 infections of isolated human islets, proteins were cross-linked and islets were lysed. Equal protein concentrations were incubated with the K1 antibody directed against dsRNA, followed by immunoprecipitation (IP). IP, output (out) and input (in) fractions were analysed for the presence of RIG-I, MDA5 and PKR. **B:** 48 h p.i. lysates from CVB3 and CVB4 infected human islets were analysed by western blot for presence of the phosphorylated form of PKR and its downstream target phospho-eIF2α. The antibodies sed recognize the phosphorylated forms of PKR and eIF2α. β-actin was used as control for

equal protein load. **C:** RNA-IP was performed from human islets infected with CVB3 or CVB4 24 h and 48 h p.i. RNA-protein complexes were cross-linked and islets were lysed. Equal amount of proteins were incubated with either TLR3 of TLR7 antibodies following IP. RNA was precipitated from IP fractions, reversely transcribed and analysed for the presence of CVB cDNA, using CVB primers (result shows one representative experiment out of three, from three different donors).

4.3.2 TLR3 and TLR7 are differentially expressed within human islets

The cellular expression and localization of TLR3 and TLR7 was investigated. The immunohistochemical analysis of cryo- and paraffin embedded pancreatic sections from healthy donors was performed. Immunostaining revealed that TLR3 was expressed in islet cells colocalizing with insulin positive cells while TLR7 showed an α-cell specific staining, suggesting that TLR3 was mainly expressed in β-cells and TLR7 in α- cells (Fig. 19).

To exclude unspecific binding of secondary antibodies, immunostaining without primary antibody was performed showing no TLR3 or TLR7 staining.

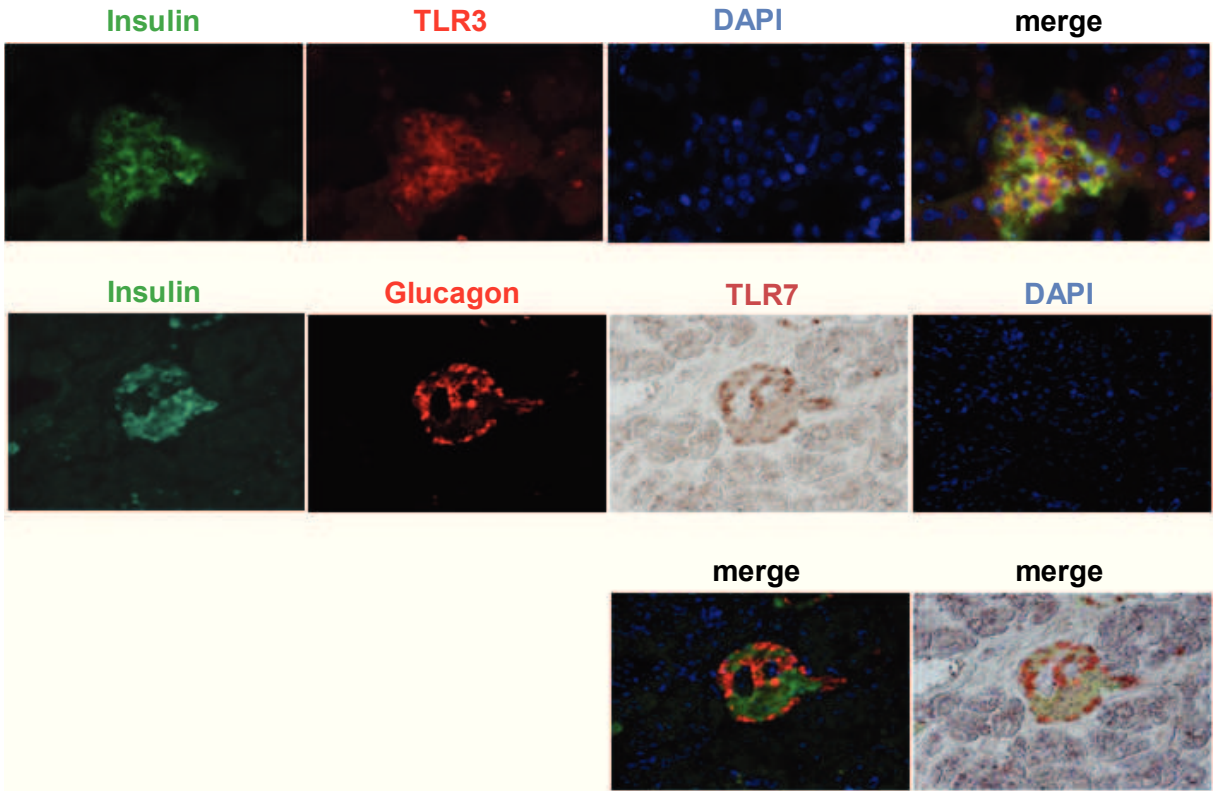

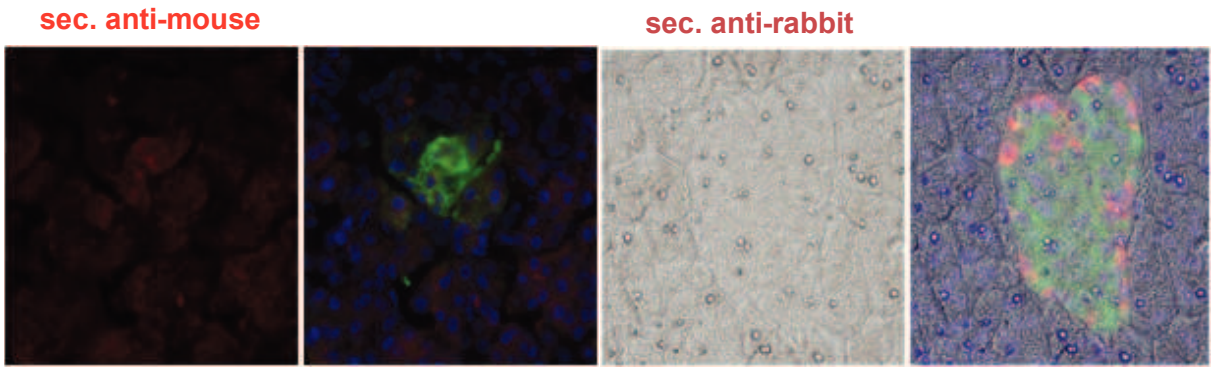

Figure 19: TLR3 is mainly expressed in β-cells while TLR7 is expressed in α-cells. Fluorescence and bright field immunostaining was performed on cryo- and paraffin sections from healthy donors. The upper panel shows fluorescent insulin staining in green, TLR3 staining in red and DAPI nuclear staining in blue. The merge image demonstrated colocalization of TLR3 with insulin positive cells indicated in yellow colour. Lower panels show fluorescent insulin and glucagon staining in green and in red and DAPI in blue. TLR7 bright field red immunostaining was colocalized with glucagon positive cells indicated by merge images. Sections incubated with only secondary antibodies against mouse and rabbit (magnification 400x).

4.3.3 TLR3 depletion decrease cytokine and chemokine gene expression in CVB3 and CVB4 infected human islets

Since TLR3 is expressed in β-cells and was shown to bind to CVB RNA, the function of TLR3 was investigated using small interfering RNA (siRNA) technique. Because commercially available TLR3 antibody did not show reliable results by western blotting, TLR3 down regulation was confirmed based on mRNA levels. To achieve high transfection efficiency, isolated human islets were dispersed by accutase treatment 48 h before transfection. siTLR3 transfection of human islets resulted in significant decrease of *TLR3* mRNA levels to 42% ± 13% (*p< 0.05) as compared to small interfering scrambled (siScr) RNA transfected control islets, 96 h after transfection (Fig. 20A).

To proof the functionality of TLR3 protein downregulation, an indirect approach was performed. Poly I:C, a known TLR3 ligand, induced strong CXCL10 secretion (Fig. 15B). Isolated human islets were siScr or siTLR3 transfected for 48 h followed by treatment with Poly I:C for additional 24h. Poly I:C induced a massive *CXCL10* gene expression in siScr transfected islets, which was clearly decreased in siTLR3 transfected human islets, from 1042.8-fold to 433.3-fold as compared to non-treated control islets (Fig. 20A).

The increase of *CXCL10* gene expression was confirmed on protein levels using CXCL10 ELISA, demonstrating a 2-fold reduction in CXCL10 secretion ad compared to siScr (Fig. 20A).
Next, the effect of TLR3 on virus-induced cytokine and chemokine gene expression was investigated. CVB3 and CVB4 infections (MOI of 20) of human islets led to increased *CXCL10*, *IFNβ*, *IL-6* and *TNFα* mRNA levels in siScr transfected islets 24 h p.i., whereas TLR3 depletion resulted in 4.5-fold and 6-fold decreased *CXCL10*, 6.5-fold and 3.7-fold decreased *IFNβ*, 1.5-fold and 1.3-fold decreased *IL-6* and 3-fold and 1.3-fold decreased *TNFα* mRNA transcription, respectively (Fig. 20B).
CXCL10 gene expression was confirmed on protein levels using CXCL10 ELISA, which showed a clear reduction of CXCL10 secretion from CVB3 and CVB4 infected islets transfected with siTLR3, as compared to siScr. CVB3 and CVB4 infections of human islets transfected with siScr led to 0.98 ng/ml ± 0.20 ng/ml and to 0.51 ng/ml ± 0.08 ng/ml secretion of CXCL10, respectively, as compared to 0.08 ng/ml ± 0.07 ng/ml from control islets. In contrast, TLR3 knock down resulted in 2-fold and 1.6-fold decrease in CXCL10 secretion from CVB3 and CVB4 infected islets. Non-infected TLR3 depleted human islets led to a low basal CXCL10 secretion of 0.15 ng/ml ± 0.14 ng/ml (Fig. 20C).
This suggests TLR3 as a sensor inducing inflammatory gene upregulation in isolated human islets following CVB3 and CVB4 infections.

A

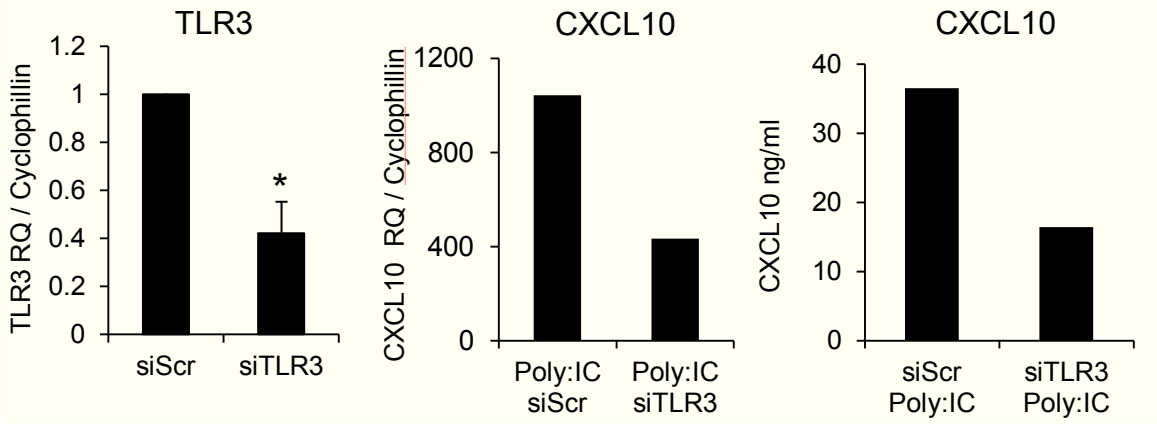

B

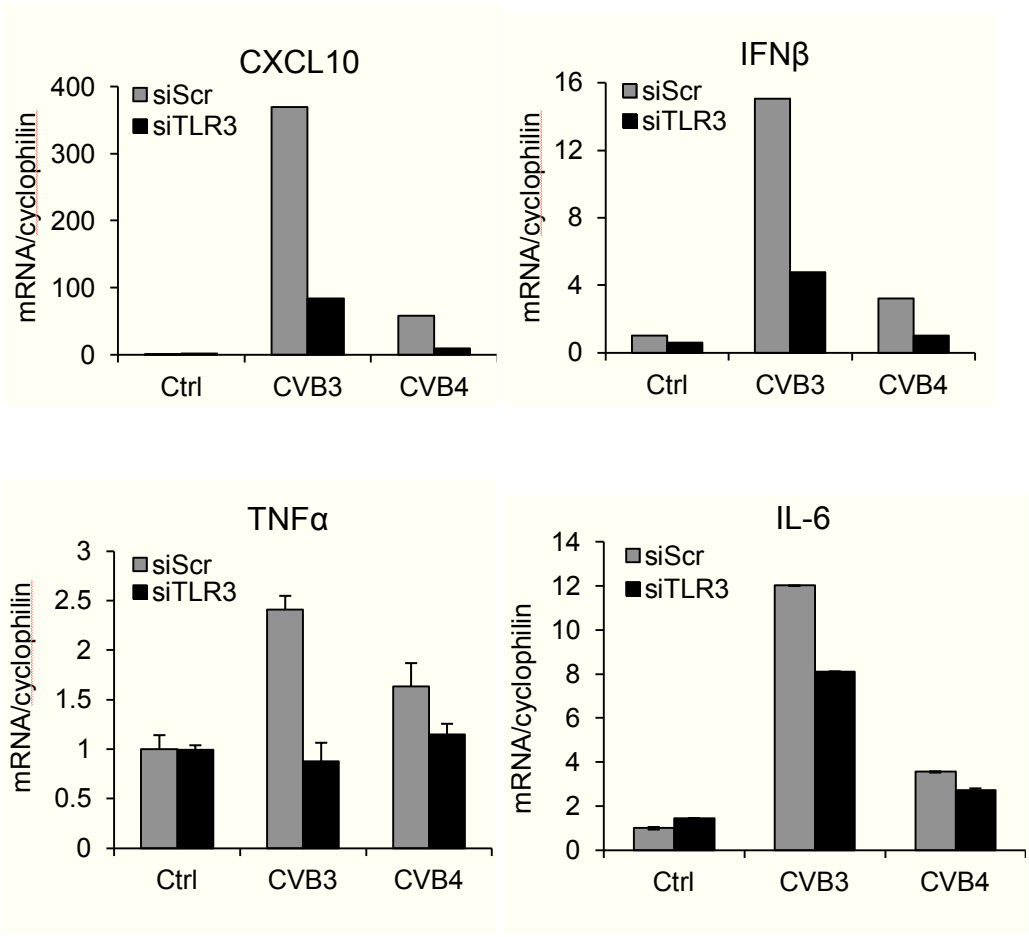

C

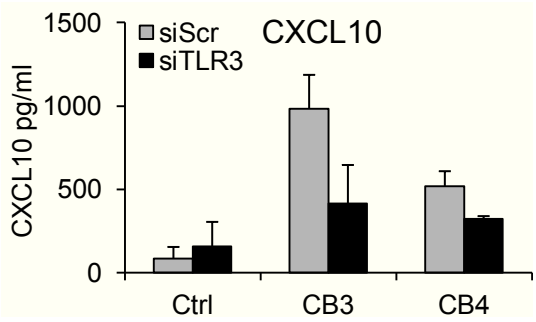

Figure 20: TLR3 is involved in CVB3 and CVB4 dependent upregulation of cytokine and chemokine gene expression. A: Human islets were treated with accutase for 5 min at 37°C and cultured for 48h. Then the islets were transfected with either siScr or siTLR3. 96 h after transfection RNA was isolated, reversely transcribed and *TLR3* gene expression was analysed (error bars indicate ± SED from three independent experiments from different donors, *p< 0.05 compared to siScr). Islets were treated and transfected as described above and 48 h after siTLR3 and siScr transfections human islets were treated with Poly I:C (25 µg/ml) for additional 24 h. *CXCL10* gene expression was analysed by qPCR. Supernatants from the same samples were analysed by CXCL10 ELISA (results show one single

experiment). **B:** 48 h after the siScr and siTLR3 transfections, isolated human islets were infected with CVB3 or CVB4 (MOI of 20). 24 h p.i. RNA was extracted and *CXCL10*, *IFNβ*, *TNFα* and *IL-6* gene expressions were analysed by qPCR (error bars represent ± technical replicate, results show one experiment). **C:** Supernatants from control and CVB3 and CVB4 infected human islets transfected with siScr and siTLR3 were analysed by CXCL10 ELISA (error bars represent ± SED from two independent experiments).

The results show the involvement of TLR3 and TLR7 in CVB infection of human islets and a distinct protein expression in α- and β-cells. TLR3 silencing confirmed TLR3 as sensor, since depletion led to decrease in expression of the cytokine and chemokine genes analysed.

4.4 CVB induced β-cell apoptosis is partially TLR3 and JNK dependent

Apoptosis is the main form of cell death in T1DM [70]. CVB serotypes, such as CVB3 and CVB4 are implicated as agents triggering T1DM in genetically susceptible individuals. *In vitro* infections of isolated human islets with CVB3 and CVB4 led to β-cell apoptosis, compared to non-infected islets. This virus induced destruction can be a precipitating event in T1DM. TLR3 and JNK were investigated as possible mediators of virus-induced β-cell apoptosis.

4.4.1 TLR3 depletion protects from CVB induced apoptosis

To investigate if TLR3 is involved in CVB3-and CVB4-induced apoptosis in isolated human islets, TLR3 was depleted and western blotting and TUNEL analyses were performed. Human islets were transfected with siScr and siTLR3 for 48 h followed by infection with CVB3 or CVB4. 24h p.i. the cells were lysed and the proteins were analysed by western blotting. siScr transfected CVB3- and CVB4-infected human islets showed cleaved caspase 3 bands. The Intensity of the bands was clearly decreased upon siTLR3 transfection, suggesting an involvement of TLR3 in CVB induced apoptosis. In contrast, there was no cleavage of caspase 3 in control conditions. VP1 expression confirmed CVB3 and CVB4 infections of islets, interestingly those bands were increased in siTLR3 transfected CVB3 and CVB4 infected islets, as compared to siScr transfected and infected islets, suggesting an effect on virus replication. β-actin was used as protein loading control (Fig. 21A).

To confirm that TLR3 had an effect on CVB3 and CVB4-induced apoptosis, a TUNEL assay was performed. Here, isolated human islets were siScr and siTLR3 transfected for 48 h followed by CVB3 or CVB4 infections. 24 h p.i. cells were fixed and double immunostaining for TUNEL and insulin was performed. Black stained nuclei in insulin positive cells were quantified and results were expressed as percentage of TUNEL positive β-cells. Results showed that CVB3 and CVB4 increased apoptosis in β-cells transfected with siScr islets from 2.7% ± 0.2% in not infected control islets to 8.7% ± 0.8% and 6.4% ± 0.7%, respectively. However, depletion of TLR3 resulted in 1.4-fold and 2-fold decrease of CVB3 and CVB4 induced apoptosis, respectively, confirming western blot analysis (Fig. 21B).

A

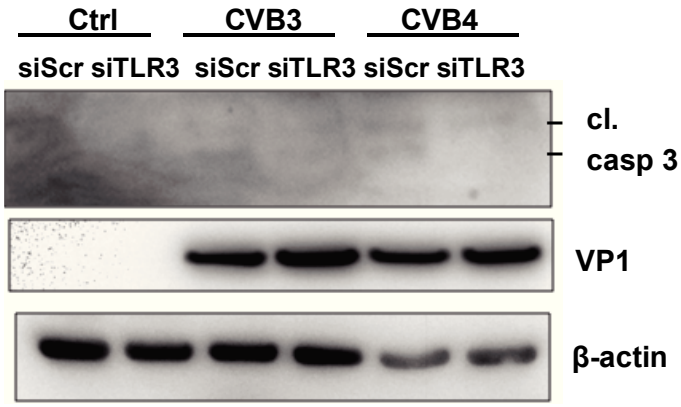

B

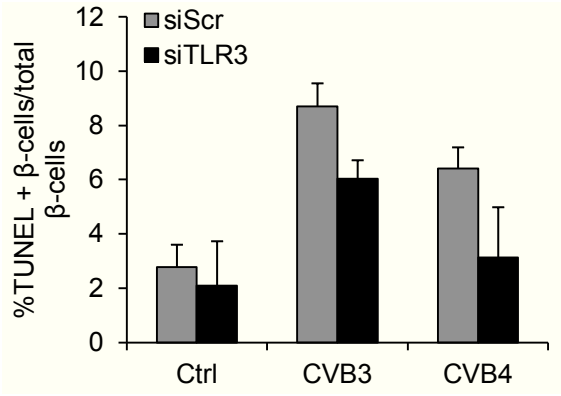

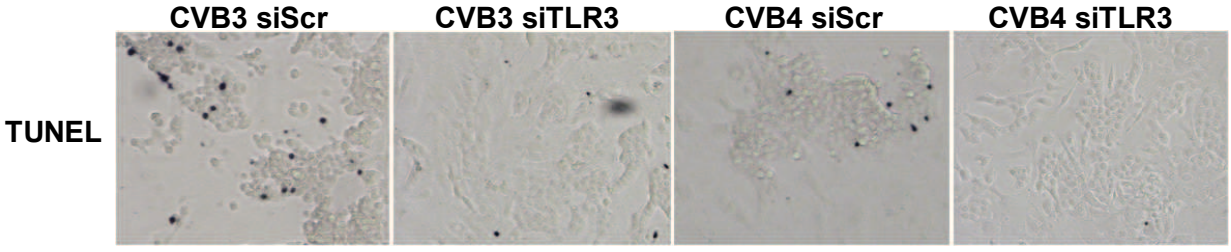

Figure 21: TLR3 depletion protects from CVB3 and CVB4 induced apoptosis. A: Human islets were treated with accutase for 5 min at 37°C and cultured for 48 h. Then the islets were transfected with either siScr or siTLR3, and 48 h after transfection the islets were infected with CVB3 or CVB4. 24 h p.i. islets were lysed and western blot analysis performed. Cleavage of caspase 3 was investigated as apoptotic marker. VP1 bands indicate infection of islets and β-actin was used as protein loading control (western blot shows one representative result out of four from four different donors) **B:** Islets were treated as described above and transfected with siScr and siTLR3 for 48 h. Then isolated human islets were infected with CVB3 or CVB4, and 24 h p.i. islets were fixed and costained with insulin and TUNEL to analyze apoptosis. TUNEL positive β-cells were quantified; values are expressed as percentage of

TUNEL positive β-cells per total β-cells (error bars indicated ± SED from two independent experiments from two different donors).

4.4.2 pJNK as mediator of CVB induced apoptosis

The β-cell line CM was used as a model cell line for the investigation of virus mediated cell apoptosis. Lysates from control treated and CVB3-infected CM cells were investigated by western blotting. Results showed a time-dependent increase in cleavage of caspase 3 upon CVB3 infection correlating with phosphorylation of JNK, already 3 h, 4 h and 5 h p.i. VP1 bands appeared at same the time points as the cleavage of caspase 3 and phosphorylation of JNK were present. β-actin was used as protein loading control (Fig. 22A).

To confirm JNK phosphorylation in infected human islets, western blot of lysates from CVB3 infected human islets was performed. JNK phosphorylation was observed after infection and 6 h and 24 h p.i. After 24 h, pJNK correlated with the cleavage of caspase 3 and the appearance of CXCL10 and VP1 bands (Fig. 22B).

To investigate a possible link between pJNK and CVB3 induced apoptosis, a JNKi (JNK inhibitor) was applied. Isolated human islets were pre-treated with JNKi following infection with CVB3 or CVB4. 48 h p.i. the islets were lysed and the proteins were analysed by western bloting. CVB3 and CVB4 infections resulted in an increase of phosphorylation of JNK and its downstream target c-Jun, as compared to non infected control islets. Pre-treatment with JNKi resulted in an abrogation of phosphorylation of JNK as well as of c-Jun, indicating successful JNK inhibition. Caspase 3 was cleaved in islet lysates from CVB3 and CVB4 infected islets in contrast to media treated control islets. Pre-treatment with JNKi revealed a decrease in the cleavage of caspase 3. In addition, pre-treatment also resulted in a decrease in VP1 bands in contrast to non pre-treated islets. The decrease in VP1 is possibly due to unspecific effects on virus replication caused by the JNKi. Thus, the decrease of cleavage of caspase 3 in JNKi pre-treated and CVB3- and CVB4-infected islets cannot be solely explained by the JNK inhibition, but rather by unspecific effects of the inhibitor on virus replication (Fig. 22C).

To exclude side effects, a vector containing a dominant negative form of JNK (dnJNK) was overexpressed in isolated human islets. As controls, islets were either treated with Lipofectamine (LF) or transfected with GFP-plasmid to exclude effects derived from the transfection procedure or protein overexpression. 48 h after transfection, islets were media treated or CVB3 infected. 48h p.i Islets were lysed and proteins were investigated by western blotting. To confirm dnJNK

overexpression and decreased JNK function, c-Jun phosphorylation and total JNK levels were investigated. Upon dnJNK overexpression and CVB3 infection, no phosphorylation of c-Jun was evident in contrast to GFP overexpressing CVB3 infected islets. In addition, total JNK bands were increased upon dnJNK transfection as compared to the control, suggesting successful dnJNK overexpression and impaired JNK function. GFP overexpression and CVB3 infections were confirmed by visualisation of GFP and VP1 bands, respectively. Results showed increase in cleavage of PARP and caspase 3 in GFP control transfected and CVB3 infected islets, which was decreased in CVB3 infected islets overexpressing dnJNK, suggesting a role for pJNK in virus induced β-cell apoptosis (Fig. 22D).

A

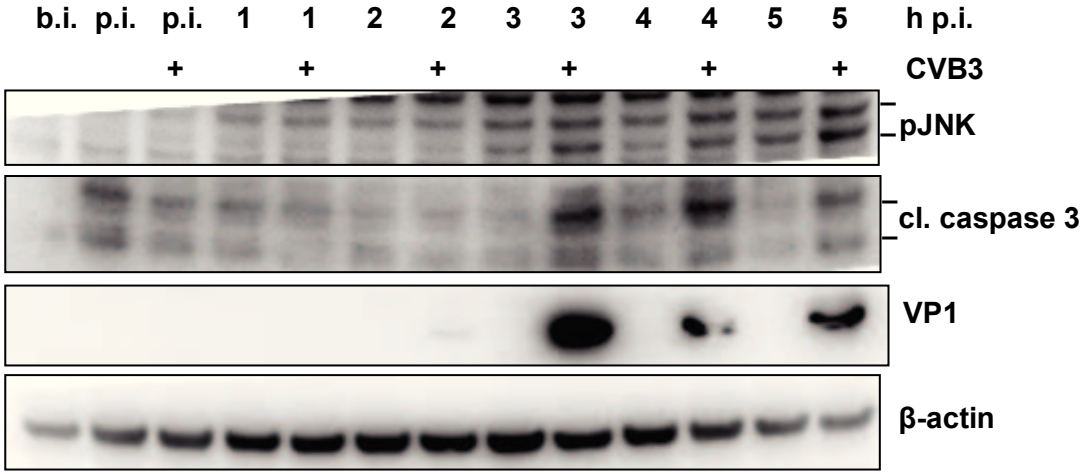

B

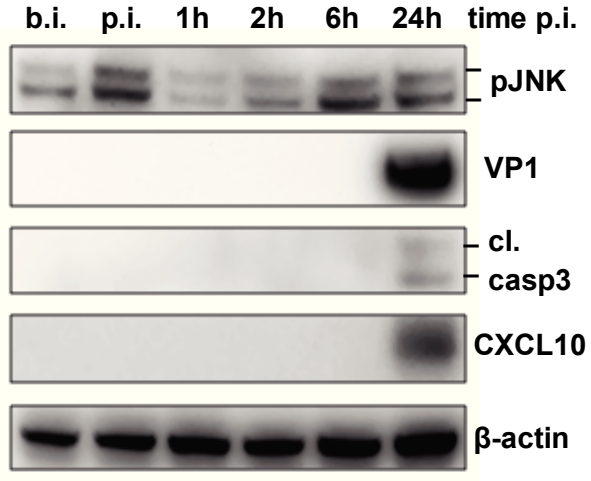

C

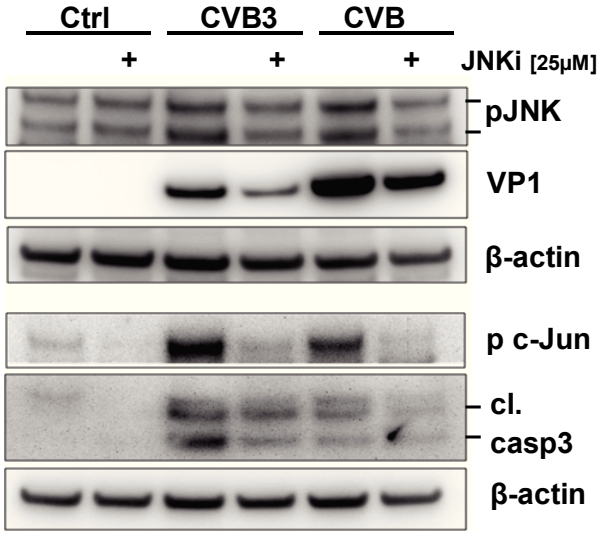

D

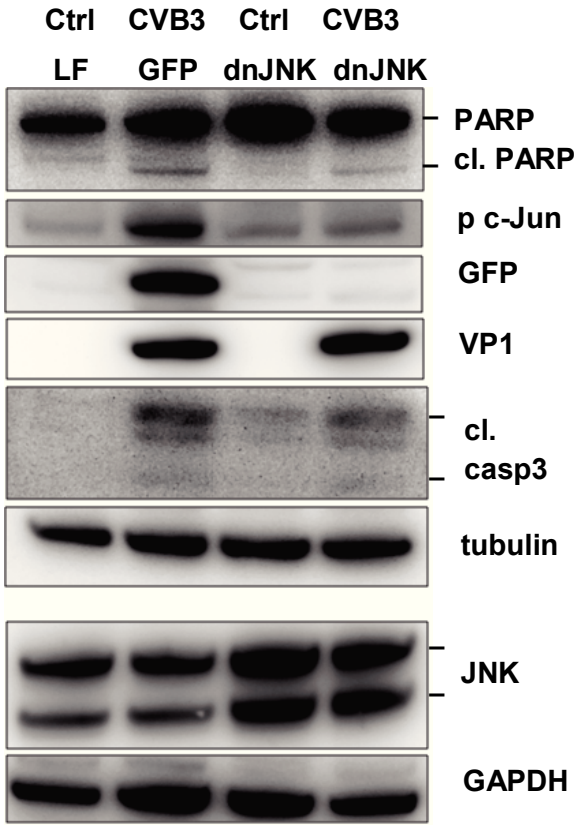

Figure 22: pJNK is involved in CVB3 induced β-cell apoptosis. A: CM cells were used as a model cell line for investigation of CVB3 induced apoptosis. Prior to infection, cells were lysed and used as control b.i. (before infection). Cells were infected with CVB3 and lysed in a time dependent manner starting after infection (p.i.) to 5h p.i., at each time point a non-infected media treated control was included. Phosphorylation of JNK and cleavage of caspase 3 were analysed during the first hours of infection. VP1 bands indicate CVB3 infection and β-actin was used as protein loading control (western blot shows one representative result out of three). **B:** Isolated human islets were lysed and used as control b.i., islets were infected with CVB3 and lysed 1 h, 2 h, 6 h, and 24 h p.i. Lysates were analysed by western blotting for phosphorylation of JNK, VP1 expression, cleavage of caspase 3 and CXCL10 expression. β-actin was used as protein loading control (western blot shows one representative result out of two from two different donors). **C:** Isolated human islets were pre-treated with the JNK inhibitor SP600125 (25μM) 1h prior to infection, during infection and p.i. Islets, pre-treated with JNKi, were CVB3 or CVB4 infected. 48 h p.i. the islets were lysed and the effects of the JNK inhibition were analysed by western blotting. pJNK and its downstream target p-c-Jun were investigated as well as cleaved caspase 3 and VP1. β-actin was used as protein loading control. **D:** Isolated human islets were dispersed for 5 min at 37°C using accutase and cultured for 48 h. Attached islets were transfected with either dnJNK- or GFP-plasmid or were treated with the transfection reagent LF (Lipofectamine). GFP and dnJNK transfected islets were infected with CVB3. In addition, LF treated and dnJNK transfected islets represent non infected controls. Islets were lysed 48 h p.i. and lysates were analysed by western blotting for total JNK, GFP and VP1 expressions as well as for phosphorylation of c-Jun and cleavage of PARP and caspase 3. Tubulin and GAPDH were used as protein loading controls (result shows one performed experiment).

4.4.3 PKR does not contribute to virus induced cell death

To investigate a possible role for PKR in the virus induced apoptosis, PKR was inhibited using two different inhibitors, 2-AP and PKRi.

Isolated human islets were infected with CVB3 and 4 and after infections, islets were treated with 2-AP. Inhibition of phosphorylation was analysed by western blotting. CVB3 infection resulted in phosphorylation of PKR, which was abrogated in islets treated with 2-AP, however VP1 bands were clearly reduced in islets treated whit 2-AP, suggesting that the inhibitor caused unspecific effects and altered the virus replication (Fig. 23A).

Since 2-AP showed no PKR specificity, another inhibitor, PKRi, was applied. CM cells were treated with different concentrations of PKRi 12 h before Poly I:C transfection. 6 h after transfection cells were lysed and proteins were analysed by western blotting.

PKR phosphorylation was decreased with increasing PKRi concentrations. Interestingly, cleavage of caspase 3 was completely preserved, suggesting that PKR might be involved in Poly I:C induced apoptosis (Fig. 23 B).

To investigate the PKR effect, isolated human islets were pre-treated with 2.5 µM PKRi for 12h before infection. 48 h p.i. TUNEL analysis showed that the PKRi inhibitor had no effect on virus induced apoptosis in isolated human islets (Fig. 23 C).

A

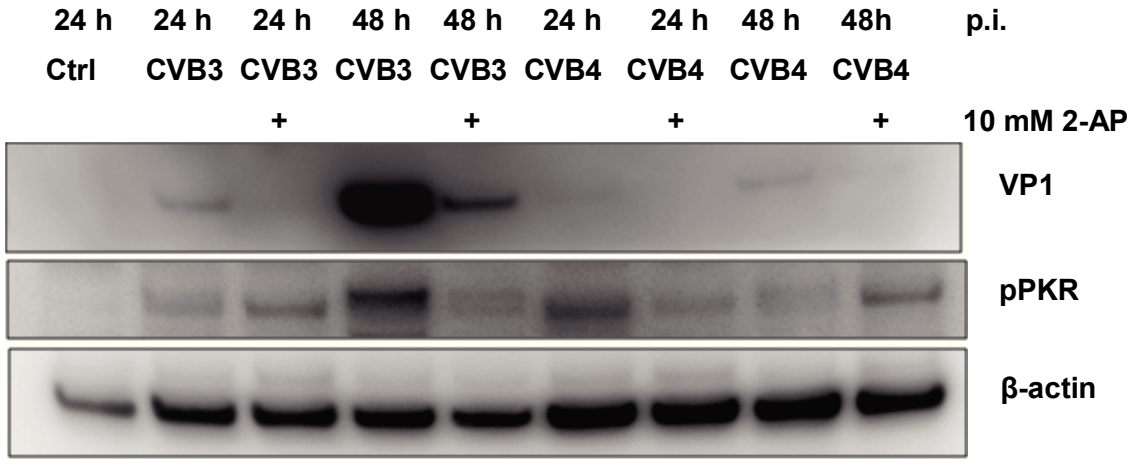

B

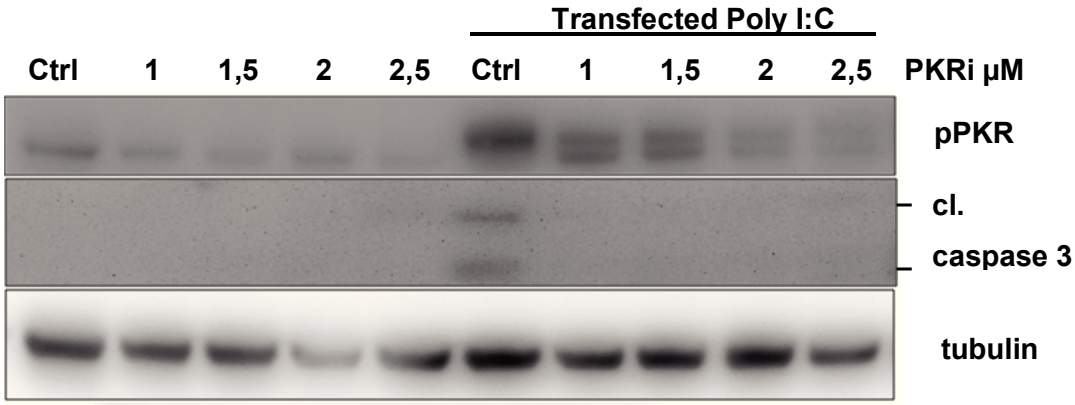

C

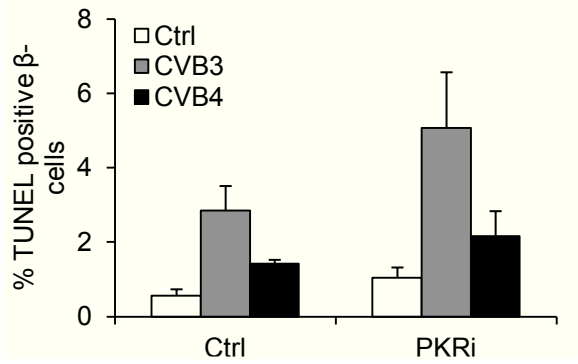

Figure 23: Inhibition of PKR had no effect on virus induced apoptosis. A: Isolated human were infected with CVB3 and CVB4 and after infection islets were exposed to 10 mM 2-AP. 24 h and 48 h p.i. islets were lysed and proteins were analysed by western blotting. β-actin was used as protein loading control (western blot shows one representative result out of two). **B:** CM cells were pre-incubated with 1 µM, 1,5 µM, 2 µM and 2,5 µM of PKRi for 12h. Following that, islets were transfected with 800 ng Poly I:C. The inhibitor was added to the transfection mixes as well as after the transfection. 6 h after transfection, cells were lysed and proteins were analysed by western blot. β-actin was used as protein loading control (western blot shows one representative result out of two). **C:** Isolated human islets were pre-treated with PKRi for 12 h, following that, islets were infected with CVB3 and CVB4. Inhibitor was present in the cell culture supernatants at every step. 48 h p.i. islets were fixed and TUNEL analysis performed (graph shows one representative result out of two).

4.5 CVB3 infects the exocrine tissue in mice

To analyse *in vivo* effects of CVB3 on islets, pancreatic sections from infected A.CA/SnJ-mice were immunohistochemically investigated. Mice infected with CVB3 were sacrificed four days p.i. and pancreas was isolated and paraffin embedded. Pancreatic paraffin sections were immunostained for VP1 and CXCL10.

Results showed a massive infection of the exocrine tissue indicated by VP1 staining with no signs of VP1 expression in islets. Interestingly, CXCL10 immunostaining showed a clear expression in β-cells, while the exocrine tissue showed no CXCL10 staining (Fig. 24).

Control mice showed no VP1 or CXCL10 positive staining.

Since islets were not infected in mice, no further studies of *in vivo* infection were performed.

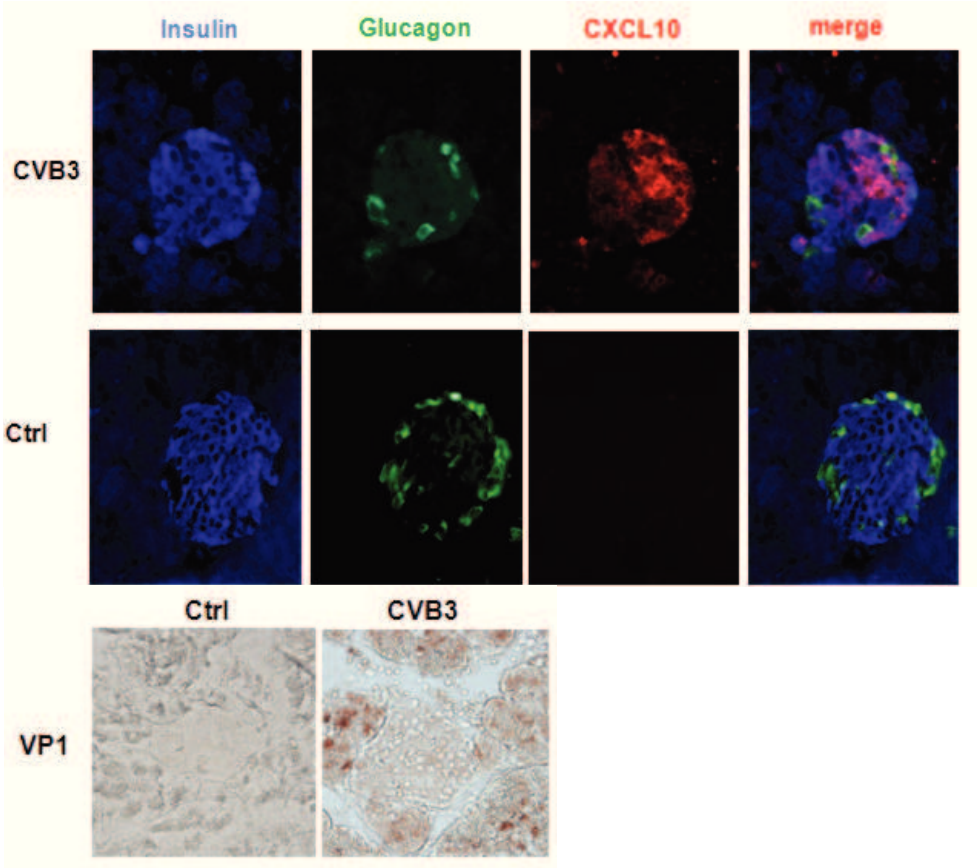

Figure 24: CVB3 infection of the exocrine tissue correlates with CXCL10 expression in β-cells in mice. A.CA/SnJ-mice were inoculated intraperitoneally with $2x10^4$ PFU of CVB3 (Nancy) or with PBS. Four days p.i., infected and control mice were sacrificed and pancreata isolated, fixed, paraffin embedded and microtome sectioned. Bright field staining for VP1 in red and fluorescent staining for insulin in blue, glucagon in green and CXCL10 in red were performed. Merge shows the colocalization of CXCL10 with either insulin positive or glucagon positive cells.

5 Discussion

T1DM is an autoimmune disease in which β-cells are selectively destroyed by the immune system. As consequence of β-cell destruction insulin levels decline, this ends finally in complete insulin deficiency. T1DM is highly associated with genetic susceptibility, however over the last decades the overall incidence is rising especially in children under the age of 5, suggesting that environmental factors contribute to the manifestation of the disease [1, 2]. T1DM is thought to result from the interaction between genetic predisposition, immune system and environmental factors [3]. Such environmental factors may be viral infections, which have been associated with T1DM for many years. So far, the best investigated viral environmental factors with the best documented connection to T1DM are human EVs [4]. Epidemiological studies and analysis of pancreatic tissue samples show the clear involvement of EV infections in T1DM patients. However, the molecular mechanisms of islet infection and how viruses can lead to the disease are still not discovered.

The present study showed that infection of isolated human islets with CVB3 or CVB4 resulted in induction of β-cell apoptosis and expression of genes involved in inflammation which were abrogated upon TLR3 depletion, suggesting that the TLR3 pathway is involved in islet infections with CVB3 and CVB4.

This study showed that infection of isolated human islets with CVB3 and CVB4 resulted in viral replication, confirming published results [108]. Immunohistochemical analysis of pancreatic tissues from T1DM patients shows a specific VP1 colocalization with insulin positive cells, suggesting a β-cell specific infection *in vivo* [101]. In my study, investigation of α- and β-cell specific infections with CVB3 and CVB4 showed that both virus serotypes infected high amounts mainly of β-cells 24 h p.i. CVB3 infected only a small amount of α-cells while CVB4 infected significantly higher numbers of this cell type, displaying different tropisms of CVB3 and CVB4. Tropism of viruses to certain cells results from different expressions of receptors and other host cellular proteins which are needed by the virus to propagate. CVBs use CAR (coxsackie and adenovirus receptor) and DAF (decay accelerating factor) to enter human cells [103, 138, 139]. CAR has been shown to be expressed in human islets, and the application of antibodies neutralizing CAR leads to strong reduction of VP1 positive cells or prevents infection with CVB3 and CVB4. In contrast DAF was not found to be expressed in human islets [140, 141]. So far it is not known which other factors can contribute to the different tropism of CVB3 and CVB4 for α- and β-cells.

Cell death, either necrosis or apoptosis, is induced as the result of various virus infections. CMV, which has been linked to T1DM [81], failed to induce apoptosis in human islets, suggesting that infection of islets did not result in cell death, at least not 72 h p.i. HAV, as CVB is a representative of the picornavirus family, also failed to induce apoptosis. The *in vitro* induced CPE in isolated human islets infected with CVB is shown to be due to cytolysis [142], however, apoptosis has also been observed [109]. At MOIs above 100 it has been shown that CVB5 induces necrosis, while low MOIs lead predominantly to apoptosis [143]. In my study, the MOI of 5 resulted in an increase of cell apoptosis. This was demonstrated by TUNEL staining and cleavage of proapoptotic proteins PARP and caspase 3 in CVB3 and CVB4 infected islets. The CVB3 and CVB4 induced apoptosis was restricted to β-cells, which correlated with β-cell infection, as mainly this cell type showed to be infected by CVB3 and CVB4. In correlation with β-cell apoptosis, the β-cell function was impaired during CVB3 and CVB4 infections indicated by GSIS 48 h p.i., confirming published data [110, 144]. This might be due to the loss of β-cells. In addition, membrane rearrangements, might lead to impaired β-cell function. Many +ssRNA viruses, such as picornaviruses replicate on intracellular membranes. Parts of the membranous structures are shown to be derived from autophagosomes [145]. Such membrane rearrangements can possibly affect formation of insulin granules, resulting in impaired insulin secretion. CVB4 infection of α-cells did not resulted in apoptosis. This implies that CVB4 infections have different outcomes in α- and β-cells. So far, there are no studies in which α-cell infections were investigated. Whether infection also resulted in necrosis in addition to apoptosis, it was not further investigated.

The engagement of PAMPs with PRRs induces the expression of chemokines and cytokines like Type I IFNs as antiviral defence mechanism [123]. The present study showed that mRNA transcription of PRRs involved in recognition of viral infections, in particular *TLR3, RIG-I, MDA5* and *PKR,* were induced after CVB3 and CVB4 infections of isolated human islets 48 h and 72 h p.i. The highest expression was observed 72 h p.i. This time-dependent increase may result from viral progeny. Due to the increasing number of viral particles, which accumulate during infection, virus spreads to neighbouring cells resulting in PRR gene expression.

Picornaviruses are thought to be sensed by MDA5 [146, 147]. However, this does not apply for all members of the picornavirus family. Various studies show the involvement of different PRRs in CVB recognition and antiviral response. MDA5 has been reported to play a role in CVB3 infection. Mice deficient in MDA5 are highly susceptibility to CVB3 infection. Virus replication was shown to be faster and to result in an increase of the mortality [148]. It has also been shown that TLR3 knockout mice are highly susceptible to CVB3 infection, resulting in increased mortality

and viral replication, which suggests that TLR3 limits CVB3 infection [149]. However, CVB3 infection of human cardiac cells is shown to be sensed by TLR7 and 8 [150]. Interestingly TLR4, which binds bacterial LPS, has been implicated in CVB3 infection, as TLR4 deficient mice infected with CVB3 display reduced levels of myocarditis and viral replication. This suggests that TLR4 exacerbates CVB3 infection [151]. CVB4 infection of TLR4 and CD14 overexpressing HEK293 cells triggers the production of pro-inflammatory cytokines [152].

In the present study it was investigated which PRR binds to CVB3 and CVB4 RNA during infection of human islets. IP analysis showed that 24 h p.i. RIG-I and MDA5 showed no binding but PKR was bound to CVB3 and CVB4 RNA. PKR is not a classical PRR, it is an antiviral protein with dsRNA binding potential. Its antiviral property is mediated through stop of translation after infection. dsRNA binding leads to dimerisation and phosphorylation of PKR. Activated PKR is phosphorylating eIF2α, leading to general inhibition of the translation [59]. High PKR expressions have also been found in VP1 positive human islets in sections from T1DM and T2DM patients, showing a clear involvement in the EV infection of the islets [100]. In my study, PKR and its downstream target eIF2α showed to be phosphorylated during CVB3 and CVB4 infections of isolated human islets, as indicated by western blot analysis.

The use of the same strategy to investigate the possible binding of CVB3 and CVB4 RNA to TLR3 and TLR7 showed unreliable results. TLR7 is binding ssRNA molecules. As CVBs are ssRNA viruses, the usage of the K1 antibody, which binds to dsRNA, could have led to misleading results. In order to avoid this, an RNA-IP has been performed with TLR3 and TLR7 antibodies. The results showed that CVB3 RNA was bound by TLR3 while CVB4 RNA was bound by both endosomal receptors TLR3 and TLR7, 24 h and 48 h p.i., suggesting an involvement of TLR3 and TLR7 in CVB3 and CVB4 RNA sensing in isolated human islets in the early phase of the infection. 48 h p.i. binding of CVB RNA to TLR3 and TLR7 was increased, possibly due to increased β-cell infection. A possible explanation for the binding of the CVB3 and CVB4 RNAs to different TLRs may be the different tropism of CVB3 and CVB4. As mentioned above, it has been shown that CVB3 mainly infected β-cells, while CVB4 infected also a certain portion of α-cells. Immmunohistochemical analysis showed that TLR3 was mainly expressed in β-cells, while TLR7 showed a strong colocalization with α-cells. This is a possible explanation why CVB3 RNA was bound to TLR3 and CVB4 RNA to TLR3 and also TLR7 (Fig. 25).

The findings observed could be additionally supported by other methods like RNA label transfer and RNA mobility shift assays.

CVBs enter cells through receptor mediated endocytosis and interaction with TLR3 and TLR7 might occur during this step. Possibly, vesicles containing virions fuse with endosomes where

virions uncoat to release their RNA which might bind to TLR3 and TLR7. However, TLR3 is usually a dsRNA binding receptor. As described above, CVBs are ssRNA viruses which form a dsRNA intermediate in the cytoplasm during replication. It raises the question, how endosomal TLR3 can be engaged by CVB dsRNA. It is conceivable that TLR3 interacts with the IRES structure of the virus genome, which contains large dsRNA regions. Another possibility is that TLR3 binds CVB dsRNA during the replication. EVs replicate on intracellular membranes derived in part from autophagosomes [145]. Phagosomes may fuse with TLR3 containing endosomes, and thus allowing TLR3 to engage with CVB dsRNA [153].

TLR3 and TLR7 might bind to the RNAs in the early phase of the infection as shown 24 h p.i., followed by binding to possibly MDA5 later in the infection. This is supported by the study of Wang et al. who suggested a cooperation of TLR3 and MDA5 in CVB3 RNA sensing, since CVB3 infection of TLR3 and MDA5 double knockout mice show a pronounced effect on mortality [41]. It has also been reported that CVB3 infection of MDA5 knockout mice does not result in an absolute IFNα deficiency, suggesting that MDA5 alone cannot be the only PRR sensing CVB3 [148]. An involvement of MDA5 is further supported by the finding that *IFIH1* gene encoding MDA5 is susceptible to T1DM [40]. As mentioned above, the present study showed no binding of MDA5 and RIG-I to CVB3 and CVB4 RNA 24 h p.i. This suggests that MDA5 and RIG-I are not involved in CVB sensing in isolated human islets. Another possible explanation is that expression of both receptors was too low in infected cells 24 h p.i. and that thus IP analysis showed no binding of those receptors to CVB3 and CVB4 RNA. This is supported by the qPCR results which showed that 24 h p.i. expression of PRRs in CVB3 and CVB4 infected cells was comparable to those in the control.

As mentioned above, the engagement of PAMPs with PRRs induces the expression of chemokines and cytokines like Type I IFNs as antiviral defence mechanism. Previous microarray studies show that upon CVB4 and CVB5 infection, various genes involved in inflammation and antiviral defence were induced [111, 114]. Schulte at al. confirmed the secretion of several cytokines and chemokines [113]. In the present study the mRNA transcription of cytokines and chemokines *CXCL10, IFNβ, IL-6, IL-1β* and *TNFα* was induced, as those of PRRs, after CVB3 and CVB4 infections of the islets and showed the same gene expression pattern as that of PRRs. Using a higher MOI of 20 resulted in earlier cytokine and chemokine gene expressions. The TLR3 knockdown using RNA interference showed that cytokine and chemokine levels especially of *CXCL10* and *IFNβ* were drastically reduced after CVB3 and CVB4 infections, supporting the involvement of TLR3 in CVB3 and CVB4 infections of human islets.

The highest induction and secretion was found for CXCL10, consistent with reported data [111, 113, 154]. The source of CXCL10 were the β-cells itself, as demonstrated by immunostaining. It has been shown that CXCL10 induced activation of the TLR4 pathway has deleterious effects on β-cell survival [137]. In my study the application of a CXCL10 neutralizing antibody had no effect on virus induced β-cell destruction, suggesting that apoptosis was induced by other mechanisms. CXCL10 attracts CXCR3 expressing cells such as activated T-cells, monocytes and natural killer cells [125]. It has been shown that CXCL10 serum levels are elevated in T1DM and in patients with a high risk to develop the disease [126-128]. In addition, CXCL10 expression has been detected in pancreatic sections from three patients who died due to fulminant T1DM. All three patients showed VP1 expression in islets which were infiltrated by CXCR3+ T-cells, suggesting an important role for CXCL10 in virus-induced insulitis [102]. This is supported by a study performed in LCMV infected RIP-GP mice where the application of CXCL10 neutralizing antibodies prevented the induction of T1DM [129].

Together with *CXCL10,* the *IFNβ* gene was highly transcribed in CVB3 and CVB4 infected islets. However, consistent with previous reports, IFNβ protein secretion was not detectable neither by IFNβ ELISA nor plaque reduction assay (data not shown) [113]. IFNα and IFNβ, which belong to the family of type I IFNs, have very strong antiviral activities. Secreted IFNβ acts in an autocrine and paracrine way. It binds to the ubiquitously expressed IFNα/β receptor (IFNAR) on neighbouring cells, which results in the expression of various ISGs (e.g. PKR, OAS1, ISG-15) through the JAK/STAT pathway [155]. The finding that IFNβ protein was not detectable in supernatants from islets infected with CVB3 or CVB4, might be explained by rapid uptake by neighbouring cells. This explanation is supported by the finding that the percentage of CVB3 and CVB4 infected β-cells decreased over time, suggesting that IFNβ can act in a paracrine manner and induce expression of proteins with antiviral activities and hence protect from CVB3 and CVB4 β-cell infection. In addition, treatment with recombinant IFNβ resulted in increased gene expression of PRRs and *CXCL10*, showing that IFNβ can stimulate antiviral activities in human islets, confirming a study demonstrating induction of the antiviral state in human islets upon IFNα stimulation [136]. Another possible explanation for the non detection of IFNβ protein might be a CVB induced disruption of protein translation or secretion. Many viruses, including picornaviruses, evade host cell defences. Viral proteins interfere with pathways inducing *IFNβ* gene expression or signalling or overcome the action of antiviral proteins [155]. It has been reported that CVB3 infection of HEK293 cells results in an only modest IRF3 induced *IFNβ* expression. The viral protease 3C cleaves the adaptor proteins MAVS and TRIF, which mediate RIG-I, MDA5 and TLR3 signalling [156].

The locally produced proinflammatory cytokines and chemokines may have adverse effects on β-cells, leading to cell death [72, 73]. IL-6 is a cytokine with various biological functions in inflammation, immune regulation, hematopoiesis and oncogenesis. Its expression is induced upon viral infections and it has been shown to be also produced in β-cells. Elevated IL-6 levels are implicated in autoimmune diseases such as multiple sclerosis (MS) and rheumatoid arthritis (RA), possibly due to its ability to inhibit TGF-β-induced T_{reg} differentiation [157]. It has been shown that IL-6 induces insulin resistance in adipose tissue and in the liver, and it may synergize with other proinflammatory cytokines to induce β-cell apoptosis [158].
IL-1β has been implicated in the co-stimulation of T-cell function, B-cell proliferation and generation of Th17 response [159]. Various studies show that IL-1β affects β-cell survival. Exposure of isolated human islets to IL-1β leads to impaired β-cell survival and function and induction [70]. It has been shown that elevated glucose concentrations trigger the production of IL-1β, resulting in IL-1β dependent Fas expression and apoptosis [160].
TNFα alone or in combination with IL-1β has also been reported to induce β-cell apoptosis [73].

TLR3 has been shown to have pro-apoptotic functions [161]. In the present study, the infection of TLR3 depleted human islets showed a decrease in CVB3 and CVB4 induced β-cell apoptosis, suggesting a role for TLR3 in virus mediated β-cell death. This was demonstrated by cleavage of caspase 3 and the TUNEL assay. This result is supported by the finding that islets isolated from TLR3 and IRF3 knockout mice exposed to Poly I:C showed decreased levels of β-cell apoptosis, suggesting a pro-apoptotic role for TLR3 in β-cells [162]. In addition, CVB 3C protein has been shown to interfere with the Type I IFN pathway, as already mentioned above, and to reduce the TLR3-TRIF-dependent apoptosis [156]. Furthermore TLR3 induces apoptosis in prostate cancer cells [163] and human breast cancer cells [164]. The Poly I:C induced apoptosis in melanoma cells was reported to be caspase 8-dependent [161]. A recent study by Sun et al. showed that both extrinsic and intrinsic apoptotic pathways are involved in TLR3 dependent apoptosis. This is due to the TLR3 dependent activation of a p53-related protein, the transactivating p63 isoform α (TAp63α), which activates both apoptotic pathways [165].
In the present study, the decrease of caspase 3 correlated with an increase in VP1 bands in TLR3 depleted islets infected with CVB3 and CVB4, suggesting that apoptosis was not induced by CVB3 and CVB4 but rather through cellular mechanism. Apoptosis is a potent antiviral mechanism, limiting viral spread [166]. Decrease of apoptosis in viral infected cells could lead to the increase in virus spread and thus to higher replication. In addition, TLR3 depletion can lead to lower gene expression and secretion of cytokines and chemokines like Type I IFNs, which

may result in a lower antiviral response and thus in higher viral replication. The finding observed is also supported by the fact that IFNβ induces the so called “antiviral state” by increasing the expression of various antiviral ISGs in neighbouring cells which are not infected. The infection of such a “warned” cell leads to apoptosis [166].

It has been shown that the JNK pathway is activated upon various stress stimuli including, UV irradiation, hyperosmolarity, and heat shock, and upon exposure of pro-inflammatory cytokines such as TNFα and IL-1β [167]. JNK is a member if a group of serin/threonin protein kinases known as mitogen activated protein kinases (MAPK). The JNK pathway is involved in cell apoptosis. JNK dependent apoptosis is mediated by the transport of proapoptotic proteins like Bax to the mitochondria, resulting in cytochrome c release from mitochondria to the cytoplasm [168]. It has been reported that the JNK pathway is also involved in virus mediated apoptosis induced by some viruses such as poliovirus [169]. The MAP kinases JNK and p38 are also involved in the TLR, MDA5 and RIG-I mediated induction of Type I IFNs [52] and it has been reported that TLR3 mediated apoptosis was dependent on JNK and p38 in a human prostate cancer cell line. This was investigated by the application of the JNK and p38 inhibitors SB203580 and SP600125 which results in the decrease of apoptosis after Poly I:C treatment [163]. In addition, it has been shown that CVB3 infection of Hela cells results in cell apoptosis which is dependent on JNK [170].

The present study showed the involvement of JNK in CVB3 infected CM cells. JNK phosphorylation was also observed in CVB3 and CVB4 infected human islets. Here, the caspase 3 cleavage correlated with the phosphorylation of JNK, demonstrated by western blotting, suggesting a possible role for pJNK in CVB3 mediated apoptosis in CM cells and human islets. In this study the application of the JNK inhibitor SP600125 also resulted in the decrease of apoptosis, as mentioned above, in CVB3 and CVB4 infected islets, as demonstrated by western blotting. However, SP600125 treatment also resulted in the decrease of VP1 bands, suggesting that the inhibitor causes alterations in CVB replication. Due to that, a dominant negative variant of JNK1 was overexpressed in isolated human islets. Overexpression resulted in increase of both isoforms of JNK, JNK1 and 2, suggesting a mutual regulation of JNK1 and 2 gene expressions. CVB3 infected isolated human islets overexpressing dnJNK1 showed less apoptosis compared to control. The results obtained imply a role for activated JNK in the CVB3 induced apoptosis in isolated human islets. However, the rescuing effect was only partial demonstrated by reduced cleavage of caspase 3 and PARP, although JNK function was absolutely inhibited demonstrated by the loss of the phosphorylation of c-Jun. Due to the restricted access to isolated human islets, the results from the dnJNK overexpressing study were

performed once and need additional confirmation. The possible relationship between TLR3 and JNK pathways was not further investigated.

Previous studies reveal that JNK activation can be mediated trough PKR [171]. In the present study it has been shown that PKR is engaged by CVB3 and CVB4 RNA, which resulted in the activation of PKR and phosphorylation of its downstream target eIF2α. A co-immunoprecipitation analysis performed in this study showed no association between PKR and JNK, suggesting that PKR had no effect on JNK activation (data not shown).

It has been clearly indicated that PKR is involved in virus induced apoptosis. This is mainly dependent on the FADD/caspase 8 pathway. In addition, it has been suggested that the phosphorylation of eIF2α and the inhibition of translation may provoke apoptosis [172]. In my study PKR inhibition with the known inhibitor 2-AP resulted in side effects including alterations in CVB3 and CVB4 replication demonstrated by the massive decrease of VP1 bands displayed by western blotting. 2-AP is a guanosine and adenosine analog. Possibly, integration of the analog during viral replication can lead to alterations in replication and less VP1 expression. The application of another PKR inhibitor, PKRi, resulted in decreased apoptosis in CM cells following Poly I:C transfection. However, PKRi had no effect on CVB3 and CVB4 induced apoptosis in isolated human islets, suggesting that PKR is not involved in the CVB mediated induction of apoptosis in human isolated islets. To eliminate side effects caused by inhibitors, other methods such as RNA interference should be applied.

This study shows for the first time the involvement of TLR3 in virus induced expression of pro-inflammatory genes and the involvement of TLR3 and JNK in virus mediated β-cell apoptosis. Apoptotic β-cells can be phagocytised by APCs leading to the presentation of viral but also of β-cell antigens. This results in activation of cytotoxic T-cells. In addition, high expression of cytokines and chemokines such as CXCL10 contribute to the attraction and the activation of immune cells. Both effects can be crucial for the initialization of autoimmunity in genetically susceptible individuals.

In conclusion, this study showed that *in vitro* infection of isolated human islets with CVB3 and CVB4 resulted in β-cell infection, apoptosis and impaired function. Both viruses induced TLR3 dependent expression of several pro-inflammatory genes and CXCL10 secretion in which the source of CXCL10 was the β-cell itself. Virus induced β-cell apoptosis was dependent on the TLR3 and JNK pathways. This study can contribute to the understanding of cellular mechanisms during CVB β-cell infection in order to develop new therapies to prevent CVB induced T1DM.

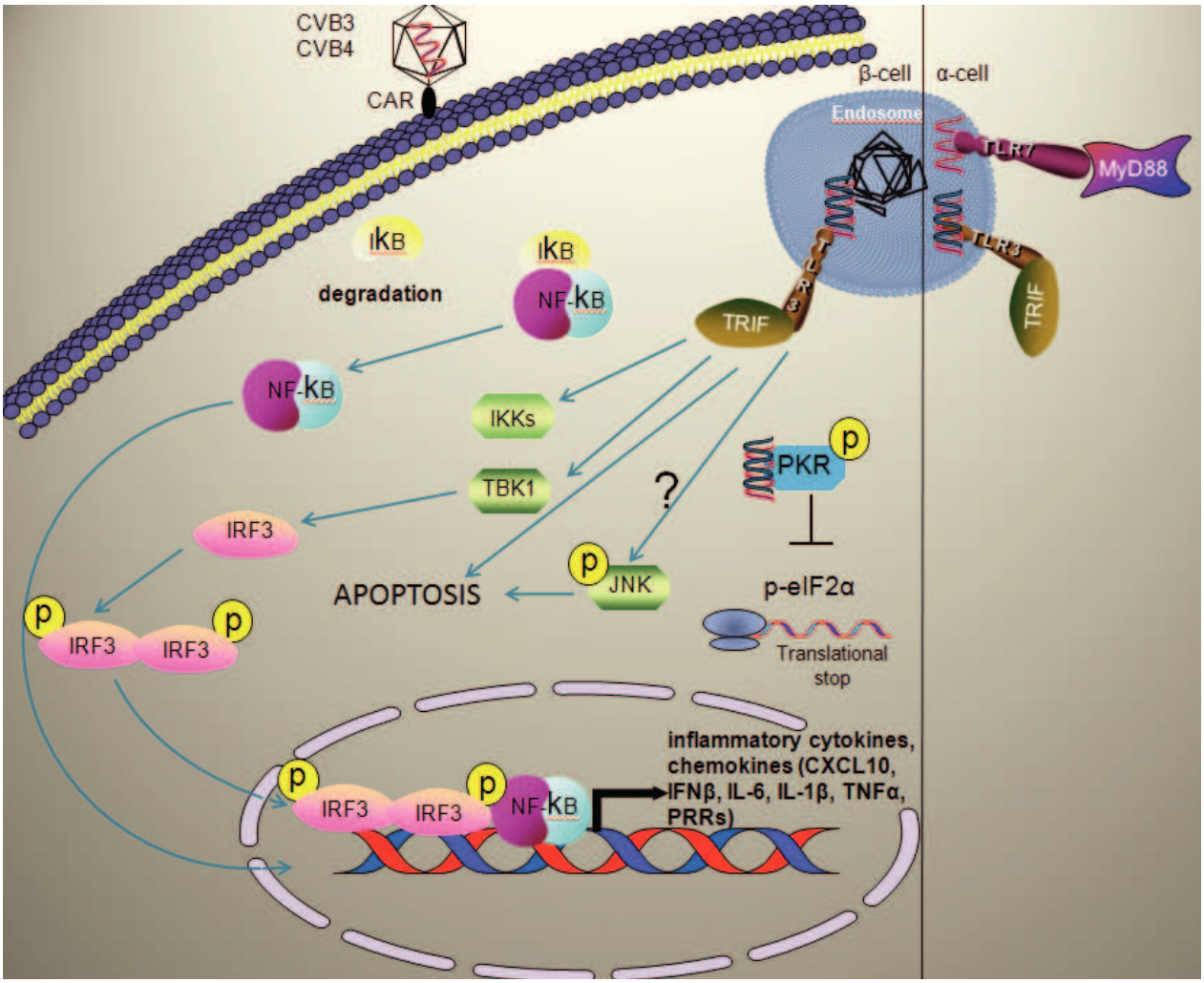

Figure 25: Proposed mechanism of CVB3 and CVB4 induced apoptosis and gene upregulation of cytokines and chemokines in α- and β-cells. CVB3 and CVB4 infections of β-cells result in binding of CVB3 and CVB4 RNA to TLR3 which leads to the activation of the TLR3 pathway and upregulation of cytokine, chemokine and PRR gene expressions. Binding of CVB3 and CVB4 RNA to PKR results in phosphorylation and activation of PKR, which in turn phosphorylates eIF2α and thus induces translational stop. In addition JNK and TLR3 induce apoptosis of β-cells. Whether JNK induced apoptosis is also TLR3 dependent is not known. CVB3 and CVB4 infection of α-cells results in binding of CVB3 and CVB4 RNA to TLR3 as well as to TLR7.

6 References

1. *Variation and trends in incidence of childhood diabetes in Europe. EURODIAB ACE Study Group.* Lancet, 2000. **355**(9207): p. 873-6.
2. *Incidence and trends of childhood Type 1 diabetes worldwide 1990-1999.* Diabet Med, 2006. **23**(8): p. 857-66.
3. Hober, D. and P. Sauter, *Pathogenesis of type 1 diabetes mellitus: interplay between enterovirus and host.* Nature Reviews Endocrinology, 2010. **6**(5): p. 279-289.
4. Coppieters, K.T., T. Boettler, and M. von Herrath, *Virus infections in type 1 diabetes.* Cold Spring Harb Perspect Med. **2**(1): p. a007682.
5. Islam, M.S. and SpringerLink (Online service), *The Islets of Langerhans* Advances in Experimental Medicine and Biology, Dordrecht: Springer Science+Business Media B.V.
6. In't Veld, P. and M. Marichal, *Microscopic anatomy of the human islet of Langerhans.* Adv Exp Med Biol. **654**: p. 1-19.
7. Dunning, B.E. and J.E. Gerich, *The role of alpha-cell dysregulation in fasting and postprandial hyperglycemia in type 2 diabetes and therapeutic implications.* Endocr Rev, 2007. **28**(3): p. 253-83.
8. Brissova, M., et al., *Assessment of human pancreatic islet architecture and composition by laser scanning confocal microscopy.* J Histochem Cytochem, 2005. **53**(9): p. 1087-97.
9. Stumvoll, M., B.J. Goldstein, and T.W. van Haeften, *Type 2 diabetes: principles of pathogenesis and therapy.* Lancet, 2005. **365**(9467): p. 1333-46.
10. Joshi, S.R., R.M. Parikh, and A.K. Das, *Insulin--history, biochemistry, physiology and pharmacology.* J Assoc Physicians India, 2007. **55 Suppl**: p. 19-25.
11. Kojima, S., et al., *A role for pancreatic polypeptide in feeding and body weight regulation.* Peptides, 2007. **28**(2): p. 459-63.
12. Steiner, D.J., et al., *Pancreatic islet plasticity: interspecies comparison of islet architecture and composition.* Islets. **2**(3): p. 135-45.
13. Wild, S., et al., *Global prevalence of diabetes: estimates for the year 2000 and projections for 2030.* Diabetes Care, 2004. **27**(5): p. 1047-53.
14. Daneman, D., *Type 1 diabetes.* Lancet, 2006. **367**(9513): p. 847-58.

15. Tracy, S., et al., *Enteroviruses, type 1 diabetes and hygiene: a complex relationship.* Rev Med Virol. **20**(2): p. 106-16.
16. Handel, A.E., et al., *Type 1 diabetes mellitus and multiple sclerosis: common etiological features.* Nat Rev Endocrinol, 2009. **5**(12): p. 655-64.
17. Coppieters, K.T., et al., *Immunology in the clinic review series: focus on type 1 diabetes and viruses: the role of viruses in type 1 diabetes: a difficult dilemma.* Clin Exp Immunol. **168**(1): p. 5-11.
18. Patterson, C.C., et al., *Incidence trends for childhood type 1 diabetes in Europe during 1989-2003 and predicted new cases 2005-20: a multicentre prospective registration study.* Lancet, 2009. **373**(9680): p. 2027-33.
19. Kyvik, K.O., A. Green, and H. Beck-Nielsen, *Concordance rates of insulin dependent diabetes mellitus: a population based study of young Danish twins.* BMJ, 1995. **311**(7010): p. 913-7.
20. Noble, J.A., et al., *The role of HLA class II genes in insulin-dependent diabetes mellitus: molecular analysis of 180 Caucasian, multiplex families.* Am J Hum Genet, 1996. **59**(5): p. 1134-48.
21. Hober, D. and F. Sane, *Enteroviral pathogenesis of type 1 diabetes.* Discov Med. **10**(51): p. 151-60.
22. van Belle, T.L., K.T. Coppieters, and M.G. von Herrath, *Type 1 diabetes: etiology, immunology, and therapeutic strategies.* Physiol Rev. **91**(1): p. 79-118.
23. Ziegler, A.G. and G.T. Nepom, *Prediction and pathogenesis in type 1 diabetes.* Immunity. **32**(4): p. 468-78.
24. Todd, J.A., *Etiology of type 1 diabetes.* Immunity. **32**(4): p. 457-67.
25. Bonifacio, E., et al., *IDDM1 and multiple family history of type 1 diabetes combine to identify neonates at high risk for type 1 diabetes.* Diabetes Care, 2004. **27**(11): p. 2695-700.
26. Erlich, H.A., et al., *HLA class II alleles and susceptibility and resistance to insulin dependent diabetes mellitus in Mexican-American families.* Nat Genet, 1993. **3**(4): p. 358-64.
27. Valdes, A.M., H.A. Erlich, and J.A. Noble, *Human leukocyte antigen class I B and C loci contribute to Type 1 Diabetes (T1D) susceptibility and age at T1D onset.* Hum Immunol, 2005. **66**(3): p. 301-13.
28. Nejentsev, S., et al., *Localization of type 1 diabetes susceptibility to the MHC class I genes HLA-B and HLA-A.* Nature, 2007. **450**(7171): p. 887-92.

29. Noble, J.A., et al., *Type 1 diabetes risk for human leukocyte antigen (HLA)-DR3 haplotypes depends on genotypic context: association of DPB1 and HLA class I loci among DR3- and DR4-matched Italian patients and controls.* Hum Immunol, 2008. **69**(4-5): p. 291-300.

30. Fennessy, M., et al., *A gene in the HLA class I region contributes to susceptibility to IDDM in the Finnish population. Childhood Diabetes in Finland (DiMe) Study Group.* Diabetologia, 1994. **37**(9): p. 937-44.

31. Bennett, S.T., et al., *Susceptibility to human type 1 diabetes at IDDM2 is determined by tandem repeat variation at the insulin gene minisatellite locus.* Nat Genet, 1995. **9**(3): p. 284-92.

32. Kennedy, G.C., M.S. German, and W.J. Rutter, *The minisatellite in the diabetes susceptibility locus IDDM2 regulates insulin transcription.* Nat Genet, 1995. **9**(3): p. 293-8.

33. Pugliese, A., et al., *The insulin gene is transcribed in the human thymus and transcription levels correlated with allelic variation at the INS VNTR-IDDM2 susceptibility locus for type 1 diabetes.* Nat Genet, 1997. **15**(3): p. 293-7.

34. Pugliese, A., et al., *The paternally inherited insulin gene B allele (1,428 FokI site) confers protection from insulin-dependent diabetes in families.* J Autoimmun, 1994. **7**(5): p. 687-94.

35. Fan, Y., et al., *Thymus-specific deletion of insulin induces autoimmune diabetes.* EMBO J, 2009. **28**(18): p. 2812-24.

36. Bottini, N., et al., *A functional variant of lymphoid tyrosine phosphatase is associated with type I diabetes.* Nat Genet, 2004. **36**(4): p. 337-8.

37. Lowe, C.E., et al., *Large-scale genetic fine mapping and genotype-phenotype associations implicate polymorphism in the IL2RA region in type 1 diabetes.* Nat Genet, 2007. **39**(9): p. 1074-82.

38. Hulme, M.A., et al., *Central role for interleukin-2 in type 1 diabetes.* Diabetes. **61**(1): p. 14-22.

39. Filippi, C.M. and M.G. von Herrath, *99th Dahlem conference on infection, inflammation and chronic inflammatory disorders: viruses, autoimmunity and immunoregulation.* Clin Exp Immunol. **160**(1): p. 113-9.

40. Nejentsev, S., et al., *Rare variants of IFIH1, a gene implicated in antiviral responses, protect against type 1 diabetes.* Science, 2009. **324**(5925): p. 387-9.

41. Wang, J.P., et al., *MDA5 and MAVS mediate type I interferon responses to coxsackie B virus.* J Virol. **84**(1): p. 254-60.
42. Diao, F., et al., *Negative regulation of MDA5- but not RIG-I-mediated innate antiviral signaling by the dihydroxyacetone kinase.* Proc Natl Acad Sci U S A, 2007. **104**(28): p. 11706-11.
43. Shigemoto, T., et al., *Identification of loss of function mutations in human genes encoding RIG-I and MDA5: implications for resistance to type I diabetes.* J Biol Chem, 2009. **284**(20): p. 13348-54.
44. Cooper, J.D., et al., *Follow-up of 1715 SNPs from the Wellcome Trust Case Control Consortium genome-wide association study in type I diabetes families.* Genes Immun, 2009. **10 Suppl 1**: p. S85-94.
45. Akira, S., S. Uematsu, and O. Takeuchi, *Pathogen recognition and innate immunity.* Cell, 2006. **124**(4): p. 783-801.
46. Akira, S., *Toll-like receptor signaling.* J Biol Chem, 2003. **278**(40): p. 38105-8.
47. Takeuchi, O. and S. Akira, *Pattern recognition receptors and inflammation.* Cell. **140**(6): p. 805-20.
48. Alexopoulou, L., et al., *Recognition of double-stranded RNA and activation of NF-kappaB by Toll-like receptor 3.* Nature, 2001. **413**(6857): p. 732-8.
49. Sharma, S., et al., *Triggering the interferon antiviral response through an IKK-related pathway.* Science, 2003. **300**(5622): p. 1148-51.
50. Sato, S., et al., *Toll/IL-1 receptor domain-containing adaptor inducing IFN-beta (TRIF) associates with TNF receptor-associated factor 6 and TANK-binding kinase 1, and activates two distinct transcription factors, NF-kappa B and IFN-regulatory factor-3, in the Toll-like receptor signaling.* J Immunol, 2003. **171**(8): p. 4304-10.
51. Jiang, Z., et al., *Toll-like receptor 3-mediated activation of NF-kappaB and IRF3 diverges at Toll-IL-1 receptor domain-containing adapter inducing IFN-beta.* Proc Natl Acad Sci U S A, 2004. **101**(10): p. 3533-8.
52. Kawai, T. and S. Akira, *TLR signaling.* Cell Death Differ, 2006. **13**(5): p. 816-25.
53. Kaiser, W.J. and M.K. Offermann, *Apoptosis induced by the toll-like receptor adaptor TRIF is dependent on its receptor interacting protein homotypic interaction motif.* J Immunol, 2005. **174**(8): p. 4942-52.
54. Han, K.J., et al., *Mechanisms of the TRIF-induced interferon-stimulated response element and NF-kappaB activation and apoptosis pathways.* J Biol Chem, 2004. **279**(15): p. 15652-61.

55. Yoneyama, M., et al., *The RNA helicase RIG-I has an essential function in double-stranded RNA-induced innate antiviral responses.* Nat Immunol, 2004. **5**(7): p. 730-7.
56. Yoneyama, M., et al., *Shared and unique functions of the DExD/H-box helicases RIG-I, MDA5, and LGP2 in antiviral innate immunity.* J Immunol, 2005. **175**(5): p. 2851-8.
57. Yoneyama, M. and T. Fujita, *RNA recognition and signal transduction by RIG-I-like receptors.* Immunol Rev, 2009. **227**(1): p. 54-65.
58. Seth, R.B., et al., *Identification and characterization of MAVS, a mitochondrial antiviral signaling protein that activates NF-kappaB and IRF 3.* Cell, 2005. **122**(5): p. 669-82.
59. Pfaller, C.K., et al., *Protein kinase PKR and RNA adenosine deaminase ADAR1: new roles for old players as modulators of the interferon response.* Curr Opin Immunol. **23**(5): p. 573-82.
60. Nakamura, T., et al., *Double-stranded RNA-dependent protein kinase links pathogen sensing with stress and metabolic homeostasis.* Cell. **140**(3): p. 338-48.
61. LaGasse, J.M., et al., *Successful prospective prediction of type 1 diabetes in schoolchildren through multiple defined autoantibodies: an 8-year follow-up of the Washington State Diabetes Prediction Study.* Diabetes Care, 2002. **25**(3): p. 505-11.
62. Kulmala, P., et al., *Prediction of insulin-dependent diabetes mellitus in siblings of children with diabetes. A population-based study. The Childhood Diabetes in Finland Study Group.* J Clin Invest, 1998. **101**(2): p. 327-36.
63. Cucca, F., et al., *A correlation between the relative predisposition of MHC class II alleles to type 1 diabetes and the structure of their proteins.* Hum Mol Genet, 2001. **10**(19): p. 2025-37.
64. Pescovitz, M.D., et al., *Rituximab, B-lymphocyte depletion, and preservation of beta-cell function.* N Engl J Med, 2009. **361**(22): p. 2143-52.
65. Skowera, A., et al., *CTLs are targeted to kill beta cells in patients with type 1 diabetes through recognition of a glucose-regulated preproinsulin epitope.* J Clin Invest, 2008. **118**(10): p. 3390-402.
66. Di Lorenzo, T.P., M. Peakman, and B.O. Roep, *Translational mini-review series on type 1 diabetes: Systematic analysis of T cell epitopes in autoimmune diabetes.* Clin Exp Immunol, 2007. **148**(1): p. 1-16.
67. Itoh, N., et al., *Mononuclear cell infiltration and its relation to the expression of major histocompatibility complex antigens and adhesion molecules in pancreas biopsy*

specimens from newly diagnosed insulin-dependent diabetes mellitus patients. J Clin Invest, 1993. **92**(5): p. 2313-22.

68. Foulis, A.K., et al., *The histopathology of the pancreas in type 1 (insulin-dependent) diabetes mellitus: a 25-year review of deaths in patients under 20 years of age in the United Kingdom.* Diabetologia, 1986. **29**(5): p. 267-74.
69. Willcox, A., et al., *Analysis of islet inflammation in human type 1 diabetes.* Clin Exp Immunol, 2009. **155**(2): p. 173-81.
70. Eizirik, D.L. and T. Mandrup-Poulsen, *A choice of death--the signal-transduction of immune-mediated beta-cell apoptosis.* Diabetologia, 2001. **44**(12): p. 2115-33.
71. Kreuwel, H.T. and L.A. Sherman, *The role of Fas-FasL in CD8+ T-cell-mediated insulin-dependent diabetes mellitus (IDDM).* J Clin Immunol, 2001. **21**(1): p. 15-8.
72. Cnop, M., et al., *Mechanisms of pancreatic beta-cell death in type 1 and type 2 diabetes: many differences, few similarities.* Diabetes, 2005. **54 Suppl 2**: p. S97-107.
73. Eizirik, D.L., M.L. Colli, and F. Ortis, *The role of inflammation in insulitis and beta-cell loss in type 1 diabetes.* Nat Rev Endocrinol, 2009. **5**(4): p. 219-26.
74. Mathis, D., L. Vence, and C. Benoist, *beta-Cell death during progression to diabetes.* Nature, 2001. **414**(6865): p. 792-8.
75. Martin Joseph Richer1, M.S.H., *Viral infections in the pathogenesis of autoimmune diseases: focus on type 1 diabetes.* Frontiers in Bioscience, 2008. **13, 4241-4257**: p. 4241-4257.
76. Goto, A., et al., *A case of fulminant type 1 diabetes associated with significant elevation of mumps titers.* Endocr J, 2008. **55**(3): p. 561-4.
77. Honeyman, M., *How robust is the evidence for viruses in the induction of type 1 diabetes?* Curr Opin Immunol, 2005. **17**(6): p. 616-23.
78. Honeyman, M.C., N.L. Stone, and L.C. Harrison, *T-cell epitopes in type 1 diabetes autoantigen tyrosine phosphatase IA-2: potential for mimicry with rotavirus and other environmental agents.* Mol Med, 1998. **4**(4): p. 231-9.
79. Honeyman, M.C., et al., *Association between rotavirus infection and pancreatic islet autoimmunity in children at risk of developing type 1 diabetes.* Diabetes, 2000. **49**(8): p. 1319-24.
80. Blomqvist, M., et al., *Rotavirus infections and development of diabetes-associated autoantibodies during the first 2 years of life.* Clin Exp Immunol, 2002. **128**(3): p. 511-5.

81. Nicoletti, F., et al., *Correlation between islet cell antibodies and anti-cytomegalovirus IgM and IgG antibodies in healthy first-degree relatives of type 1 (insulin-dependent) diabetic patients.* Clin Immunol Immunopathol, 1990. **55**(1): p. 139-47.

82. Jaidane, H., et al., *Enteroviruses and type 1 diabetes: towards a better understanding of the relationship.* Reviews in Medical Virology, 2010. **20**(5): p. 265-280.

83. Zoll, J., et al., *The structure-function relationship of the enterovirus 3'-UTR.* Virus Res, 2009. **139**(2): p. 209-16.

84. Whitton, J.L., *Immunopathology during coxsackievirus infection.* Springer Semin Immunopathol, 2002. **24**(2): p. 201-13.

85. Gamble, D.R., et al., *Viral antibodies in diabetes mellitus.* Br Med J, 1969. **3**(5671): p. 627-30.

86. Yoon, J.W., et al., *Isolation of a virus from the pancreas of a child with diabetic ketoacidosis.* N Engl J Med, 1979. **300**(21): p. 1173-9.

87. Banatvala, J.E., et al., *Coxsackie B, mumps, rubella, and cytomegalovirus specific IgM responses in patients with juvenile-onset insulin-dependent diabetes mellitus in Britain, Austria, and Australia.* Lancet, 1985. **1**(8443): p. 1409-12.

88. Clements, G.B., D.N. Galbraith, and K.W. Taylor, *Coxsackie B virus infection and onset of childhood diabetes.* Lancet, 1995. **346**(8969): p. 221-3.

89. Tauriainen, S., et al., *Enteroviruses in the pathogenesis of type 1 diabetes.* Seminars in Immunopathology, 2011. **33**(1): p. 45-55.

90. Hiltunen, M., et al., *Islet cell antibody seroconversion in children is temporally associated with enterovirus infections. Childhood Diabetes in Finland (DiMe) Study Group.* J Infect Dis, 1997. **175**(3): p. 554-60.

91. Lonnrot, M., et al., *Enterovirus infection as a risk factor for beta-cell autoimmunity in a prospectively observed birth cohort: the Finnish Diabetes Prediction and Prevention Study.* Diabetes, 2000. **49**(8): p. 1314-8.

92. Lonnrot, M., et al., *Enterovirus RNA in serum is a risk factor for beta-cell autoimmunity and clinical type 1 diabetes: a prospective study. Childhood Diabetes in Finland (DiMe) Study Group.* J Med Virol, 2000. **61**(2): p. 214-20.

93. Salminen, K., et al., *Enterovirus infections are associated with the induction of beta-cell autoimmunity in a prospective birth Cohort study.* Journal of Medical Virology, 2003. **69**(1): p. 91-98.

94. Oikarinen, S., et al., *Enterovirus RNA in Blood Is Linked to the Development of Type 1 Diabetes.* Diabetes, 2011. **60**(1): p. 276-279.

95. Fuchtenbusch, M., et al., *No evidence for an association of coxsackie virus infections during pregnancy and early childhood with development of islet autoantibodies in offspring of mothers or fathers with type 1 diabetes.* J Autoimmun, 2001. **17**(4): p. 333-40.

96. Graves, P.M., et al., *Prospective study of enteroviral infections and development of beta-cell autoimmunity. Diabetes autoimmunity study in the young (DAISY).* Diabetes Res Clin Pract, 2003. **59**(1): p. 51-61.

97. Stene, L.C. and M. Rewers, *Immunology in the clinic review series; focus on type 1 diabetes and viruses: the enterovirus link to type 1 diabetes: critical review of human studies.* Clin Exp Immunol. **168**(1): p. 12-23.

98. Oikarinen, M., et al., *Type 1 diabetes is associated with enterovirus infection in gut mucosa.* Diabetes. **61**(3): p. 687-91.

99. Mercalli, A., et al., *No evidence of enteroviruses in the intestine of patients with type 1 diabetes.* Diabetologia. **55**(9): p. 2479-88.

100. Richardson, S.J., et al., *The prevalence of enteroviral capsid protein vp1 immunostaining in pancreatic islets in human type 1 diabetes.* Diabetologia, 2009. **52**(6): p. 1143-51.

101. Dotta, F., et al., *Coxsackie B4 virus infection of beta cells and natural killer cell insulitis in recent-onset type 1 diabetic patients.* Proc Natl Acad Sci U S A, 2007. **104**(12): p. 5115-20.

102. Tanaka, S., et al., *Enterovirus infection, CXC chemokine ligand 10 (CXCL10), and CXCR3 circuit: a mechanism of accelerated beta-cell failure in fulminant type 1 diabetes.* Diabetes, 2009. **58**(10): p. 2285-91.

103. Bergelson, J.M., et al., *Isolation of a common receptor for Coxsackie B viruses and adenoviruses 2 and 5.* Science, 1997. **275**(5304): p. 1320-3.

104. Bergelson, J.M., et al., *Coxsackievirus B3 adapted to growth in RD cells binds to decay-accelerating factor (CD55).* J Virol, 1995. **69**(3): p. 1903-6.

105. Oikarinen, M., et al., *Analysis of pancreas tissue in a child positive for islet cell antibodies.* Diabetologia, 2008. **51**(10): p. 1796-802.

106. Shibasaki, S., et al., *Expression of toll-like receptors in the pancreas of recent-onset fulminant type 1 diabetes.* Endocr J. **57**(3): p. 211-9.

107. Yeung, W.C., W.D. Rawlinson, and M.E. Craig, *Enterovirus infection and type 1 diabetes mellitus: systematic review and meta-analysis of observational molecular studies.* BMJ. **342**: p. d35.

108. Roivainen, M., et al., *Functional impairment and killing of human beta cells by enteroviruses: the capacity is shared by a wide range of serotypes, but the extent is a characteristic of individual virus strains.* Diabetologia, 2002. **45**(5): p. 693-702.

109. Roivainen, M., et al., *Mechanisms of coxsackievirus-induced damage to human pancreatic beta-cells.* J Clin Endocrinol Metab, 2000. **85**(1): p. 432-40.

110. Grieco, F.A., et al., *Immunology in the clinic review series; focus on type 1 diabetes and viruses: how viral infections modulate beta cell function.* Clin Exp Immunol. **168**(1): p. 24-9.

111. Ylipaasto, P., et al., *Global profiling of coxsackievirus- and cytokine-induced gene expression in human pancreatic islets.* Diabetologia, 2005. **48**(8): p. 1510-22.

112. Olsson, A., et al., *Inflammatory gene expression in Coxsackievirus B-4-infected human islets of Langerhans.* Biochem Biophys Res Commun, 2005. **330**(2): p. 571-6.

113. Barbara M. Schulte, 2 Kjerstin H.W. Lanke,2 Jon D. Piganelli,3 Esther D. Kers-Rebel,1 Rita Bottino,3, R.J.F.H. Massimo Trucco, 4 Timothy R.D.J. Radstake,4 Marten A. Engelse,5, and J.M.G. Eelco J.P. de Koning, 2 Gosse J. Adema,1 and Frank J.M. van Kuppeveld2, *Cytokine and Chemokine Production by Human Pancreatic Islets Upon Enterovirus Infection.* **Diabetes**, 2012.

114. Ylipaasto, P., et al., *Enterovirus-induced gene expression profile is critical for human pancreatic islet destruction.* Diabetologia.

115. Munz, C., et al., *Antiviral immune responses: triggers of or triggered by autoimmunity?* Nat Rev Immunol, 2009. **9**(4): p. 246-58.

116. Kaufman, D.L., et al., *Autoimmunity to two forms of glutamate decarboxylase in insulin-dependent diabetes mellitus.* J Clin Invest, 1992. **89**(1): p. 283-92.

117. Atkinson, M.A., et al., *Cellular immunity to a determinant common to glutamate decarboxylase and coxsackie virus in insulin-dependent diabetes.* J Clin Invest, 1994. **94**(5): p. 2125-9.

118. Varela-Calvino, R., et al., *T-Cell reactivity to the P2C nonstructural protein of a diabetogenic strain of coxsackievirus B4.* Virology, 2000. **274**(1): p. 56-64.

119. Horwitz, M.S., et al., *Diabetes induced by Coxsackie virus: initiation by bystander damage and not molecular mimicry.* Nat Med, 1998. **4**(7): p. 781-5.

120. Schloot, N.C., et al., *Molecular mimicry in type 1 diabetes mellitus revisited: T-cell clones to GAD65 peptides with sequence homology to Coxsackie or proinsulin peptides do not crossreact with homologous counterpart.* Hum Immunol, 2001. **62**(4): p. 299-309.

121. Horwitz, M.S., et al., *Coxsackieviral-mediated diabetes: induction requires antigen-presenting cells and is accompanied by phagocytosis of beta cells.* Clin Immunol, 2004. **110**(2): p. 134-44.

122. Seewaldt, S., et al., *Virus-induced autoimmune diabetes: most beta-cells die through inflammatory cytokines and not perforin from autoreactive (anti-viral) cytotoxic T-lymphocytes.* Diabetes, 2000. **49**(11): p. 1801-9.

123. Lind, K., M.H. Huhn, and M. Flodstrom-Tullberg, *Immunology in the clinic review series; focus on type 1 diabetes and viruses: the innate immune response to enteroviruses and its possible role in regulating type 1 diabetes.* Clin Exp Immunol. **168**(1): p. 30-8.

124. Berg, A.K., O. Korsgren, and G. Frisk, *Induction of the chemokine interferon-gamma-inducible protein-10 in human pancreatic islets during enterovirus infection.* Diabetologia, 2006. **49**(11): p. 2697-703.

125. Baggiolini, M., B. Dewald, and B. Moser, *Human chemokines: an update.* Annu Rev Immunol, 1997. **15**: p. 675-705.

126. Nicoletti, F., et al., *Serum concentrations of the interferon-gamma-inducible chemokine IP-10/CXCL10 are augmented in both newly diagnosed Type I diabetes mellitus patients and subjects at risk of developing the disease.* Diabetologia, 2002. **45**(8): p. 1107-10.

127. Devaraj, S. and I. Jialal, *Increased secretion of IP-10 from monocytes under hyperglycemia is via the TLR2 and TLR4 pathway.* Cytokine, 2009. **47**(1): p. 6-10.

128. Shigihara, T., et al., *Significance of serum CXCL10/IP-10 level in type 1 diabetes.* J Autoimmun, 2006. **26**(1): p. 66-71.

129. Christen, U., et al., *Among CXCR3 chemokines, IFN-gamma-inducible protein of 10 kDa (CXC chemokine ligand (CXCL) 10) but not monokine induced by IFN-gamma (CXCL9) imprints a pattern for the subsequent development of autoimmune disease.* J Immunol, 2003. **171**(12): p. 6838-45.

130. Foulis, A.K., M.A. Farquharson, and A. Meager, *Immunoreactive alpha-interferon in insulin-secreting beta cells in type 1 diabetes mellitus.* Lancet, 1987. **2**(8573): p. 1423-7.

131. Richardson, S.J., et al., *Immunopathology of the human pancreas in type-I diabetes.* Semin Immunopathol. **33**(1): p. 9-21.

132. Bell, Y.C., B.L. Semler, and E. Ehrenfeld, *Requirements for RNA replication of a poliovirus replicon by coxsackievirus B3 RNA polymerase.* J Virol, 1999. **73**(11): p. 9413-21.

133. **Kärber, G.**, *Beitrag zur kollektiven Behandlung pharmakologischer Reihenversuche. Arch Exp Pathol Pharmakol* 1931. **162**: p. 480-483

134. Pichlmair, A., et al., *Activation of MDA5 requires higher-order RNA structures generated during virus infection.* J Virol, 2009. **83**(20): p. 10761-9.

135. Grasl-Kraupp, B., et al., *In situ detection of fragmented DNA (TUNEL assay) fails to discriminate among apoptosis, necrosis, and autolytic cell death: a cautionary note.* Hepatology, 1995. **21**(5): p. 1465-8.

136. Hultcrantz, M., et al., *Interferons induce an antiviral state in human pancreatic islet cells.* Virology, 2007. **367**(1): p. 92-101.

137. Schulthess, F.T., et al., *CXCL10 impairs beta cell function and viability in diabetes through TLR4 signaling.* Cell Metab, 2009. **9**(2): p. 125-39.

138. Shafren, D.R., et al., *Coxsackieviruses B1, B3, and B5 use decay accelerating factor as a receptor for cell attachment.* J Virol, 1995. **69**(6): p. 3873-7.

139. Bewley, M.C., et al., *Structural analysis of the mechanism of adenovirus binding to its human cellular receptor, CAR.* Science, 1999. **286**(5444): p. 1579-83.

140. Chehadeh, W., et al., *Persistent infection of human pancreatic islets by coxsackievirus B is associated with alpha interferon synthesis in beta cells.* J Virol, 2000. **74**(21): p. 10153-64.

141. Ylipaasto, P., et al., *Enterovirus infection in human pancreatic islet cells, islet tropism in vivo and receptor involvement in cultured islet beta cells.* Diabetologia, 2004. **47**(2): p. 225-39.

142. Elshebani, A., et al., *Effects on isolated human pancreatic islet cells after infection with strains of enterovirus isolated at clinical presentation of type 1 diabetes.* Virus Res, 2007. **124**(1-2): p. 193-203.

143. Rasilainen, S., et al., *Mechanisms of coxsackievirus B5 mediated beta-cell death depend on the multiplicity of infection.* J Med Virol, 2004. **72**(4): p. 586-96.

144. Frisk, G. and H. Diderholm, *Tissue culture of isolated human pancreatic islets infected with different strains of coxsackievirus B4: assessment of virus replication and effects on islet morphology and insulin release.* Int J Exp Diabetes Res, 2000. **1**(3): p. 165-75.

145. Shi, J. and H. Luo, *Interplay between the cellular autophagy machinery and positive-stranded RNA viruses.* Acta Biochim Biophys Sin (Shanghai). **44**(5): p. 375-84.

146. Gitlin, L., et al., *Essential role of mda-5 in type I IFN responses to polyriboinosinic:polyribocytidylic acid and encephalomyocarditis picornavirus.* Proc Natl Acad Sci U S A, 2006. **103**(22): p. 8459-64.

147. Kato, H., et al., *Differential roles of MDA5 and RIG-I helicases in the recognition of RNA viruses.* Nature, 2006. **441**(7089): p. 101-5.

148. Huhn, M.H., et al., *Melanoma differentiation-associated protein-5 (MDA-5) limits early viral replication but is not essential for the induction of type 1 interferons after Coxsackievirus infection.* Virology. **401**(1): p. 42-8.

149. Richer, M.J., et al., *Toll-like receptor 3 signaling on macrophages is required for survival following coxsackievirus B4 infection.* PLoS ONE, 2009. **4**(1): p. e4127.

150. Triantafilou, K., et al., *Human cardiac inflammatory responses triggered by Coxsackie B viruses are mainly Toll-like receptor (TLR) 8-dependent.* Cell Microbiol, 2005. **7**(8): p. 1117-26.

151. Fairweather, D., et al., *IL-12 receptor beta 1 and Toll-like receptor 4 increase IL-1 beta- and IL-18-associated myocarditis and coxsackievirus replication.* J Immunol, 2003. **170**(9): p. 4731-7.

152. Triantafilou, K. and M. Triantafilou, *Coxsackievirus B4-induced cytokine production in pancreatic cells is mediated through toll-like receptor 4.* J Virol, 2004. **78**(20): p. 11313-20.

153. Kemball, C.C., M. Alirezaei, and J.L. Whitton, *Type B coxsackieviruses and their interactions with the innate and adaptive immune systems.* Future Microbiol. **5**(9): p. 1329-47.

154. Skog, O., O. Korsgren, and G. Frisk, *Modulation of innate immunity in human pancreatic islets infected with enterovirus in vitro.* J Med Virol. **83**(4): p. 658-64.

155. Bonjardim, C.A., P.C. Ferreira, and E.G. Kroon, *Interferons: signaling, antiviral and viral evasion.* Immunol Lett, 2009. **122**(1): p. 1-11.

156. Mukherjee, A., et al., *The coxsackievirus B 3C protease cleaves MAVS and TRIF to attenuate host type I interferon and apoptotic signaling.* PLoS Pathog. **7**(3): p. e1001311.

157. Kimura, A. and T. Kishimoto, *IL-6: regulator of Treg/Th17 balance.* Eur J Immunol. **40**(7): p. 1830-5.

158. Kristiansen, O.P. and T. Mandrup-Poulsen, *Interleukin-6 and diabetes: the good, the bad, or the indifferent?* Diabetes, 2005. **54 Suppl 2**: p. S114-24.

159. Dinarello, C.A., *Immunological and inflammatory functions of the interleukin-1 family.* Annu Rev Immunol, 2009. **27**: p. 519-50.

160. Maedler, K., et al., *Glucose induces beta-cell apoptosis via upregulation of the Fas receptor in human islets.* Diabetes, 2001. **50**(8): p. 1683-90.

161. Weber, A., et al., *Proapoptotic signalling through Toll-like receptor-3 involves TRIF-dependent activation of caspase-8 and is under the control of inhibitor of apoptosis proteins in melanoma cells.* Cell Death Differ. **17**(6): p. 942-51.

162. Dogusan, Z., et al., *Double-stranded RNA induces pancreatic beta-cell apoptosis by activation of the toll-like receptor 3 and interferon regulatory factor 3 pathways.* Diabetes, 2008. **57**(5): p. 1236-45.

163. Paone, A., et al., *Toll-like receptor 3 triggers apoptosis of human prostate cancer cells through a PKC-alpha-dependent mechanism.* Carcinogenesis, 2008. **29**(7): p. 1334-42.

164. Salaun, B., et al., *TLR3 can directly trigger apoptosis in human cancer cells.* J Immunol, 2006. **176**(8): p. 4894-901.

165. Sun, R., et al., *Toll-like receptor 3 (TLR3) induces apoptosis via death receptors and mitochondria by up-regulating the transactivating p63 isoform alpha (TAP63alpha).* J Biol Chem. **286**(18): p. 15918-28.

166. Barber, G.N., *Host defense, viruses and apoptosis.* Cell Death Differ, 2001. **8**(2): p. 113-26.

167. Bogoyevitch, M.A. and B. Kobe, *Uses for JNK: the many and varied substrates of the c-Jun N-terminal kinases.* Microbiol Mol Biol Rev, 2006. **70**(4): p. 1061-95.

168. Lei, K., et al., *The Bax subfamily of Bcl2-related proteins is essential for apoptotic signal transduction by c-Jun NH(2)-terminal kinase.* Mol Cell Biol, 2002. **22**(13): p. 4929-42.

169. Autret, A., et al., *Poliovirus induces Bax-dependent cell death mediated by c-Jun NH2-terminal kinase.* J Virol, 2007. **81**(14): p. 7504-16.

170. Kim, S.M., et al., *Coxsackievirus B3 infection induces cyr61 activation via JNK to mediate cell death.* J Virol, 2004. **78**(24): p. 13479-88.

171. Zhang, P., et al., *Protein kinase PKR-dependent activation of mitogen-activated protein kinases occurs through mitochondrial adapter IPS-1 and is antagonized by vaccinia virus E3L.* J Virol, 2009. **83**(11): p. 5718-25.

172. Garcia, M.A., E.F. Meurs, and M. Esteban, *The dsRNA protein kinase PKR: virus and cell control.* Biochimie, 2007. **89**(6-7): p. 799-811.

7 Appendix

Published studies with my contribution

XOMA 052, an Anti-IL-1β Monoclonal Antibody, Improves Glucose Control and β-Cell Function in the Diet-Induced Obesity Mouse Model

Alexander M. Owyang,* Kathrin Maedler,* Lisa Gross, Johnny Yin, Lin Esposito, Luan Shu, Jaaee Jadhav, Erna Domsgen, Jennifer Bergemann, Steve Lee, and Seema Kantak

Preclinical Research and Development (A.M.O., L.G., J.Y., L.E., S.L., S.K.), XOMA (US) LLC, Berkeley, California 94710; and Centre for Biomolecular Interactions (K.M., L.S., J.J., E.D., J.B.), University of Bremen, D-28359 Bremen, Germany

Recent evidence suggests that IL-1β-mediated glucotoxicity plays a critical role in type 2 diabetes mellitus. Although previous work has shown that inhibiting IL-1β can lead to improvements in glucose control and β-cell function, we hypothesized that more efficient targeting of IL-1β with a novel monoclonal antibody, XOMA 052, would reveal an effect on additional parameters affecting metabolic disease. In the diet-induced obesity model, XOMA 052 was administered to mice fed either normal or high-fat diet (HFD) for up to 19 wk. XOMA 052 was administered as a prophylactic treatment or as a therapy. Mice were analyzed for glucose tolerance, insulin tolerance, insulin secretion, and lipid profile. In addition, the pancreata were analyzed for β-cell apoptosis, proliferation, and β-cell mass. Mice on HFD exhibited elevated glucose and glycated hemoglobin levels, impaired glucose tolerance and insulin secretion, and elevated lipid profile, which were prevented by XOMA 052. XOMA 052 also reduced β-cell apoptosis and increased β-cell proliferation. XOMA 052 maintained the HFD-induced compensatory increase in β-cell mass, while also preventing the loss in β-cell mass seen with extended HFD feeding. Analysis of fasting insulin and glucose levels suggests that XOMA 052 prevented HFD-induced insulin resistance. These studies provide new evidence that targeting IL-1β *in vivo* could improve insulin sensitivity and lead to β-cell sparing. This is in addition to previously reported benefits on glycemic control. Taken together, the data presented suggest that XOMA 052 could be effective for treating many aspects of type 2 diabetes mellitus. **(*Endocrinology* 151: 2515–2527, 2010)**

Type 2 diabetes mellitus (T2DM) is a worldwide epidemic. Obesity and a sedentary lifestyle are major risk factors for developing T2DM (1). T2DM occurs when the β-cell fails to produce sufficient amounts of insulin to maintain normoglycemia as a result of impaired β-cell function and/or decreased β-cell mass (2), a condition generally accompanied by insulin resistance (3). Effective treatments are necessary to prevent β-cell failure.

Obesity and insulin resistance have been associated with chronic inflammation (4–6). Several inflammatory molecules and pathways have been linked to insulin resistance, including IL-1β, TNF-α, IL-6, and the nuclear factor-κB pathway (7). Recent studies show that inflammatory markers (*e.g.* C-reactive protein and IL-1β) are elevated in individuals with T2DM and in patients with a significantly increased risk to develop the disease (8, 9).

IL-1β expression level and function are tightly regulated by a complex system of IL-1 family members and their receptors. IL-1β binds to the IL-1 receptor type I (IL-1RI) expressed on all nucleated cells and highly ex-

ISSN Print 0013-7227 ISSN Online 1945-7170
Printed in U.S.A.

doi: 10.1210/en.2009-1124 Received September 21, 2009. Accepted February 23, 2010.
First Published Online March 23, 2010
* A.M.O. and K.M. contributed equally to the study.

Abbreviations: Con A, Concanavalin A; D10, D10.G4.1; DIO, diet-induced obesity; FFA, free fatty acids; GK, Goto-Kakizaki; HbA_{1c}, glycated hemoglobin; HDL, high-density lipoprotein; HFD, high-fat/high-sucrose diet; hIL-1β, human IL-1β; HOMA-IR, homeostatic model of assessment-insulin resistance; IL-1RI, IL-1 receptor type I; ipGTT, ip glucose tolerance test; ipITT, ip insulin tolerance test; mIL-1β, mouse IL-1β; ND, normal diet; T2DM, type 2 diabetes mellitus.

pressed on pancreatic islets (10), which triggers the recruitment of the IL-1 receptor accessory protein to form the active signaling complex. The natural inhibitor IL-1Ra binds to IL-1RI but does not allow the recruitment of IL-1 receptor accessory protein (11, 12). IL-1β specifically impairs survival of pancreatic β-cells and severely affects β-cell insulin secretion (13). Moreover, blocking IL-1β by specific IL-1β antibodies protects from the cytotoxic effect induced by conditioned medium of activated mononuclear cells (14), indicating that IL-1β may play an important role in the molecular mechanisms underlying autoimmune β-cell destruction.

IL-1β has long been associated with autoimmune type 1 diabetes mellitus (15) and is also seen increasingly as a key player in T2DM (16), although this has been under debate (17). Studies on isolated islets have shown that IL-1β is produced by the β-cell in response to chronic glucose exposure (18–20). Elevated IL-1β expression was observed in β-cells in pancreatic sections from autopsies from patients with T2DM by immunostaining, as well as by laser microdissection (18, 21), indicating that IL-β may mediate β-cell destruction also in T2DM. Elevated pancreatic β-cell expression of IL-1β under hyperglycemic conditions has also been observed in two animal models, *Psammomys obesus* and the Goto-Kakizaki (GK) rat (18, 22).

Blocking IL-1β as a therapeutic strategy for T2DM has been examined in several studies. *In vitro*, recombinant IL-1Ra protected β-cells from glucose-induced apoptosis and impaired function. Daily injection of recombinant IL-1Ra in mice fed a high-fat/high-sucrose diet (HFD) improved glycemia, glucose stimulated insulin secretion, and β-cell survival (23) and reversed the islet inflammatory phenotype in the GK rat (24). Importantly, results from a recent clinical study in patients with T2DM showed that recombinant IL-1Ra improved glycemic control and β-cell function (25).

Because IL-1Ra has a short half-life, and must block the ubiquitous IL-1RI to neutralize IL-1 activity, we were interested in testing the efficacy of an agent that specifically targets the ligand IL-1β, which is usually secreted only in the local environment during inflammation. In the present study, we show that inhibiting IL-1β with the monoclonal antibody XOMA 052 improves glycemic control, β-cell function and survival, dyslipidemia, and insulin sensitivity in the diet-induced obesity (DIO) model of T2DM.

Materials and Methods

D10.G4.1 (D10) assay

Resting D10 cells (TIB-224; American Type Culture Collection, Manassas, VA) (26) were seeded in triplicate at 2×10^4 cells/well and were activated with 2.5 μg/ml of concanavalin A (Con A) in combination with recombinant IL-1β (R&D Systems, Minneapolis, MN). Proliferation was measured after 72 h by Alamar Blue redox viability dye. To determine the potency of XOMA 052, cells were treated with IL-1β and various amounts of XOMA 052. IC_{50} values were determined using the curve-fitting software program Prism (GraphPad Software, La Jolla, CA). EC_{50} values for recombinant and native forms of IL-1β were derived from dose-response curves generated by titrations of recombinant cytokine or lipopolysaccharide-stimulated peripheral blood mononuclear cell supernatants.

In vivo assay for IL-1β activity

Female C57BL/6 mice were pretreated with PBS or XOMA 052, ip. Twenty-four hours later, they were injected sc with 20 ng of human IL-1β (hIL-1β) or mouse IL-1β (mIL-1β). Two hours after IL-1β injection, blood was collected via retroorbital bleed. Induction of IL-6 was measured by mIL-6 ELISA (BD PharMingen, San Diego, CA).

Animals

C57BL/6J male mice were obtained from The Jackson Laboratory (Bar Harbor, ME) at 5 wk of age. Beginning at 6 wk of age, mice were fed either a normal diet (ND) (Harlan Teklad Rodent Diet 8604, containing 12.2, 57.6, and 30.2% calories from fat, carbohydrate, and protein, respectively; Harlan Laboratories, Inc., Indianapolis, IN) or a HFD (containing 58, 26, and 16% calories from fat, carbohydrate, and protein, respectively; "Surwit" Research Diets, New Brunswick, NJ) (27) for 12–19 wk. Animals fed a HFD developed DIO.

Prophylactic studies

C57BL/6J male mice were treated twice weekly with ip injections of XOMA 052 or isotype control (antikeyhole limpet hemocyanin IgG_2) or daily ip injections of recombinant IL-1Ra (10 mg/kg, Kineret; Amgen, Thousand Oaks, CA) or vehicle control, starting at 6 wk of age. Body weight and food consumption were monitored weekly.

Therapeutic studies

The HFD was initiated in 6-wk-old C57BL/6 male mice without drug injections. After 10 wk, XOMA 052 and vehicle were given twice weekly for an additional 9 wk.

Treatment groups

The following treatment groups were examined: 1) ND IgG (mice on ND and isotype control), 2) ND XOMA 052 (mice on ND and XOMA 052), 3) HFD IgG (mice on HFD and isotype control), 4) HFD XOMA 052 (mice on HFD and XOMA 052) (for both prophylactic and therapeutic studies), 5) ND C (mice on ND and vehicle control), 6) ND IL-1Ra (mice on ND and IL-1Ra), 7) HFD C (mice on HFD and vehicle control), and 8) HFD IL-1Ra (mice on HFD and vehicle IL-1Ra) (for prophylactic studies).

Independent experiments were performed at three different institutions: at XOMA (US) LLC, at The Jackson Laboratory–West (Sacramento, CA), and at the University of Bremen.

All animals were housed in a temperature-controlled room with a 12-h light, 12-h dark cycle and were allowed free access to food and water according to the protocol and approved by the

XOMA Institutional Animal Care and Use Committee and The Jackson Laboratory–West Institutional Animal Care and Use Committee, in compliance with the Guide for the Care and Use of Laboratory Animals and the Bremen Senate in agreement with the National Institutes of Health Animal Care Guidelines and Section 8 of the German animal protection law.

Intraperitoneal glucose tolerance test (ipGTT) and ip insulin tolerance test (ipITT)

After 4, 8, and 12 wk of diet and treatment (prophylactic studies), or 10 and 19 wk of diet (therapeutic studies), all animals underwent *in vivo* assays. For ipGTTs, mice were fasted 12 h overnight and injected ip with glucose (40%; Phoenix Pharmaceuticals, Inc., St. Josephs, MO) at a dose of 1 g/kg body weight. Blood samples were obtained at time points 0, 15, 30, 60, 90, and 120 min (prophylactic study) and at 0 and 30 min (therapeutic studies) for glucose measurements using a Glucometer (Freestyle; TheraSense, Inc., Alameda, CA). For stimulated insulin secretion, a dose of 2 g/kg body weight of glucose was injected, and blood samples were obtained retroorbitally at time points 0 and 30 min. Serum insulin concentrations were determined using a mouse insulin ultrasensitive ELISA (ALPCO, Salem, NH). Stimulation index for insulin production was calculated by dividing the 30-min insulin values (stimulated) by the 0-min value (basal).

For ipITTs, mice were injected ip with 0.75 U/kg body weight recombinant human insulin (Novolin; Novo Nordisk, Bagsværd, Denmark) after 5-h fasting, and glucose concentration was determined with the Freestyle Glucometer.

Histochemical analyses and β-cell mass

After 12 wk (prophylactic study) or 19 wk (therapeutic study) of diet and treatment, pancreata were weighed and fixed overnight in 4% paraformaldehyde at 4 C under continuous shaking, followed by paraffin embedding, orienting pancreata such that sections were cut along the head-tail axis.

Apoptosis, proliferation, and β-cell mass were analyzed as described previously (23). Samples were evaluated in a randomized manner by two independent investigators (J.J. and K.M.) who were blinded to the treatment conditions. Data are presented as means ± SE and were analyzed by paired, Student's *t* test or by ANOVA with a Bonferroni correction for multiple group comparisons. Histochemical analyses were performed on two of three prophylactic studies and four of five therapeutic studies.

Homeostatic model of assessment-insulin resistance (HOMA-IR)

HOMA-IR was calculated using the method employed by Odegaard *et al.* (28): fasting insulin (ng/ml) × fasting glucose (mmol/liter) = HOMA-IR.

IL-1β expression analysis

Total RNA from the epididymal fat pad, hypothalamus, and pancreatic islets was extracted from mice in a prophylactic study. Total RNA was isolated using the RNeasy Lipid Tissue kit (QIAGEN, Inc., Valencia, CA). For quantitative analysis, we used the LightCycler Quantitative PCR System (Roche Diagnostics, Indianapolis, IN) with a commercial kit (LightCycler FastStart DNA Master plus SYBR Green I; Roche Diagnostics). Mouse primers used were as follows: 5′-gttggccaggctggtgtccag-3′ and 5′-ctgtgatgagctgctcagggtgg-3′ (tubulin), and 5′-gaccttccaggatgaggaca-3′ and 5′-agctcatatgggtccgacag-3′ (IL-1β).

Serum lipid analysis

Serum obtained by cardiac puncture at the time of killing was analyzed for serum lipids by the University of California, Los Angeles, Lipid and Lipoprotein Laboratory as described previously (29). All lipid assays were performed in triplicate. An external control sample with known analyte concentration was run for each assay to assure accuracy. Free plasma glycerol concentrations were also determined and used to correct the triglyceride values. Non-HDL cholesterol was calculated by subtracting HDL levels from total cholesterol.

Glycated hemoglobin (HbA_{1c})

HbA_{1c} was measured at the end of the study using A1CNow+ (Bayer Healthcare, Sunnyvale, CA).

Results

XOMA 052 neutralizes IL-1β activity *in vitro* and *in vivo*

The human engineered anti-IL-1β IgG2 antibody, XOMA 052, was developed for human therapeutic use and has a very high affinity [dissociation constant (K_D) = 0.3 pM] to hIL-1β and a 10,000-fold lower affinity to mIL-1β of 3.0 nM (Roell, M., H. Issafras, R. Bauer, K. Michelson, N. Mendoza, S. Vanegas, L. Gross, P. Larsen, D. Bedinger, D. Bohmann, G. Nonet, N. Liu, S. Lee, S. Kantak, A. Horwitz, J. Hunter, A. Owyang, A. Mirax, J. Corbin, and M. White, unpublished observations).

To determine the neutralization activity of XOMA 052 *in vitro*, we used the mouse D10 proliferation assay. Human, rhesus macaque, and mIL-1β are able to stimulate D10 cells with a similar potency of 0.2–0.3 pM (Fig. 1A). In neutralization experiments with D10 cells, XOMA 052 had an IC_{50} against hIL-1β in the low pM range (2.5 ± 0.4 pM; Fig. 1B). Interestingly, XOMA 052 was also able to neutralize mIL-1β activity, with an IC_{50} of 2.6 ± 0.4 nM (Fig. 1B). Neutralization of IL-1 activity was specific for IL-1β, because XOMA 052 did not neutralize IL-1α (Supplemental Fig. 1, published on The Endocrine Society's Journals Online web site at http://endo.endojournals.org).

We next tested the ability of XOMA 052 to neutralize IL-1β *in vivo*. C57BL/6 mice were pretreated with various doses of antibody. Twenty-four hours later, mice were injected with 20 ng of either hIL-1β or mIL-1β. Mouse IL-6 in the serum was measured after 2 h. As expected, XOMA 052 at a low dose was able to neutralize the *in vivo* activity of hIL-1β (Fig. 1C). The antibody achieved 73% inhibition of IL-6 induction at 0.15 mg/kg and 66% inhibition at 15 mg/kg. XOMA 052 could also neutralize mIL-1β, but only at the higher dose of 15 mg/kg, achieving 47% inhibition (Fig. 1D). Thus, although designed for

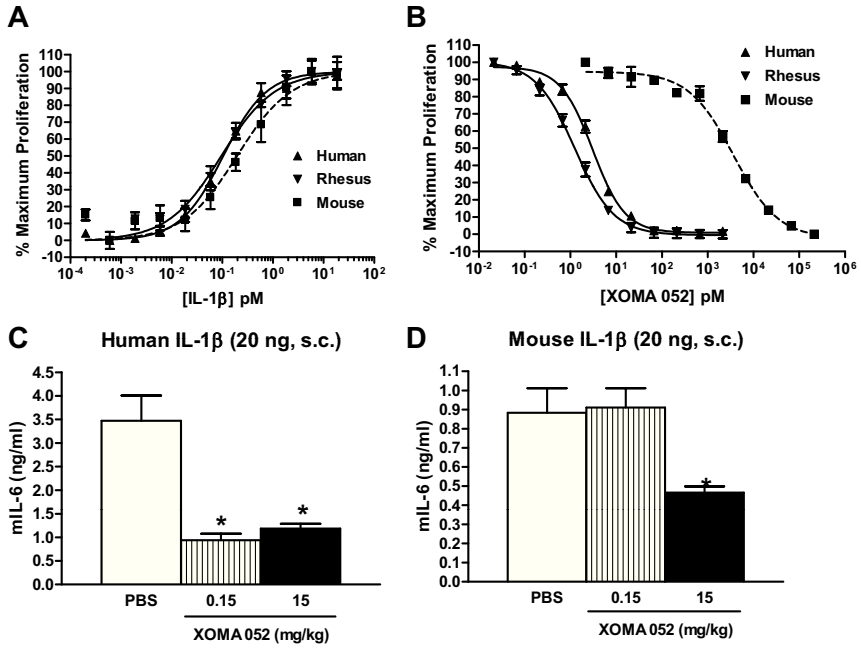

FIG. 1. XOMA 052 neutralizes IL-1β activity *in vitro* and *in vivo*. A, Stimulation of D10 cells by recombinant IL-1β. D10 cells were stimulated with 2.5 μg/ml Con A and serial dilutions of IL-1β from the indicated species. Proliferation was assessed after 72 h by Alamar Blue. B, Neutralization of recombinant IL-1β activity. D10 cells were stimulated with 2.5 μg/ml Con A, 0.6 pM of IL-1β from the indicated species, and serial dilutions of XOMA 052. Proliferation was assessed after 72 h by Alamar Blue. IC_{50} at 0.6 pM hIL-1β is 2.5 ± 0.4 pM of XOMA 052 (n = 6 experiments). IC_{50} at 0.6 pM rhesus IL-1β is 2.7 ± 0.7 pM (n = 3). IC_{50} at 0.6 pM mIL-1β is 2.6 ± 0.4 nM (n = 7). ▲, Human; ▼, rhesus; ■, mIL-1β. C, Serum IL-6 levels of hIL-1β-treated mice pretreated with PBS, 0.15 mg/kg (3 μg) XOMA 052, or 15 mg/kg (300 μg) XOMA 052. Representative of three or more experiments. n = 5 mice/group. *, $P < 0.01$ *vs.* PBS by unpaired *t* test. D, Serum IL-6 levels of mIL-1β-treated mice pretreated with PBS, 0.15 mg/kg (3 μg) XOMA 052, or 15 mg/kg (300 μg) XOMA 052. Representative of two experiments (n = 5 mice/group). *, $P < 0.05$ *vs.* PBS by unpaired *t* test.

human use, XOMA 052 exhibits sufficient potency for studies in murine models.

XOMA 052 has no effect on weight gain or food intake in mice

To assess the effect of specifically inhibiting IL-1β in T2DM, studies with XOMA 052 were performed in the DIO model. Mice were fed ND or HFD ("Surwit") (30). Two types of studies were performed, based on prophylactic and therapeutic administration of XOMA 052. In both cases, 5- to 6-wk-old C57BL/6J mice were fed either ND or HFD, and either XOMA 052 or IgG_2 isotype control antibody was administered twice weekly. In the prophylactic studies, XOMA 052 treatment was administered in parallel with the different diets at 5–6 wk of age for 12–14 wk. In the therapeutic studies, mice were fed the diets for 19 wk with treatment administered from wk 11–19 of the diet.

Mice fed HFD gained more weight than the ND group, which reached significance at 3 wk. XOMA 052 had no effect on food intake (data not shown) nor on weight gain. After 12 wk of treatment, body weight of control mice was 32 ± 0.7 g on HFD *vs.* 26 ± 0.9 g on ND, $P < 0.01$, and of XOMA 052-treated mice, 32 ± 1.2 g on HFD *vs.* 28 ± 0.4 g on ND, $P < 0.01$ (prophylactic study). In the therapeutic study (9 wk of antibody treatment), body weight of control mice was 43 ± 3.6 g on HFD *vs.* 28 ± 1.2 g on ND, $P < 0.01$, and of XOMA 052-treated mice, 42 ± 4.9 g on HFD *vs.* 31 ± 1.5 g on ND, $P < 0.01$.

XOMA 052 improves glucose tolerance, insulin secretion, and insulin sensitivity in mice

Prophylactic studies

After 4 wk on diet, untreated HFD mice developed glucose intolerance as measured by ipGTT. After 8 wk of diet, HFD mice displayed elevated fasting glucose levels relative to ND mice (90 ± 3 mg/dl for untreated HFD control mice *vs.* 77 ± 4 mg/dl for ND control mice, $P < 0.05$), which was prevented by XOMA 052 treatment in the HFD group (76 ± 4 mg/dl, $P < 0.05$). The study was performed in three independent experiments with four to eight mice in each group, respectively, and showed similar results in each experiment. Figure 2A, *left panel*, shows fasting glucose after 12 wk on diet. Additionally, average long-term glycemic control was assessed in the prophylactic studies by measuring the HbA_{1c} levels in serum. After 12 wk on HFD, untreated mice had elevated HbA_{1c} compared with ND mice, which was reduced to control levels by XOMA 052 treatment ($P < 0.01$; Fig. 2B, *left panel*). In treated HFD mice, XOMA 052 was able to significantly improve glucose tolerance after 4, 8, and 12 wk on HFD (ipGTT after 12 wk on diet; Fig. 2C, *left panel*). Area under the curve analysis revealed significantly lower glucose levels in the XOMA 052-treated HFD mice ($P < 0.05$; Fig. 2D, *left panel*). Treatment of mice with daily injections of 10 mg/kg recombinant IL-1Ra improved fasting glucose (Fig. 2A, *right panel*), HbA_{1c} (Fig. 2B, *right panel*), and glucose tolerance (Fig. 2, C and D, *right panel*), with results similar to XOMA 052 treatment.

Because inhibition of IL-1β led to an improvement in glycemic control, mice were assessed for the effect of XOMA 052 on insulin secretion. Fasted mice were challenged with 2 g/kg glucose, and insulin secretion was assessed before (0 min) and 30 min after glucose injection. In parallel with the hyperglycemia, high-fat feeding resulted

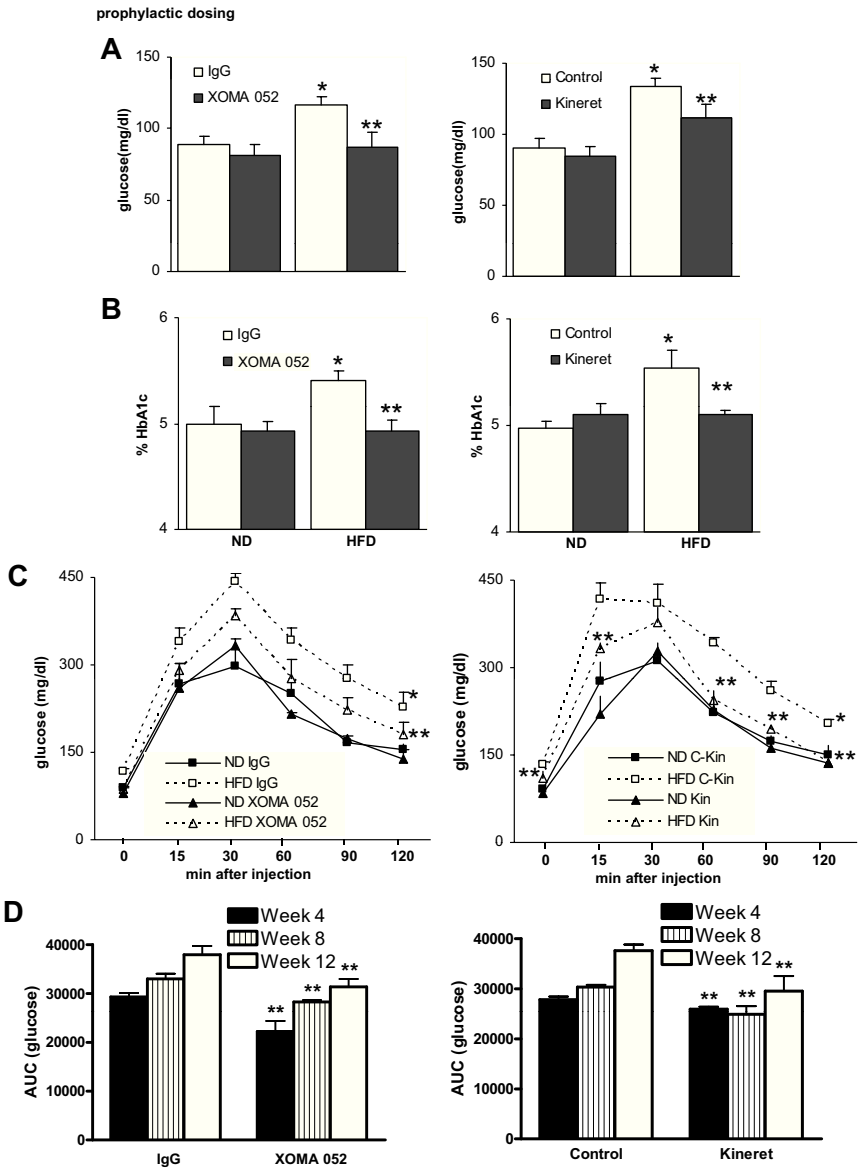

FIG. 2. XOMA 052 improves glucose tolerance in mice: prophylactic study. Mice were fed a ND or HFD and injected twice weekly with either IgG_2 (control) or XOMA 052 at 1 mg/kg (*left panel*) or daily with either 10 mg/kg recombinant IL-1Ra or vehicle (*right panel*) for 12 wk. Data shown are from one representative experiment out of three (n = 4 mice/group). A, Fasting serum glucose after 12 wk of diet. B, $GHbA_{1c}$ after 12 wk of diet. C, ipGTT. Blood glucose levels in mice after 12 wk of diet and XOMA 052 treatment after overnight fasting (0 min) and after ip injection of 1 g/kg body weight glucose. D, Area under the curve (AUC) analysis of ipGTT results from the HFD groups after 4, 8, and 12 wk of diet. Data show mean ± SE. *, $P < 0.05$ HFD *vs.* ND, same treatment; **, $P < 0.05$ XOMA 052 *vs.* IgG_2, same diet. Kin, Kineret; C-Kin, vehicle control.

in hyperinsulinemia (Fig. 3A) compared with ND mice. Fasting insulin levels were 2.1-fold higher in untreated HFD mice compared with ND ($P < 0.05$; Fig. 3A). In addition, untreated HFD mice also failed to considerably increase their insulin levels in response to a glucose challenge, whereas control ND mice exhibited a stimulatory index of 2.2 and the ND-XOMA 052 mice of 2.7, respectively (Fig. 3B). HFD mice under XOMA 052 treatment exhibited significantly lower fasting insulin levels than untreated HFD mice (1.3-fold difference, $P < 0.001$; Fig. 3A), and glucose stimulated insulin secretion was restored (1.4-fold increased stimulatory index compared with untreated HFD control, $P < 0.05$; Fig. 3B).

Normalization of fasting insulin levels in treated HFD mice suggests a possible effect of XOMA 052 on insulin resistance. This observation was confirmed by the analysis of HOMA-IR (Fig. 3C). HOMA-IR is shown as the product of fasting insulin and fasting glucose as employed previously (28). In untreated mice, HOMA-IR was elevated 4-fold by the HFD, which was greatly reduced by XOMA 052 (2.4-fold decrease compared with the untreated HFD control; Fig. 3C). To further assess the effect of XOMA 052 treatment on insulin resistance, we performed an ITT by measuring glucose concentrations after ip injection of insulin at 0.75 U/kg of body weight (ip-ITT). No significant differences in glucose levels were observed between treated and untreated animals of the ND group (Fig. 3D). Untreated HFD-mice showed elevated glucose levels throughout the test compared with ND mice. In contrast, in the XOMA 052-treated HFD mice, glucose levels were significantly lower than the untreated HFD mice before and at 90 min after the insulin injection ($P < 0.05$; Fig. 3D). Area under the curve analysis revealed significantly lower glucose levels in the XOMA 052-treated HFD mice at wk 8 and 12 (Fig. 3E; $P < 0.05$).

The impaired glucose and insulin tolerance in DIO mice correlated with an increase in IL-1β expression. IL-1β mRNA was significantly elevated by HFD in the epididymal fat, hypothalamus, and pancreatic islets (Fig. 3F). This was significantly reduced by XOMA 052 treatment.

Therapeutic studies

XOMA 052 also was tested for its ability to improve glycemia and insulin secretion under conditions of existing impaired glucose tolerance. The study was performed in five independent experiments with eight to 10 mice in each group, respectively, and showed similar results in each experiment. Untreated mice on HFD for 10 wk dis-

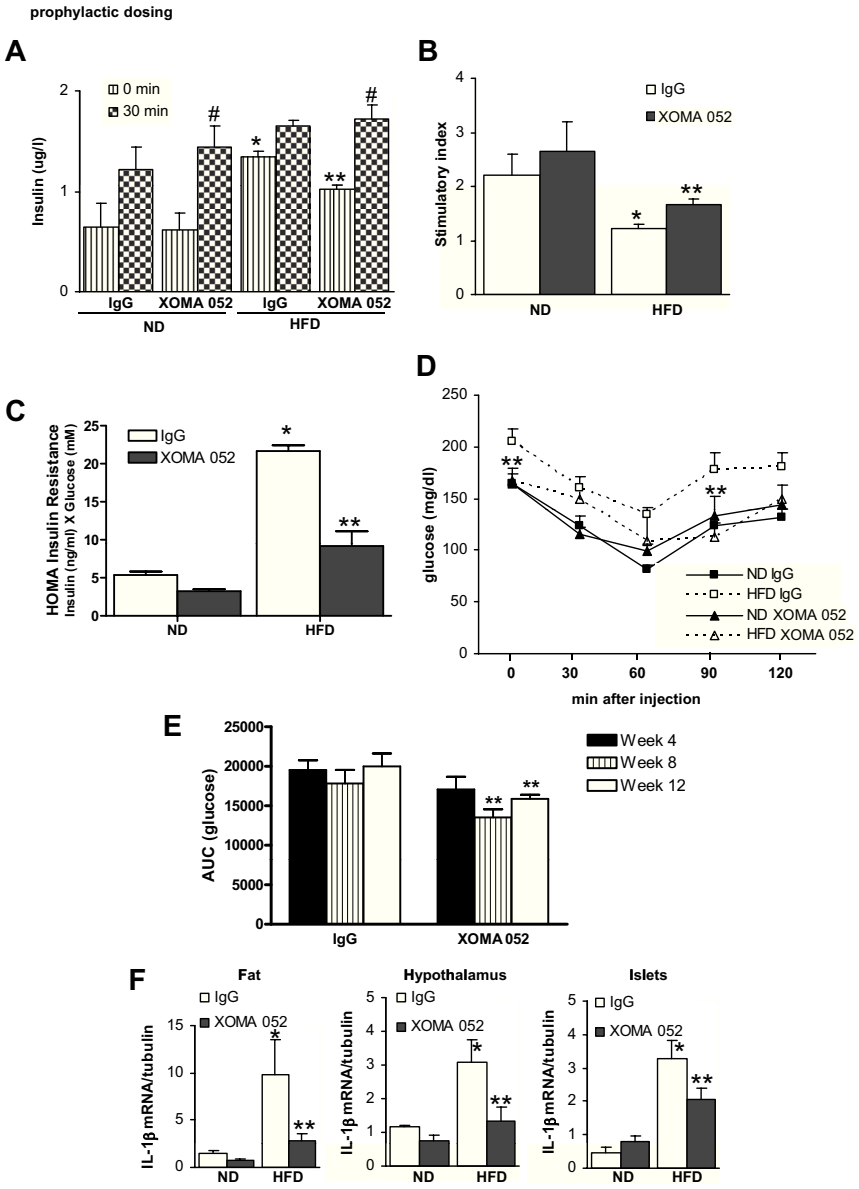

FIG. 3. XOMA 052 improves insulin secretion and insulin sensitivity in mice: prophylactic study. Mice were fed a ND or HFD and injected twice weekly with either IgG2 (control) or XOMA 052 at 1 mg/kg for 12 wk. Data shown are from one representative experiment out of five (n = 4 mice/group). A, Serum insulin was measured during a GTT before (0 min) and 30 min after glucose injection (2 g/kg body weight). B, Insulin stimulatory index as a ratio of stimulated (30 min) over basal (0 min) insulin. C, HOMA-IR of mice as a product of fasting insulin and glucose levels after 13 wk of diet and treatment (n = 5 mice/group). D, ipITT after 5 h fast. Glucose levels were measure before (0 min) and 30, 60, 90, and 120 min after ip injection of 0.75 U/kg insulin (n = 4 mice/group). E, Area under the curve analysis of ipITT results from the HFD groups after 4, 8, and 12 wk of diet. F, mRNA expression of IL-1β in fat, hypothalamus, and islet tissue after 12 wk of diet and treatment with IgG_2 or XOMA 052. Representative of three experiments. Data show mean ± SE. *, $P < 0.05$ HFD *vs.* ND, same treatment; **, $P < 0.05$ XOMA 052 *vs.* IgG_2, same diet; #, $P < 0.05$ stimulated compared with basal insulin secretion.

played increased fasting glucose (1.4-fold increase for HFD *vs.* ND mice, $P < 0.0001$; Fig. 4A), as well as impaired glucose tolerance (1.3-fold increase in glucose levels 30 min after glucose injection for HFD *vs.* ND mice, $P < 0.0001$; Fig. 4A). The two diet groups were separated into control and XOMA 052 groups, and the diet was continued with XOMA 052 or isotype control administration for 9 wk. Figure 4B shows fasting and stimulated glucose levels (during ipGTT) at the end of the study. Isotype control injected mice on HFD showed higher fasting glucose levels and higher stimulated glucose levels compared with ND mice (Fig. 4B). The elevated stimulated glucose was lowered significantly by XOMA 052 treatment (Fig. 4B). In parallel, serum insulin was measured before and after glucose injection. After 10 wk of diet, fasting insulin levels were 1.4-fold higher in HFD than ND mice ($P < 0.05$; Fig. 4C), and glucose stimulated insulin secretion was abolished by the HFD ($P < 0.0001$; Fig. 4D). When HFD mice were treated with XOMA 052, glucose-stimulated insulin secretion was significantly restored ($P < 0.05$; Fig. 4F). Although stimulatory index was decreased in the control HFD group compared with the control ND group (Fig. 4F), stimulatory index was improved by XOMA 052 treatment (1.7-fold increased compared with the HFD control group, $P < 0.05$; Fig. 4F). As an indicator of insulin resistance, HOMA-IR was assessed before and after treatment. At 10 wk of diet, HOMA-IR was elevated more than 2-fold in HFD (Fig. 4G) and was further increased after 19 wk of HFD (2.9-fold increased in the HFD *vs.* ND control mice, Fig. 4H). Nine weeks of XOMA 052 treatment inhibited the HFD-induced increase in HOMA-IR (1.3-fold decrease in the HFD-XOMA 052 *vs.* HFD control, $P < 0.01$; Fig. 4H).

XOMA 052 improves β-cell survival and restores β-cell mass

To investigate whether the XOMA 052 effects on improved glucose tolerance and insulin secretion were accompanied by improved β-cell survival, we analyzed β-cell apoptosis, proliferation, and β-cell mass in all four groups of mice in the prophylactic and all four groups in the therapeutic studies after 12 and 19 wk of diet, respectively. After 12 wk of diet, islet β-cell apoptosis was increased by HFD feeding (2.3-fold increase in the

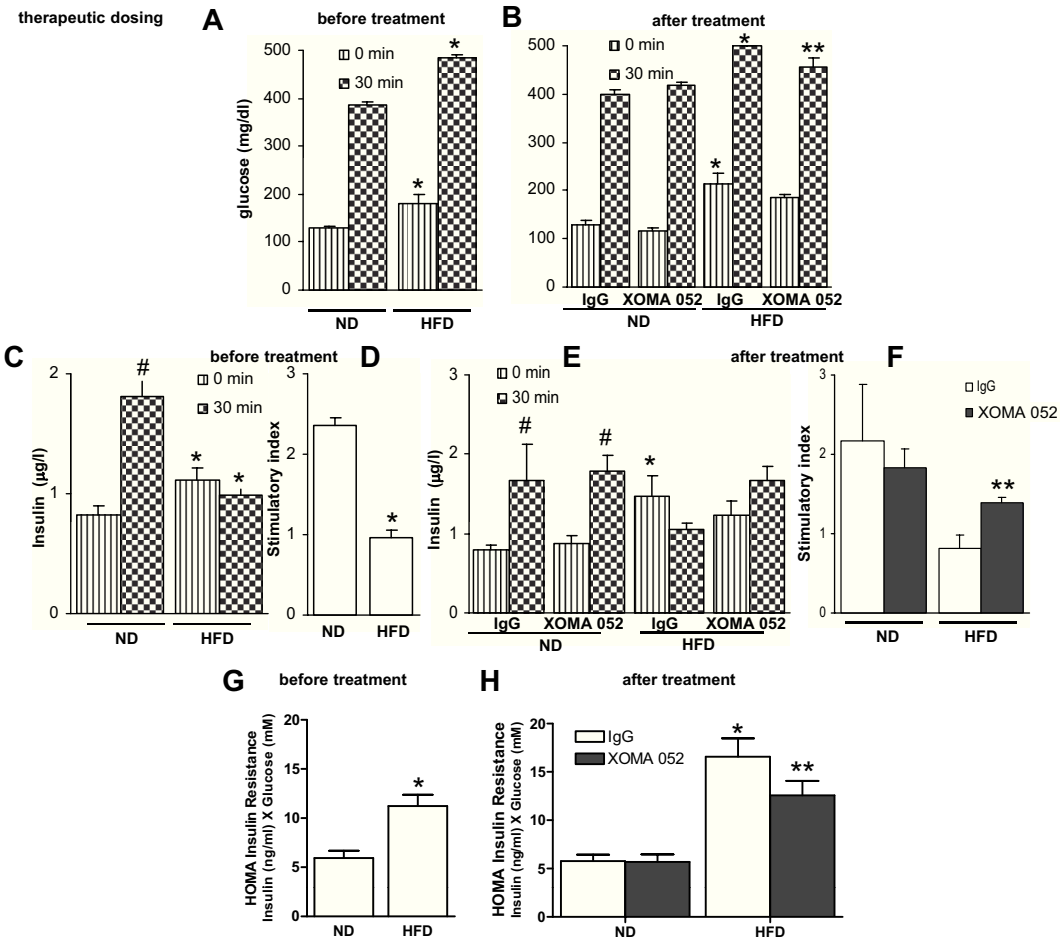

FIG. 4. XOMA 052 improves glucose tolerance, insulin secretion, and insulin sensitivity in mice: therapeutic study. Mice were fed a ND or HFD for 19 wk. After 10 wk of diet, mice underwent *in vivo* assessment and then injected twice weekly with either IgG_2 (control) or XOMA 052 at 1 mg/kg from wk 11–19. Data shown are from one representative experiment. Serum glucose (A and B) and serum insulin (C and E) levels in mice after 10 wk of diet before treatment (A and C) and after XOMA 052 treatment (B and E) after overnight fasting (0 min) and after ip injection of 2 g/kg body weight glucose. D and F, Insulin stimulatory index as a ratio of stimulated (30 min) over basal (0 min) insulin before (D) and after (F) treatment. G and H, HOMA-IR of mice as a product of fasting insulin and glucose levels before (G) and after (H) XOMA 052 treatment (n = 4–5 mice/group except A, C, D, and G, which are 12 mice/diet group before antibody treatment). Representative of five experiments. Data show mean ± SE. *, $P < 0.05$ HFD *vs.* ND, same treatment; **, $P < 0.05$ XOMA 052 *vs.* IgG_2, same diet; #, $P < 0.05$ stimulated compared with basal insulin secretion.

HFD *vs.* ND control, $P < 0.001$; Fig. 5C). In contrast, XOMA 052 completely restored β-cell survival: it decreased β-cell apoptosis and also increased proliferation. XOMA 052 also decreased β-cell apoptosis under ND conditions (3-fold reduction in XOMA 052-treated ND mice *vs.* control ND mice, $P < 0.05$; Fig. 5C). Previously, we reported increased β-cell mass in mice after 12 wk of HFD despite the tendency for increased β-cell apoptosis at that time point (23). Also, in the current studies, the HFD-induced changes in apoptosis and proliferation were not reflected in the β-cell mass results. HFD feeding induced a compensatory increase in β-cell mass in both control and XOMA 052 HFD-treated groups ($P < 0.05$; Fig. 5E).

In line with the results after 12 wk of diet, HFD feeding induced apoptosis and reduced proliferation after 19 wk of diet (Fig. 5, F and G, respectively). As in the prophylactic studies, in the therapeutic studies, XOMA 052 significantly inhibited apoptosis ($P < 0.001$; Fig. 5F) and increased proliferation ($P < 0.001$; Fig. 5G) in HFD-fed mice. In contrast to the findings after 12 wk of diet, no compensatory increase in β-cell mass was observed in control mice after 19 wk on HFD compared with those on ND (Fig. 5H). Importantly, the compensatory increase in β-cell mass was maintained in XOMA 052-treated mice after 19 wk ($P < 0.001$; Fig. 5H).

XOMA 052 protects from HFD-induced changes in lipid levels

At the end of each study, we measured serum lipid levels. HFD treatment has been shown to increase levels of serum lipids, and elevation of lipids is known to affect insulin action and secretion (31). Levels of triglycerides, free fatty acids (FFA), total cholesterol, and high-density lipoprotein (HDL) were analyzed after 12 and 19 wk of

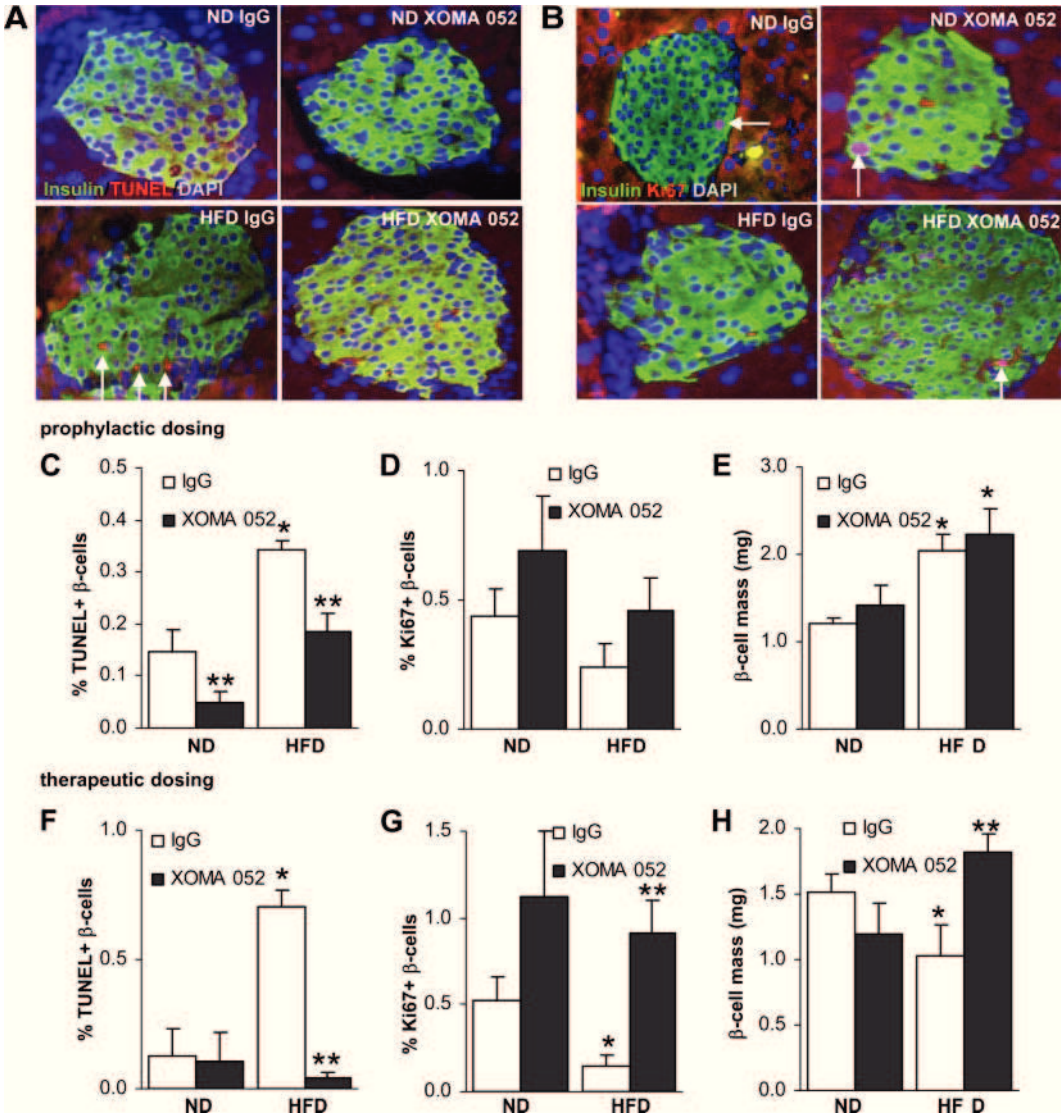

FIG. 5. XOMA 052 improves β-cell survival and restores β-cell mass. A, Triple staining for terminal deoxynucleotidyl transferase dUTP nick end labeling (TUNEL) in *red*, insulin in *green*, and 4′,6-diamidino-2-phenylindole (DAPI) in *blue* was performed on fixed, paraffin-embedded islet sections (magnification, ×250). *White arrows* indicate TUNEL positive β-cells (triple stained). B, Triple staining for proliferation by Ki67-antibody in *red*, insulin in *green*, and DAPI in *blue* was performed on fixed, paraffin-embedded mouse pancreas sections (magnification, ×250). *White arrows* indicate Ki67 positive β-cells (triple stained). C and F, Results are expressed as percentage of TUNEL-positive β-cells ± SE. The mean number of β-cells scored was 8191 ± 830 (C) or 7098 ± 3011 (F) for each treatment condition in two (C) or four (F) independent experiments. D and G, Results are expressed as percentage of Ki67-positive β-cells ± SE. The mean number of β-cells scored was 5370 ± 619 (D) or 3338 ± 916 (G) for each treatment condition in two (D) or four (G) independent experiments. E and H, β-Cell mass per pancreas was estimated as the product of the relative cross-sectional area of β-cells (determined by quantification of the cross-sectional area occupied by β-cells divided by the cross-sectional area of total tissue) and the weight of the pancreas. Ten sections per mouse spanning the width of the pancreas were included in the analysis. Data show mean ± SE from two (prophylactic; C–E) or four (therapeutic; F–H) independent experiments. *, $P < 0.05$ HFD *vs.* ND, same treatment; **, $P < 0.05$ XOMA 052 *vs.* IgG_2, same diet.

diet and treatment. Non-HDL cholesterol was calculated by subtracting HDL levels from total cholesterol.

Triglyceride levels, FFA, total cholesterol, and non-HDL cholesterol were increased by HFD feeding after 12 and 19 wk in the control IgG-treated mice [12 wk, $P < 0.05$ (Fig. 6, A–D); 19 wk, $P < 0.05$ (Fig. 6, E–H)]. Treatment of HFD mice with XOMA 052 significantly reduced lipid levels relative to untreated HFD mice, and HDL levels were unaffected by XOMA 052 (data not shown). In the prophylactic study, there was a 35% reduction in triglycerides, a 29% reduction in FFA, a 22% reduction in total cholesterol, and a 73% reduction in non-HDL cholesterol in XOMA 052-treated HFD compared with control HFD mice ($P < 0.05$; Fig. 6, A–D). The results of the therapeutic studies were consistent with the prophylactic results (Fig. 6, E–H). There was a 22% reduction in triglycerides, a 14% reduction in FFA, a 16% reduction in total cholesterol, and a 76% reduction in non-HDL cholesterol in XOMA 052-treated HFD compared with control HFD mice ($P < 0.05$; Fig. 6, D–F).

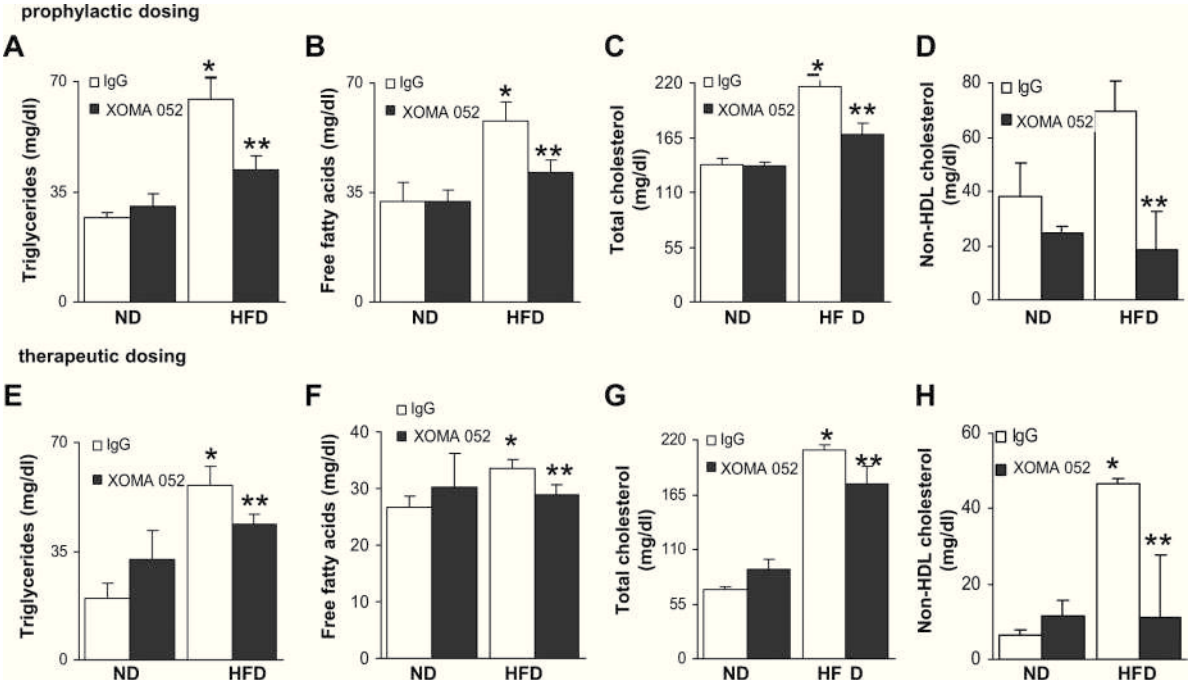

FIG. 6. XOMA 052 prevents HFD-induced changes in lipid levels. Mice were fed a ND or HFD for 12 wk and injected from wk 0 to 12 with 1 mg/kg XOMA 052 (prophylactic) or for 19 wk and injected from wk 11–19 with 1 mg/kg XOMA 052 (therapeutic). Fasting serum was obtained at the end of the study and triglycerides (A and E), FFA (B and F), and total cholesterol (C and G) were measured. Non-HDL cholesterol (D and H) was calculated by subtracting HDL from total cholesterol. A–D, Prophylactic study, performed in three separate experiments. Data show results from one representative experiment. E–H, Therapeutic study, performed in five separate experiments. Data show results from one representative experiment. Data show mean ± SE. *, $P < 0.05$ HFD *vs.* ND, same treatment; **, $P < 0.05$ XOMA 052 *vs.* IgG_2, same diet.

The protective effect of XOMA 052 treatment was seen for all three lipid measures (*i.e.* triglycerides, cholesterol, and FFA), which all reached significance in two out of three prophylactic studies; significance was reached for triglycerides in two, for cholesterol in five, and for FFA in three out of five therapeutic studies. The prophylactic study experiments were performed three times and the therapeutic study experiments five times in three animal facilities. The use of multiple animal facilities may help explain variations observed in serum lipid levels between study experiments.

Discussion

Novel treatments for diabetes which target the preservation of the β-cell are urgently needed. In the present study, we show that specific inhibition of IL-1β by an antibody preserved β-cell mass and function sufficiently to maintain normoglycemia in a DIO model. The effect on glycemic control observed for XOMA 052 was accompanied by improved insulin secretion, improved lipid profile, decreased β-cell apoptosis, and increased β-cell proliferation.

An important advantage of XOMA 052 over the previously studied IL-1 pathway inhibitor IL-1Ra is that, due to its longer circulatory half-life, XOMA 052 may be administered much less frequently than the daily injections of recombinant IL-1Ra required to achieve similar results. The effects of XOMA 052 were observed despite the fact that the affinity and *in vivo* potency of XOMA 052 for mIL-1β is 1000- to 10,000-fold lower than for hIL-1β. Thus, in comparison with IL-1Ra, which inhibits both IL-1α and IL-1β, the longer half-life and specificity of XOMA 052 for IL-1β may provide major advantages for use as a therapy in human patients.

The initial doses of XOMA 052 in the DIO model were based on previous work in the collagen-induced arthritis model. Because the DIO model requires 12–14 wk of dosing, and XOMA 052 is a human antibody, we wished to avoid a potential mouse antihuman antibody response; 5 mg/kg was the top dose attempted, which is the lowest effective dose in collagen-induced arthritis (our unpublished observations). We have performed preliminary experiments with 0.01, 0.1, 1, and 5 mg/kg; 0.1 and 1 mg/kg XOMA 052 have so far been the optimal doses for improving metabolic parameters.

Although the link between inflammation and insulin resistance is substantial (4), *in vivo* evidence of a role for IL-1β on the β-cell itself and in insulin resistance has not yet been demonstrated in a model of T2DM. Previous work used recombinant IL-1Ra, which blocks both IL-1α and IL-1β. Other studies lack data on insulin resistance

and stimulated insulin secretion (32). The present work provides evidence *in vivo* that IL-1β is a key mediator of β-cell dysfunction, survival, and peripheral insulin sensitivity.

The effect of IL-1β antibody on insulin sensitivity was calculated by the HOMA-IR model. The calculated HOMA-IR measure of insulin resistance was significantly higher in the HFD-fed mice and was normalized by XOMA 052 treatment. Although the HOMA-IR index is not the most accurate method for assessing insulin resistance compared with the hyperinsulinemic-euglycemic clamp, the combined result of normalized HOMA-IR and improved insulin sensitivity during an ipITT indicate a protective effect of XOMA 052 on insulin sensitivity. In line with our observation, administration of recombinant IL-1Ra improved insulin sensitivity (as assessed by HOMA-IR) in the GK rat (24).

The ability of XOMA 052 to improve glycemic control and β-cell function was observed consistently across eight independent experiments. A recent study with another anti-IL-1β antibody, 1400.24.17, also showed a reduction in HbA_{1c} but did not show an effect on fasting plasma glucose (32). There was no significant effect of the 1400.24.17 antibody on serum lipid levels. Although we report some variation in effect on serum lipid levels among the mice, our multiple studies with XOMA 052 show a consistent trend of lipid lowering effects. Osborn *et al.* (32) report results of one experiment with eight to 12 mice in each group, which could be a possible explanation for the lack of observed effect on plasma glucose and lipid levels.

In the current study, we included the additional approach of a therapeutic study. Treatment with XOMA 052 was initiated in mice that were already obese and that demonstrated hyperglycemia and impaired glucose tolerance, as well as impaired insulin secretion. Importantly, in the therapeutic study, serum glucose levels, which were elevated during the HFD feeding, could be decreased by XOMA 052 treatment for an additional 9 wk, even when the HFD feeding was maintained. In addition, glucose stimulated insulin secretion, which was abolished by the HFD, was restored by XOMA 052 treatment. β-Cell survival was also significantly improved. This therapeutic study design, rather than previously described prophylactic studies (where the HFD was started concomitantly with the drugs), better reflects the situation of an overweight patient with progressing T2DM.

After 19 wk of diet, β-cell apoptosis was increased from 0.15% with ND to 0.7% with HFD. These data are comparable with β-cell apoptosis in humans published by Butler *et al.* (33) using a large collection of autopsy pancreata from nondiabetic control individuals and patients with T2DM. In general, numbers of apoptotic cells are low due to the rapid clearance by macrophages within 5–10 min *in vivo*. Therefore, *in situ* apoptosis data are difficult to extrapolate to the *in vivo* situation. In a previous study, we were unable to show significant changes in apoptosis *in vivo* after 12 wk of diet (23). The fact that we measured a significant increase in apoptosis in each pancreas, which was prevented by XOMA 052 treatment, led us to the assumption that there is indeed an effect on β-cell survival by long-term HFD diet, especially over 19 wk.

One important mechanism to adapt to conditions of higher insulin demand (*e.g.* due to obesity-induced insulin resistance) is the extraordinary capacity of the β-cell to increase its mass to maintain normoglycemia (33). This adaptive capacity was observed in the present study, where HFD feeding increased β-cell mass after 12 wk, although we had observed impaired β-cell turnover at this time point, consistent with our previous studies (23, 34). After 19 wk of diet, we observed that the compensatory capacity of the β-cell could not be maintained in the untreated control group but was rescued in the XOMA 052-treated mice, with those animals also showing increased β-cell proliferation, decreased apoptosis, and increased β-cell mass relative to control animals.

The lipid-lowering effects of XOMA 052 in both prophylactic and therapeutic studies are interesting in light of the potential cardiovascular risks of current diabetes drugs (35). Recent reports have highlighted the role of inflammation, and IL-1β itself, in atherosclerosis and congestive heart failure (36, 37). We are currently exploring the potential benefit of inhibiting IL-1β with XOMA 052 in animal models of atherosclerosis. In addition, the ability of XOMA 052 to improve the lipid profile also suggests that the antibody could reduce peripheral insulin resistance (38).

An effect of IL-1β on the insulin sensitivity of adipocytes has been suggested by observations of its effects on insulin signaling in such cells *in vitro* (39), as well as through its established role as an inducer of IL-6 (40). However, the effect of IL-1Ra on insulin sensitivity has been debated because increased IL-1Ra serum levels have been shown in some studies to correlate with obesity and insulin resistance (41–45). Nevertheless, in a previous study in DIO mice, daily recombinant IL-1Ra injections for 12 wk did not impair insulin sensitivity as assessed by ipITT. Moreover, basal insulin levels, which were increased by the HFD due to insulin resistance, could be maintained at normal levels in the IL-1Ra-treated group (23). Recent results from the Whitehall Study show that endogenous IL-1Ra levels are increased before the onset of T2DM (46), which is consistent with findings in mice fed with a HFD. With the progression of diabetes, endogenous IL-1Ra has been shown to decrease in parallel with the development of hyperglycemia and decreased β-cell mass

in mice (34). Lower levels of endogenous IL-1Ra were also measured in patients with T2DM (47).

Given the protective effect of XOMA 052 on both improved β-cell function and lipid profile, there are questions regarding what tissue is primarily affected by IL-1β blockade and what cells produce IL-1β under diabetogenic conditions. Intraislet IL-1β expression in T2DM was found in our earlier study (18). In line with this previous observation, recent data from β-cells derived through laser microdissection show increased IL-1β in T2DM (21), which has also been confirmed by Igoillo-Esteve *et al.* (48). However, the major role of IL-1β in the pathogenesis of T2DM is so far not completely established. Infiltration of macrophages in adipose tissue has been found in obesity in mice and humans. This is linked to the development of insulin resistance (49, 50) and involves the production of inflammatory cytokines, among them IL-1β. Recently, IL-1β production in response to obesity was also observed in the hypothalamus and was connected to an inflammatory response and insulin resistance (51). We therefore investigated the possibility that blocking IL-1β may inhibit the increase in IL-1β in the tissues where diabetes-induced IL-1β production has been shown. In all the tested tissues, the hypothalamus, the epididymal fat pads, as well as in isolated pancreatic islets, we found IL-1β mRNA present in the HFD-fed mice. In contrast, XOMA 052 significantly inhibited IL-1β gene expression in all three tissues. These data confirm the well-known phenomenon of IL-1β to induce its own expression (52, 53), which has recently been shown in β-cells (10). Importantly, IL-1β stimulates pro-IL-1β mRNA in human islet cultures, which is completely blocked by XOMA 052 or IL-1Ra (10). Thus, IL-1β treatment of human islets results in IL-1β autostimulation, which is inhibited by IL-1β blockade. Similarly, we show here that the increase in IL-1β mRNA induced by the HFD did not occur in mice where IL-1β was blocked by XOMA 052. These data indicate that a cycle of increased IL-1β expression in IL-1β-expressing tissue can be blocked by XOMA 052, and thus provide a possible mechanism of XOMA 052-induced protection from the establishment of severe impairment of insulin action and insulin secretion. Although we have not investigated the cellular source of IL-1β production in the isolated islets, we believe that the production of IL-1β in the insulin target tissue plays an important role in the interorgan network with the β-cell.

The work presented here provides the first proof in animals that IL-1β inhibition is effective in T2DM even after disease onset, suggesting that antibody therapy may be successful at treating many aspects of T2DM. The present DIO model of HFD-treated mouse, although a standard for metabolic research, has a distinct pathogenesis from diabetes pathophysiology in humans. Therefore, results from clinical trials using XOMA 052 will help in understanding whether regulating IL-1β is an effective therapy for T2DM. In favor of our data, early results from a phase I clinical trial of XOMA 052 show an overall reduction in HbA_{1c} and an increase in stimulated insulin secretion for at least 3 months in T2DM patients with established disease and who have received a single dose of XOMA 052 (54).

Acknowledgments

We thank Dr. Lawrence W. Castellani for serum lipid analysis and Dr. Alan Solinger, Dr. Clint Rogers, and Dr. Rhonda Hansen for critical reading of the manuscript.

Address all correspondence and requests for reprints to: Seema Kantak, Ph.D., Preclinical Research and Development, XOMA (US) LLC, 2910 Seventh Street, Berkeley, California 94710. E-mail: kantak@xoma.com.

K.M. is supported by the German Research Foundation (Deutsche Forschungsgemeinschaft, Emmy Noether Programm, MA4172/1-1).

Disclosure Summary: A.M.O., L.G., J.Y., S.L., and S.K. are employed by XOMA (US) LLC. K.M. consults for XOMA (US) LLC. L.E. was previously employed by XOMA (US) LLC. L.S., J.J., E.D., and J.B. have nothing to disclose.

References

1. **Zimmet P, Alberti KG, Shaw J** 2001 Global and societal implications of the diabetes epidemic. Nature 414:782–787
2. **Nolan CJ, Prentki M** 2008 The islet β-cell: fuel responsive and vulnerable. Trends Endocrinol Metab 19:285–291
3. **Hotamisligil GS** 2006 Inflammation and metabolic disorders. Nature 444:860–867
4. **Wellen KE, Hotamisligil GS** 2005 Inflammation, stress, and diabetes. J Clin Invest 115:1111–1119
5. **Qatanani M, Lazar MA** 2007 Mechanisms of obesity-associated insulin resistance: many choices on the menu. Genes Dev 21:1443–1455
6. **Tilg H, Moschen AR** 2008 Inflammatory mechanisms in the regulation of insulin resistance. Mol Med 14:222–231
7. **Schenk S, Saberi M, Olefsky JM** 2008 Insulin sensitivity: modulation by nutrients and inflammation. J Clin Invest 118:2992–3002
8. **Alexandraki K, Piperi C, Kalofoutis C, Singh J, Alaveras A, Kalofoutis A** 2006 Inflammatory process in type 2 diabetes: the role of cytokines. Ann NY Acad Sci 1084:89–117
9. **Spranger J, Kroke A, Möhlig M, Hoffmann K, Bergmann MM, Ristow M, Boeing H, Pfeiffer AF** 2003 Inflammatory cytokines and the risk to develop type 2 diabetes: results of the prospective population-based European prospective investigation into cancer and nutrition (EPIC)-Potsdam study. Diabetes 52:812–817
10. **Böni-Schnetzler M, Boller S, Debray S, Bouzakri K, Meier DT, Prazak R, Kerr-Conte J, Pattou F, Ehses JA, Schuit FC, Donath MY** 2009 Free fatty acids induce a proinflammatory response in islets via the abundantly expressed interleukin-1 receptor I. Endocrinology 150:5218–5229
11. **Allantaz F, Chaussabel D, Banchereau J, Pascual V** 2007 Microar-

ray-based identification of novel biomarkers in IL-1-mediated diseases. Curr Opin Immunol 19:623–632
12. **Dinarello CA** 1998 Interleukin-1, interleukin-1 receptors and interleukin-1 receptor antagonist. Int Rev Immunol 16:457–499
13. **Mandrup-Poulsen T** 2003 Apoptotic signal transduction pathways in diabetes. Biochem Pharmacol 66:1433–1440
14. **Bendtzen K, Mandrup-Poulsen T, Nerup J, Nielsen JH, Dinarello CA, Svenson M** 1986 Cytotoxicity of human pI 7 interleukin-1 for pancreatic islets of Langerhans. Science 232:1545–1547
15. **Eizirik DL, Mandrup-Poulsen T** 2001 A choice of death—the signal-transduction of immune-mediated β-cell apoptosis. Diabetologia 44:2115–2133
16. **Donath MY, Mandrup-Poulsen T** 2008 The use of interleukin-1-receptor antagonists in the treatment of diabetes mellitus. Nat Clin Pract Endocrinol Metab 4:240–241
17. **Cnop M, Welsh N, Jonas JC, Jorns A, Lenzen S, Eizirik DL** 2005 Mechanisms of pancreatic β-cell death in type 1 and type 2 diabetes: many differences, few similarities. Diabetes 54(Suppl 2):S97–S107
18. **Maedler K, Sergeev P, Ris F, Oberholzer J, Joller-Jemelka HI, Spinas GA, Kaiser N, Halban PA, Donath MY** 2002 Glucose-induced β cell production of IL-1β contributes to glucotoxicity in human pancreatic islets. J Clin Invest 110:851–860
19. **Venieratos PD, Drossopoulou GI, Kapodistria KD, Tsilibary EC, Kitsiou PV** 2010 High glucose induces suppression of insulin signalling and apoptosis via upregulation of endogenous IL-1β and suppressor of cytokine signalling-1 in mouse pancreatic β cells. Cell Signal 22:791–800
20. **Zhou R, Tardivel A, Thorens B, Choi I, Tschopp J** 2010 Thioredoxin-interacting protein links oxidative stress to inflammasome activation. Nat Immunol 11:136–140
21. **Böni-Schnetzler M, Thorne J, Parnaud G, Marselli L, Ehses JA, Kerr-Conte J, Pattou F, Halban PA, Weir GC, Donath MY** 2008 Increased interleukin (IL)-1β messenger ribonucleic acid expression in β-cells of individuals with type 2 diabetes and regulation of IL-1β in human islets by glucose and autostimulation. J Clin Endocrinol Metab 93:4065–4074
22. **Mine T MK, Okutsu T, Mitsui A, Kitahara Y** 2004 Gene expression profile in the pancreatic islets of Goto-Kakizaki (GK) rats with repeated postprandial hyperglycemia. Diabetes 53(Suppl2):2475A
23. **Sauter NS, Schulthess FT, Galasso R, Castellani LW, Maedler K** 2008 The antiinflammatory cytokine interleukin-1 receptor antagonist protects from high-fat diet-induced hyperglycemia. Endocrinology 149:2208–2218
24. **Ehses JA, Lacraz G, Giroix MH, Schmidlin F, Coulaud J, Kassis N, Irminger JC, Kergoat M, Portha B, Homo-Delarche F, Donath MY** 2009 IL-1 antagonism reduces hyperglycemia and tissue inflammation in the type 2 diabetic GK rat. Proc Natl Acad Sci USA 106:13998–14003
25. **Larsen CM, Faulenbach M, Vaag A, Vølund A, Ehses JA, Seifert B, Mandrup-Poulsen T, Donath MY** 2007 Interleukin-1-receptor antagonist in type 2 diabetes mellitus. N Engl J Med 356:1517–1526
26. **Kaye J, Porcelli S, Tite J, Jones B, Janeway Jr CA** 1983 Both a monoclonal antibody and antisera specific for determinants unique to individual cloned helper T cell lines can substitute for antigen and antigen-presenting cells in the activation of T cells. J Exp Med 158:836–856
27. **Surwit RS, Feinglos MN, Rodin J, Sutherland A, Petro AE, Opara EC, Kuhn CM, Rebuffé-Scrive M** 1995 Differential effects of fat and sucrose on the development of obesity and diabetes in C57BL/6J and A/J mice. Metabolism 44:645–651
28. **Odegaard JI, Ricardo-Gonzalez RR, Goforth MH, Morel CR, Subramanian V, Mukundan L, Red Eagle A, Vats D, Brombacher F, Ferrante AW, Chawla A** 2007 Macrophage-specific PPARγ controls alternative activation and improves insulin resistance. Nature 447:1116–1120
29. **Warnick GR** 1986 Enzymatic methods for quantification of lipoprotein lipids. Methods Enzymol 129:101–123
30. **Surwit RS, Kuhn CM, Cochrane C, McCubbin JA, Feinglos MN** 1988 Diet-induced type II diabetes in C57BL/6J mice. Diabetes 37:1163–1167
31. **LeRoith D** 2002 β-Cell dysfunction and insulin resistance in type 2 diabetes: role of metabolic and genetic abnormalities. Am J Med 113(Suppl 6A):3S–11S
32. **Osborn O, Brownell SE, Sanchez-Alavez M, Salomon D, Gram H, Bartfai T** 2008 Treatment with an Interleukin 1β antibody improves glycemic control in diet-induced obesity. Cytokine 44:141–148
33. **Butler AE, Janson J, Bonner-Weir S, Ritzel R, Rizza RA, Butler PC** 2003 β-Cell deficit and increased β-cell apoptosis in humans with type 2 diabetes. Diabetes 52:102–110
34. **Glas R, Sauter NS, Schulthess FT, Shu L, Oberholzer J, Maedler K** 2009 Purinergic $P2X_7$ receptors regulate secretion of interleukin-1 receptor antagonist and β cell function and survival. Diabetologia 52:1579–1588
35. **DeSouza C, Fonseca V** 2009 Therapeutic targets to reduce cardiovascular disease in type 2 diabetes. Nat Rev Drug Discov 8:361–367
36. **Braunwald E** 2008 Biomarkers in heart failure. N Engl J Med 358:2148–2159
37. **Apostolakis S, Vogiatzi K, Krambovitis E, Spandidos DA** 2008 IL-1 cytokines in cardiovascular disease: diagnostic, prognostic and therapeutic implications. Cardiovasc Hematol Agents Med Chem 6:150–158
38. **Ginsberg HN** 2000 Insulin resistance and cardiovascular disease. J Clin Invest 106:453–458
39. **Jager J, Grémeaux T, Cormont M, Le Marchand-Brustel Y, Tanti JF** 2007 Interleukin-1β-induced insulin resistance in adipocytes through down-regulation of insulin receptor substrate-1 expression. Endocrinology 148:241–251
40. **Dinarello CA** 1996 Biologic basis for interleukin-1 in disease. Blood 87:2095–2147
41. **Abbatecola AM, Ferrucci L, Grella R, Bandinelli S, Bonafè M, Barbieri M, Corsi AM, Lauretani F, Franceschi C, Paolisso G** 2004 Diverse effect of inflammatory markers on insulin resistance and insulin-resistance syndrome in the elderly. J Am Geriatr Soc 52:399–404
42. **Meier CA, Bobbioni E, Gabay C, Assimacopoulos-Jeannet F, Golay A, Dayer JM** 2002 IL-1 receptor antagonist serum levels are increased in human obesity: a possible link to the resistance to leptin? J Clin Endocrinol Metab 87:1184–1188
43. **Ruotsalainen E, Salmenniemi U, Vauhkonen I, Pihlajamäki J, Punnonen K, Kainulainen S, Laakso M** 2006 Changes in inflammatory cytokines are related to impaired glucose tolerance in offspring of type 2 diabetic subjects. Diabetes Care 29:2714–2720
44. **Salmenniemi U, Ruotsalainen E, Pihlajamäki J, Vauhkonen I, Kainulainen S, Punnonen K, Vanninen E, Laakso M** 2004 Multiple abnormalities in glucose and energy metabolism and coordinated changes in levels of adiponectin, cytokines, and adhesion molecules in subjects with metabolic syndrome. Circulation 110:3842–3848
45. **Somm E, Cettour-Rose P, Asensio C, Charollais A, Klein M, Theander-Carrillo C, Juge-Aubry CE, Dayer JM, Nicklin MJ, Meda P, Rohner-Jeanrenaud F, Meier CA** 2006 Interleukin-1 receptor antagonist is upregulated during diet-induced obesity and regulates insulin sensitivity in rodents. Diabetologia 49:387–393
46. **Herder C, Brunner EJ, Rathmann W, Strassburger K, Tabák AG, Schloot NC, Witte DR** 2009 Elevated levels of the anti-inflammatory interleukin-1 receptor antagonist precede the onset of type 2 diabetes: the Whitehall II study. Diabetes Care 32:421–423
47. **Marculescu R, Endler G, Schillinger M, Iordanova N, Exner M, Hayden E, Huber K, Wagner O, Mannhalter C** 2002 Interleukin-1 receptor antagonist genotype is associated with coronary atherosclerosis in patients with type 2 diabetes. Diabetes 51:3582–3585
48. **Igoillo-Esteve M, Marselli L, Cunha DA, Ladrière L, Ortis F, Weir**

G, Marchetti P, Eizirik DL, Cnop M 2009 Exposure of human islets to palmitate mimics the mild inflammatory response observed in islets from type 2 diabetic individuals. Diabetologia 52:S164

49. **Weisberg SP, McCann D, Desai M, Rosenbaum M, Leibel RL, Ferrante Jr AW** 2003 Obesity is associated with macrophage accumulation in adipose tissue. J Clin Invest 112:1796–1808
50. **Xu H, Barnes GT, Yang Q, Tan G, Yang D, Chou CJ, Sole J, Nichols A, Ross JS, Tartaglia LA, Chen H** 2003 Chronic inflammation in fat plays a crucial role in the development of obesity-related insulin resistance. J Clin Invest 112:1821–1830
51. **Milanski M, Degasperi G, Coope A, Morari J, Denis R, Cintra DE, Tsukumo DM, Anhe G, Amaral ME, Takahashi HK, Curi R, Oliveira HC, Carvalheira JB, Bordin S, Saad MJ, Velloso LA** 2009 Saturated fatty acids produce an inflammatory response predominantly through the activation of TLR4 signaling in hypothalamus: implications for the pathogenesis of obesity. J Neurosci 29:359–370
52. **Warner SJ, Auger KR, Libby P** 1987 Human interleukin 1 induces interleukin 1 gene expression in human vascular smooth muscle cells. J Exp Med 165:1316–1331
53. **Dinarello CA** 1988 Biology of interleukin 1. FASEB J 2:108–115
54. **Donath MY, CW, Brunner A, Keller C, Whitmore J, Der K, Zayed H, Scannon PJ, Feldstein JD, Dinarello CA, Solinger AM,** XOMA 052, a potential disease modifying anti-IL-1β antibody, shows sustained HbA1c reductions 3 months after a single injection with no increases in safety parameters in subjects with type 2 diabetes. Proc American Diabetes Association 69th Scientific Sessions, New Orleans, LA, 2009 (Abstract 113-OR)

Islets 1:3, 256-259; November/December 2009; © 2009 Landes Bioscience

CXCL10

A path to β-cell death

Federico Paroni, Erna Domsgen and Kathrin Maedler*
Centre for Biomolecular Interactions Bremen; University of Bremen; Germany

The ability of the β-cells to control blood glucose levels depends on their function and mass. In both, type 1 and type 2 diabetes mellitus the main processes leading to β-cell failure are apoptosis and loss of function.

Many studies demonstrate how cytokines and chemokines have an active role in triggering the immune-response against the β-cell population. In a recent study we have identified that the chemokine CXCL10 may play an active role in triggering β-cell destruction.

We have identified the Toll like receptor 4 as the receptor for CXCL10 and as new pathway for the induction of β-cell apoptosis. Our findings may open new therapeutic approaches to fight onset and progression of the disease.

Key words: diabetes, β-cells, apoptosis, proliferation, inflammation, CXCL10

Submitted: 05/18/09

Revised: 05/25/09

Accepted: 05/26/09

Previously published online:
www.landesbioscience.com/journals/islets/article/9110

*Correspondence to:
Kathrin Maedler; Email: kmaedler@uni-bremen.de

Addendum to: Schulthess FT, Paroni F, Sauter NS, Shu L, Ribaux P, Haataja L, et al. CXCL10 impairs beta cell function and viability in diabetes through TLR4 signaling. JCell Metab. 2009 Feb;9(2):125-39. PMID: 19187771; DOI: 10.1016/j.cmet.2009.01.003

As evidenced by numerous studies from human pancreata and mouse models, β-cell apoptosis is the main process leading to β-cell mass depletion.[1,2]

Apoptosis in type 1 diabetes (T1DM) is triggered by an auto-immune reaction; the interaction between antigen presenting cells and T-cells leads to prolonged presence in high intra-islet concentrations of inflammatory mediators: cytokines, chemokines, reactive oxygen species (ROS) and other death effectors, which all lead to specific destruction of the β-cells and disease development.[3-5]

Similarly, T2DM is characterized by the presence of immune cell infiltration,[6] toxic amyloid oligomer deposition,[7,8] elevated levels of cytokines in the serum as well as inside the pancreatic islets,[9] and apoptotic β-cells, leading to the decrease of β-cell mass and disease progression.

Hyperglycemia and hyperlipidemia, so called "lipoglucotoxicity" then initiates a vicious cycle in β-cell destruction.[10] Through the accumulation of oxidative protein folding, elevated ER stress markers are present in diabetes,[11] however, it remains to be clarified whether ER stress is causative for β-cell failure.[12,13] The constant activation of sub-clinical levels of pro-inflammatory cytokines can lead to the expression of high levels of several markers involved in the acute immune response such as CRP, IL-1β, TNFα, IL-8, MCP-1,[14] and to disease development through activation of the classical apoptotic machinery including activation of caspases and c-jun terminal kinase (JNK).[15]

Besides that, acute or chronic viral infection can be a contributing factor to T1DM and T2DM through the activation of the inflammatory cascade,[16] specifically, viral infection causes high levels of one member of the chemokine family, the Interferon-γ-inducible protein (IP-10),[17] also known as chemokine (C-X-C motif) ligand 10 (CXCL10).

Increased CXCL10 serum levels have been found present in both T1DM[18,19] and T2DM patients[20] as well as in patients with high risk to develop T1DM[18] and T2DM.[21] It acts as a potent chemo-attractant for mononuclear cells, T-cells, B-cells and NK-cells. Particularly, the production of the chemokine CXCL10 is present prior to the onset or at least at an early stage of the disease development.[22,23]

In our recent study we point out that CXCL10 is able by itself to trigger apoptosis in isolated human islets. Detailed analysis of CXCL10-induced apoptosis in

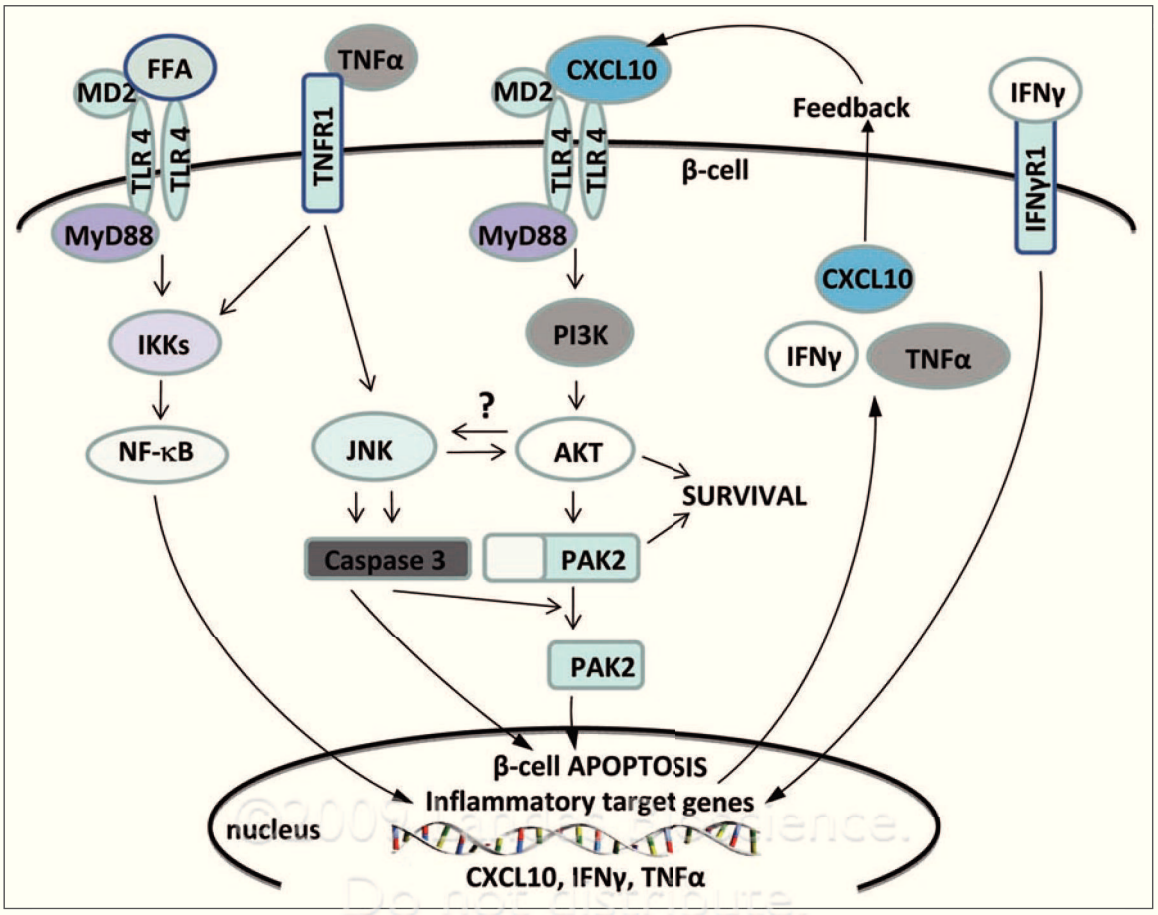

Figure 1. Our hypothetical model how CXCL10 signaling and production leads to β-cell apoptosis. Binding of CXCL10 to TLR4, TNFα to TNFR1, IFNγ to IFNγR1 result in their own gene upregulation. FFA may enhance such proinflammatory target gene production. Expression and secretion of CXCL10, IFNγ and TNFα lead to a feedback signaling ending in an ampligied self induction and apoptosis. We hypothesize that binding of CXCL10 on TLR4 results in MyD88-dependent activation of PI3K and AKT followed by a possible crosstalk between JNK and AKT. Activated JNK leads to cleavage of Caspase 3 and cleavage of PAK2 ending in a switch from survival of β-cell apoptosis.

islets identified apoptotic cells frequently in doublets, which suggests that proliferating cells are vulnerable to apoptosis.[24] This observation is in line with earlier studies from diabetic mouse models.[25-27]

In obese state, there is an increase in β-cell mass due to replication of already existing β-cells.[28] Mice fed a high fat diet adapt to the higher insulin demand by increasing their functional β-cell mass due to β-cell hyperplasia rather than hypertrophy.[28] Also, β-cell replication is the primary mechanism for maintaining postnatal β-cell mass shown in mice[29] as well as in humans.[30] β-cell replication rapidly decreases with age, shown in mice at the age of around 6 months[31] and in humans as early as at the age of ~1 year[30] and further decreases to almost undetectable levels.[1,32] The capacity of the β-cell to adapt to a higher insulin demand declines with aging.[33,34] Nevertheless, the important capacity to adapt insulin secretion to the metabolic demand through increasing β-cell mass is maintained at older age.[1,35] Logically, this could be achieved by β-cell replication, which was observed in human β-cells in obesity[1] and pregnancy,[36] but to a much lesser extend than in rodents.[31]

Given that the switch from β-cell proliferation and adaptation to apoptosis and β-cell failure may occur as a general mechanism in diabetes progression, we further investigated CXCL10 signaling as a model for such deleterious activity in β-cells. One signal which is essential for β-cell survival is the PI3K/Akt pathway.[37] Despite the pre-apoptotic effect of CXCL10, Akt is highly and prolonged activated. Why does apoptosis occur in the presence of such protective factor? It is well established that CXCL10 exerts its activity by its natural receptor CXCR3.[38-40] In our study we demonstrate that the pro-apoptotic CXCL10 effect is CXCR3-independent.[24] Instead, Toll like receptor 4 (TLR4) signaling mediated such pro-apoptotic machinery (**Fig. 1**).

TLR 4 signaling is able to trigger the expression of JNK.[41] Given that, CXCL10 activates JNK, induces caspase 3 cleavage which in turn cleaves the protein activated kinase 2 PAK-2 and ends in reversing the Akt signal from proliferation to apoptosis (**Fig. 1**).

JNK activation could have a different starting point, either via a direct or indirect activation by TLR4,[41] or through a crosstalk with PI3K/Akt.[42] CXCL10 may give the initial burst and triggers a downstream activation of the apoptotic signal that involves both PI3K/Akt and JNK pathways (**Fig. 1**).

Insulin injection in patients is able to downregulate TLR4 expression that can end in an anti-inflammatory effect.[43] Insulin could exert its action in an insulin receptor-dependent manner. Binding of FFA to TLR4 results in an insulin resistance condition, initiated through the classical TLR4 signaling cascade with downstream production of inflammatory molecules. Indeed, FFA stimulated NFκB activation leads to IL-6 and TNFα production in macrophages and adipocytes[41] and to the production of other cytokines including CXCL10 at the end.[44-46] This could be further amplified by interferon-γ (IFNγ), also shown to be elevated in obesity[14] and the main inducer of CXCL10.[22] Human adipocytes were identified as a source of CXCL10 expression and secretion which suggests the chemokine as an inducer of obesity related inflammation.[47] A recent study which shows association of CXCL10 with both BMI and waist circumference[48] supports such interplay of FFAs with cytokines and chemokines and links obesity, inflammation and diabetes.

Indeed, we have detected the presence of CXCL10 in β-cells not only in T1DM and T2DM, but also in obese non-diabetic patients. The presence of CXCL10 in obese patients could be a result of the elevated circulating FFA concentrations.[49] If this pathway is true and exclusive, obesity must consequently lead to diabetes, but firstly, this occurs in only 10–20% of the patients[50] and secondly, pro-diabetic factors have been shown independently of diabetes progression.[51] The body must have an extensive stock of protective mechanisms to block such progression which demands further extensive research.

The fact that TLR downstream pathway is known to be activated by several agents such as LPS,[52] FFA[41] and virus infection[16] leading to cytokine and chemokine which in turn target the whole metabolic system invites to speculate on an essential role of TLR4 in metabolic disturbances including insulin resistance and diabetes. Our data will bring a new insight on the involvement of chemokines in the development of T1DM and T2DM, and perhaps, TLR4 could be a potential therapeutic target for preventing the disease. By recruiting MyD88 to the receptor complex, TLR4 shares downstream pathways with IL-1β signaling.[53] Similar to our study, IL-1β expression has been found in islets from patients with T2DM.[54] Antagonizing IL-1β signaling by the naturally occurring interleukin-1receptor antagonist (IL-1Ra) showed that IL-1Ra treatment could improve β-cell function in patients with T2DM in a recent trial[55] and improved glycemia and β-cell survival in mouse models of T1DM & T2DM.[56-62] It is therefore possible that the use of neutralizing antibodies to CXCL10 alone or in combination with antagonizing IL-1β[63] provides a potent new strategy for the therapy of T1DM and T2DM to rescue the β-cell.

Acknowledgements

This work was supported by the German Research Foundation (DFG, Emmy Noether Programm, MA4172/1-1), the Juvenile Diabetes Research Foundation (JDRF 26-2008-861) and the European Foundation for the Study of Diabetes (EFSD)/Merck Sharp & Dohme (MSD) European Studies on Beta Cell Function and Survival. The authors thank the members of the Islet Biology laboratory in Bremen for critical discussion.

References

1. Butler AE, Janson J, Bonner-Weir S, Ritzel R, Rizza RA, Butler PC. Beta-cell deficit and increased beta-cell apoptosis in humans with type 2 diabetes. Diabetes 2003; 52:102-10.
2. Kurrer MO, Pakala SV, Hanson HL, Katz JD. Beta cell apoptosis in T cell-mediated autoimmune diabetes. Proc Natl Acad Sci USA 1997; 94:213-8.
3. Eizirik DL, Darville MI. beta-cell apoptosis and defense mechanisms: lessons from type 1 diabetes. Diabetes 2001; 50:64-9.
4. Eizirik DL, Mandrup-Poulsen T. A choice of death—the signal-transduction of immune-mediated beta-cell apoptosis. Diabetologia 2001; 44:2115-33.
5. Mandrup-Poulsen T. Apoptotic signal transduction pathways in diabetes. Biochem Pharmacol 2003; 66:1433-40.
6. Ehses JA, Boni-Schnetzler M, Faulenbach M, Donath MY. Macrophages, cytokines and beta-cell death in Type 2 diabetes. Biochem Soc Trans 2008; 36:340-2.
7. Haataja L, Gurlo T, Huang CJ, Butler PC. Islet amyloid in type 2 diabetes, and the toxic oligomer hypothesis. Endocr Rev 2008; 29:303-16.
8. Kahn SE. The importance of the beta-cell in the pathogenesis of type 2 diabetes mellitus. Am J Med 2000; 108:2-8.
9. Alexandraki K, Piperi C, Kalofoutis C, Singh J, Alaveras A, Kalofoutis A. Inflammatory Process in Type 2 Diabetes: The Role of Cytokines. Ann N Y Acad Sci 2006; 1084:89-117.
10. Poitout V, Robertson RP. Glucolipotoxicity: fuel excess and beta-cell dysfunction. Endocr Rev 2008; 29:351-66.
11. Laybutt DR, Preston AM, Akerfeldt MC, Kench JG, Busch AK, Biankin AV, Biden TJ. Endoplasmic reticulum stress contributes to beta cell apoptosis in type 2 diabetes. Diabetologia 2007; 50:752-63.
12. Akerfeldt MC, Howes J, Chan JY, Stevens VA, Boubenna N, McGuire HM, et al. Cytokine-induced beta-cell death is independent of endoplasmic reticulum stress signaling. Diabetes 2008; 57:3034-44.
13. Sundar Rajan S, Srinivasan V, Balasubramanyam M, Tatu U. Endoplasmic reticulum (ER) stress & diabetes. Indian J Med Res 2007; 125:411-24.
14. Kolb H, Mandrup-Poulsen T. An immune origin of type 2 diabetes? Diabetologia 2005; 48:1038-50.
15. Donath MY, Storling J, Maedler K, Mandrup-Poulsen T. Inflammatory mediators and islet beta-cell failure: a link between type 1 and type 2 diabetes. J Mol Med 2003; 81:455-70.
16. Xagorari A, Chlichlia K. Toll-like receptors and viruses: induction of innate antiviral immune responses. The open microbiology journal 2008; 2:49-59.
17. Christen U, Von Herrath MG. IP-10 and type 1 diabetes: a question of time and location. Autoimmunity 2004; 37:273-82.
18. Nicoletti F, Conget I, Di Mauro M, Di Marco R, Mazzarino MC, Bendtzen K, et al. Serum concentrations of the interferon-gamma-inducible chemokine IP-10/CXCL10 are augmented in both newly diagnosed Type I diabetes mellitus patients and subjects at risk of developing the disease. Diabetologia 2002; 45:1107-10.
19. Shimada A, Morimoto J, Kodama K, Suzuki R, Oikawa Y, Funae O, et al. Elevated serum IP-10 levels observed in type 1 diabetes. Diabetes Care 2001; 24:510-5.
20. Xu H, Nakayama K, Ogawa S, Sugiura A, Kato T, Sato T, et al. Elevated plasma concentration of IP-10 in patients with type 2 diabetes mellitus. Nippon Jinzo Gakkai Shi 2005; 47:524-30.
21. Herder C, Baumert J, Thorand B, Koenig W, de Jager W, Meisinger C, et al. Chemokines as risk factors for type 2 diabetes: results from the MONICA/KORA Augsburg study, 1984–2002. Diabetologia 2006; 49:921-9.
22. Cardozo AK, Proost P, Gysemans C, Chen MC, Mathieu C, Eizirik DL. IL-1beta and IFNgamma induce the expression of diverse chemokines and IL-15 in human and rat pancreatic islet cells, and in islets from pre-diabetic NOD mice. Diabetologia 2003; 46:255-66.
23. Li D, Zhu SW, Liu DJ, Liu GL. Expression of interferon inducible protein-10 in pancreas of mice. World J Gastroenterol 2005; 11:4750-2.
24. Schulthess FT, Paroni F, Sauter NS, Shu L, Ribaux P, Haataja L, et al. CXCL10 impairs beta cell function and viability in diabetes through TLR4 signaling. Cell Metab 2009; 9:125-39.
25. Ritzel RA, Butler PC. Replication increases beta-cell vulnerability to human islet amyloid polypeptide-induced apoptosis. Diabetes 2003; 52:1701-8.
26. Donath MY, Gross DJ, Cerasi E, Kaiser N. Hyperglycemia-induced beta-cell apoptosis in pancreatic islets of *Psammomys obesus* during development of diabetes. Diabetes 1999; 48:738-44.
27. Meier JJ, Ritzel RA, Maedler K, Gurlo T, Butler PC. Increased vulnerability of newly forming beta cells to cytokine-induced cell death. Diabetologia 2006; 49:83-9.
28. Hull RL, Kodama K, Utzschneider KM, Carr DB, Prigeon RL, Kahn SE. Dietary-fat-induced obesity in mice results in beta cell hyperplasia but not increased insulin release: evidence for specificity of impaired beta cell adaptation. Diabetologia 2005; 48:1350-8.
29. Georgia S, Bhushan A. Beta cell replication is the primary mechanism for maintaining postnatal beta cell mass. J Clin Invest 2004; 114:963-8.

30. Meier JJ, Butler AE, Saisho Y, Monchamp T, Galasso R, Bhushan A, et al. Beta-cell replication is the primary mechanism subserving the postnatal expansion of beta-cell mass in humans. Diabetes 2008; 57:1584-94.
31. Teta M, Rankin MM, Long SY, Stein GM, Kushner JA. Growth and regeneration of adult beta cells does not involve specialized progenitors. Dev Cell 2007; 12:817-26.
32. Maedler K, Schumann DM, Schulthess F, Oberholzer J, Bosco D, Berney T, Donath MY. Aging correlates with decreased beta-cell proliferative capacity and enhanced sensitivity to apoptosis: a potential role for Fas and pancreatic duodenal homeobox-1. Diabetes 2006; 55:2455-62.
33. Tschen SI, Dhawan S, Gurlo T, Bhushan A: Age-dependent decline in beta-cell proliferation restricts the capacity of beta-cell regeneration in mice. Diabetes 58:1312-1320, 2009
34. Rankin MM, Kushner JA: Adaptive beta-cell proliferation is severely restricted with advanced age. Diabetes 58:1365-1372, 2009
35. Butler PC, Meier JJ, Butler AE, Bhushan A. The replication of beta cells in normal physiology, in disease and for therapy. Nat Clin Pract Endocrinol Metab 2007; 3:758-68.
36. Van Assche FA, Aerts L, De Prins F. A morphological study of the endocrine pancreas in human pregnancy. Br J Obstet Gynaecol 1978; 85:818-20.
37. Tuttle RL, Gill NS, Pugh W, Lee JP, Koeberlein B, Furth EE, et al. Regulation of pancreatic beta-cell growth and survival by the serine/threonine protein kinase Akt1/PKBalpha. Nat Med 2001; 7:1133-7.
38. Luster AD, Greenberg SM, Leder P. The IP-10 chemokine binds to a specific cell surface heparan sulfate site shared with platelet factor 4 and inhibits endothelial cell proliferation. J Exp Med 1995; 182:219-31.
39. Cole AM, Ganz T, Liese AM, Burdick MD, Liu L, Strieter RM. Cutting edge: IFN-inducible ELR-CXC chemokines display defensin-like antimicrobial activity. J Immunol 2001; 167:623-7.
40. Soejima K, Rollins BJ. A functional IFNgamma-inducible protein-10/CXCL10-specific receptor expressed by epithelial and endothelial cells that is neither CXCR3 nor glycosaminoglycan. J Immunol 2001; 167:6576-82.
41. Shi H, Kokoeva MV, Inouye K, Tzameli I, Yin H, Flier JS. TLR4 links innate immunity and fatty acid-induced insulin resistance. J Clin Invest 2006; 116:3015-25.
42. Aikin R, Maysinger D, Rosenberg L. Cross-talk between phosphatidylinositol 3-kinase/AKT and c-jun NH2-terminal kinase mediates survival of isolated human islets. Endocrinology 2004; 145:4522-31.
43. Ghanim H, Mohanty P, Deopurkar R, Sia CL, Korzeniewski K, Abuaysheh S, et al. Acute modulation of toll-like receptors by insulin. Diabetes Care 2008; 31:1827-31.
44. Giarratana N, Penna G, Amuchastegui S, Mariani R, Daniel KC, Adorini L. A vitamin D analog down-regulates proinflammatory chemokine production by pancreatic islets inhibiting T cell recruitment and type 1 diabetes development. J Immunol 2004; 173:2280-7.
45. Hoshino K, Kaisho T, Iwabe T, Takeuchi O, Akira S. Differential involvement of IFNbeta in Toll-like receptor-stimulated dendritic cell activation. Int Immunol 2002; 14:1225-31.
46. Selvarajoo K. Discovering differential activation machinery of the Toll-like receptor 4 signaling pathways in MyD88 knockouts. FEBS Lett 2006; 580:1457-64.
47. Herder C, Hauner H, Kempf K, Kolb H, Skurk T. Constitutive and regulated expression and secretion of interferon-gamma-inducible protein 10 (IP-10/CXCL10) in human adipocytes. Int J Obes (Lond) 2007; 31:403-10.
48. Herder C, Schneitler S, Rathmann W, Haastert B, Schneitler H, Winkler H, et al. Low-grade inflammation, obesity and insulin resistance in adolescents. J Clin Endocrinol Metab 2007; 92:4569-74.
49. Shimabukuro M, Zhou YT, Levi M, Unger RH. Fatty acid-induced beta cell apoptosis: a link between obesity and diabetes. Proc Natl Acad Sci USA 1998; 95:2498-502.
50. Bonner-Weir S. Islet growth and development in the adult. J Mol Endocrinol 2000; 24:297-302.
51. Solinas G, Vilcu C, Neels JG, Bandyopadhyay GK, Luo JL, Naugler W, et al. JNK1 in hematopoietically derived cells contributes to diet-induced inflammation and insulin resistance without affecting obesity. Cell Metab 2007; 6:386-97.
52. Pedron T, Girard R, Chaby R. TLR4-dependent lipopolysaccharide-induced shedding of tumor necrosis factor receptors in mouse bone marrow granulocytes. J Biol Chem 2003; 278:20555-64.
53. Kenny EF, O'Neill LAJ. Signalling adaptors used by Toll-like receptors: An update. Cytokine 2008; 43:342-9.
54. Maedler K, Sergeev P, Ris F, Oberholzer J, Joller-Jemelka HI, Spinas GA, et al. Glucose-induced beta-cell production of interleukin-1beta contributes to glucotoxicity in human pancreatic islets. J Clin Invest 2002; 110:851-60.
55. Larsen CM, Faulenbach M, Vaag A, Volund A, Ehses JA, Seifert B, et al. Interleukin-1-receptor antagonist in type 2 diabetes mellitus. N Engl J Med 2007; 356:1517-26.
56. Sandberg JO, Andersson A, Eizirik DL, Sandler S. Interleukin-1 receptor antagonist prevents low dose streptozotocin induced diabetes in mice. Biochem Biophys Res Commun 1994; 202:543-8.
57. Nicoletti F, Di Marco R, Barcellini W, Magro G, Schorlemmer HU, Kurrle R, et al. Protection from experimental autoimmune diabetes in the non-obese diabetic mouse with soluble interleukin-1 receptor. Eur J Immunol 1994; 24:1843-7.
58. Sandberg JO, Eizirik DL, Sandler S. IL-1 receptor antagonist inhibits recurrence of disease after syngeneic pancreatic islet transplantation to spontaneously diabetic non-obese diabetic (NOD) mice. Clin Exp Immunol 1997; 108:314-7.
59. Stoffels K, Gysemans C, Waer M, Laureys J, Bouillon R, Mathieu C. Interleukin-1 receptor antagonist inhibits primary non-function and prolongs graft survival time of xenogeneic islets transplanted in sponaeously diabetic autoimmune NOD mice. Diabetologia 2002; 45:424.
60. Tellez N, Montolio M, Estil-les E, Escoriza J, Soler J, Montanya E. Adenoviral overproduction of interleukin-1 receptor antagonist increases beta cell replication and mass in syngeneically transplanted islets, and improves metabolic outcome. Diabetologia 2007; 50:602-11.
61. Satoh M, Yasunami Y, Matsuoka N, Nakano M, Itoh T, Nitta T, et al. Successful islet transplantation to two recipients from a single donor by targeting proinflammatory cytokines in mice. Transplantation 2007; 83:1085-92.
62. Sauter NS, Schulthess FT, Galasso R, Castellani LW, Maedler K. The antiinflammatory cytokine interleukin-1 receptor antagonist protects from high-fat diet-induced hyperglycemia. Endocrinology 2008; 149:2208-18.
63. Donath MY, Weder C, Whitmore J, Bauer RJ, Der K, Scannon PJ, et al. XOMA 052, an anti-IL-10 antibody, in a double-blind, placebocontrolled, dose escalation study of the safety and pharmacokinetics in patients with type 2 diabetes mellitus—a new approach to therapy. Diabetologia 2008; 51:7.

Acknowledgments

I would like to thank Kathrin Mädler for giving me the opportunity to perform my PhD thesis in her lab and for her support throughout my work.

My special thanks goes to Federico Paroni, who worked with me on this project for several years, for his ideas and his support.

I would also like to thank Andreas Dotzauer for his friendship, his support and help throughout my whole university period.

I want to thank all the lab members, especially Payal Shah, Gitanjeli Dharmadhikari, Amin Ardestani, Zara Azizi, Jennifer Bergemann, Katharina Stolz, Katrin Zien, Wei He and many others for their friendship and support and care.

Ausserdem möchte ich mich herzlich bei meinen Freundinnen Hanna Rehberger, Miriam Trefas, Sarah Trefas, Janka Dießelhorst und Eva Zabel und Leena Krämer bedanken, die mich durch die ganze Phase der Doktorarbeit begleitet haben, immer ein Ohr für mich offen hatten, mich immer unterstütz haben und an mich gedacht haben.

Der grösste Dank gilt meiner Familie, Maja Domsgen, Semira Domsgen und Erich Domsgen, ohne die, diese Arbeit nicht möglich gewesen wäre. Sie haben mich stetz unterstützt, immer an mich geglaubt und sich aufopferungsvoll um mich gekümmert.

Daher widme ich diese Arbeit meiner Familie.